HIGH PERFORMANCE IN LOW-FLOW SOLAR DOMESTIC HOT WATER SYSTEMS

by

MYRNA DAYAN

A thesis submitted in partial fulfillment of
the requirements for the degree of

MASTER OF SCIENCE
MECHANICAL ENGINEERING

at the

UNIVERSITY OF WISCONSIN-MADISON

1998

ABSTRACT

Low-flow solar hot water heating systems employ flow rates on the order of 1/5 to 1/10 of the conventional flow. Low-flow systems are of interest because the reduced flow rate allows smaller diameter tubing, which is less costly to install. Further, low-flow systems result in increased tank stratification. Lower collector inlet temperatures are achieved through stratification and the useful energy produced by the collector is increased.

The disadvantage of low-flow systems is the collector heat removal factor, F_R, decreases with decreasing flow rate. A serpentine collector has the potential to perform better than a conventional header-riser collector in low-flow systems due to the earlier onset of turbulent flow which enhances the internal heat transfer coefficient. The onset of turbulent flow is a function of the tube diameter and flow rate per tube.

Many solar domestic hot water systems require an auxiliary electric source to operate a pump in order to circulate fluid through the solar collector. A photovoltaic driven pump can be used to replace the standard electrical pump. PV driven pumps provide an ideal means of controlling the flow rate, as pumps will only circulate fluid when there is sufficient radiation. The reduction of parasitic pumping power can also reduce on-peak utility demand. The PV pump, if adequately designed, decreases the system performance by a negligible amount.

There has been some confusion as to whether optimum flow rates exist in a solar domestic hot water system utilizing a heat exchanger between the collector and the storage tank, as commonly employed for freeze protection. It was found that there exists thermal optimum or at least economical optimum flow rates when it is considered that low flow rates incur less hydraulic costs. Peak performance was always found to occur when the heat exchanger tank-side flow rate was approximately equal to the average load flow rate. For low collector-side flow rates, a small deviation from the optimum flow rate will dramatically effect system performance. However, system performance is insensitive to flow rate for high collector-side flow rates.

Antifreeze solutions have temperature dependent properties such as density and specific heat. The effect of large temperature dependent property variations experienced by ethylene glycol and propylene glycol affect the optimum flow rate through the collector-side of the heat exchanger. The increased viscosity of the glycol at low temperatures impedes the onset of turbulence, which is detrimental to the heat exchanger UA.

ACKNOWLEDGEMENTS

It was an honor to work under the supervision of Professor Beckman and Professor Klein. Their guidance helped achieve my goals in developing this thesis. I would like to thank them for their probing questions always pushing my research further. Thanks to Professor Klein's development and continual improvements, EES was a fundamental tool for the development of this thesis. I would also like to thank Professor Mitchell for his input through his classes, especially his heat transfer class which helped my research.

Thank you to both the former and present TRNSYS engineers, Nathan Blair and Paul Williams, who were always willing to answer my hundreds of TRNSYS and computer related questions.

Thank you to my fellow lab mates who provided a great atmosphere in the laboratory. A special thanks goes to Ian who motivated me through all those long study sessions in the Memorial Library. Thanks to the guys in room 1337 for providing the lab humor. Thank you to all of you for keeping the lab spirit high.

Without my family providing me with their love and support, this would not have been possible. Thanks Mum and Dad for absolutely everything, you are both the best parents anybody could have.

Prax thank you so much for putting up with me during the trials and tribulations of my research and giving me encouragement when I needed it the most.

Some look at things as they are and ask "why?"
I dream for things that never were and ask "why not?"

Author unknown

TABLE OF CONTENTS

LIST OF FIGURES

CHAPTER 1: INTRODUCTION

CHAPTER 2: LOW-FLOW SOLAR DOMESTIC HOT WATER SYSTEMS

CHAPTER 3: COLLECTOR PERFORMANCE

CHAPTER 4: PV DRIVEN PUMP

CHAPTER 5: HEAT EXCHANGER ANALYSIS

CHAPTER 6: OVERALL SYSTEM PERFORMANCE

LIST OF TABLES

CHAPTER 1: INTRODUCTION

CHAPTER 5: HEAT EXCHANGER ANALYSIS

CHAPTER 6: OVERALL SYSTEM PERFORMANCE

NOMENCLATURE

a	thermal voltage	V
A_c	collector area	m^2
C_b	contact resistance	W/m.K
Cp	specific heat	J/kg.K
D	nominal pipe diameter	m
D_i	inner diameter of tube	m
D_o	outer diameter	m
f	friction factor	
F'	collector efficiency factor	
F_R	collector heat removal factor	
g	gravitational acceleration	m/s^2
G_T	solar radiation	W/m^2
h	head	m
h_{fi}	internal heat transfer coefficient	W/m^2K
h_i	heat transfer coefficient of inner fluid	$W/m^2.K$
h_o	heat transfer coefficient of outer fluid	$W/m^2.K$
I	current	A
I_D	diode current	A
I_L	light current	A
I_{mp}	maximum power point current	A
I_o	dark current	A
I_{sc}	short circuit current	A
I_{sh}	shunt resistance current	A
k	conductivity	W/m.K

K	minor loss coefficient	
L	length	m
$\dot{m}$	flow rate	kg/s
N	number of tubes in parallel in a serpentine collector	
N_G	number of glass covers	
N_s	number of cells in series in a module	
NTU	number of transfer units	
Nu	Nusselt number	
P	power	W
P	pressure drop	Pa
Pr	Prandtl number	
Q	flow	gpm
$Q_{auxiliary}$	auxiliary heat	W
Q_{hx}	heat exchanger heat transfer	W
Q_{load}	load	W
Q_u	solar collector useful energy	W
R	resistance	m.K/W
Re	Reynolds number	
R_s	series resistance	Ω
R_{sh}	shunt resistance	Ω
S_L	longitudinal pitch of tube bank	m
S_T	transverse pitch of tube bank	m
SF	solar fraction	
T_a	ambient temperature	K
T_b	temperature at the base of the plate	K
T_c	cell temperature	K
T_{ci}	inlet fluid temperature of cold fluid	K
T_{hi}	inlet temperature of hot fluid	K

T_i	temperature of collector inlet fluid	K
T_o	fluid outlet temperature	K
T_{pm}	plate mean temperature	K
U_{back}	collector back loss coefficient	W/m^2.K
U_{edge}	collector edge loss coefficient	W/m^2.K
U_L	overall collector loss coefficient	W/m^2.K
U_{top}	collector top loss coefficient	W/m^2.K
$\bar{v}$	velocity	m/s
V	voltage	V
V_{mp}	maximum power point voltage	V
V_{oc}	open circuit voltage	V
W	tube spacing	m

Symbols

δ	absorber plate thickness	m
β	collector tilt	degrees
ρ	density	kg/m^3
ε	heat exchanger effectiveness	
ε	material bandgap energy	eV
$(\tau\ \alpha\ )_{av}$	average transmission-absorption product	
$\varepsilon_{\ g}$	glass emittance	
$\eta_{\ i}$	collector efficiency	
$\mu_{\ I,sc}$	temperature coefficient for short circuit current	A/K
$\varepsilon_{\ p}$	plate emittance	
$\mu_{\ V,oc}$	temperature coefficient for open circuit voltage	V/K

CHAPTER 1: INTRODUCTION

Increasing environmental concerns and escalating conventional energy supply costs are creating a resurgence of interest in solar energy (CANMET, 1993). The changing infrastructure of utilities in the United States has provided an opportunity for new initiatives in Solar Domestic Hot Water (SDHW) Systems. In particular, the opportunity exists for utilities to market SDHW systems to customers with both customer and utility cost savings.

A significant area of interest is the development of low-flow solar domestic hot water systems. Previous work indicates that the total flow volume through the collector for an average day should be matched to the volume supplied to the load by solar for an average day for direct SDHW systems (IEA, 1996).

Low-flow systems are capable of reducing equipment and installation costs which together account for approximately two-thirds of the total SDHW system cost. Low-flow systems allow equipment to be considerably sized down; piping and pumps are smaller. Cost advantages are in terms of decreased material costs, less parasitic pumping power required from the utility and reduced costs with installing lightweight systems. The thermodynamic advantage of low-flow systems is increased tank stratification, which leads to improved system performance.

In many climates, freeze protection is required in the form of a glycol-water heat exchanger. Low-flow systems influence the heat exchanger performance. The flow rates required on either side of the heat exchanger need to be determined in order to optimize system performance.

Low-flow solar domestic hot water systems also offer a new area of investigation: PV pumping. The lower pumping power now required by low-flow systems can be met with a PV pump. The PV driven pump offers many advantages in terms of better control strategies and no need for an auxiliary power source.

1.1 Water Heating Costs

Residential water heating accounts for approximately 18 % of the annual energy consumption in the residential sector of the United States (DOE, 1997). The residential sector energy use is shown in Figure 1.1.

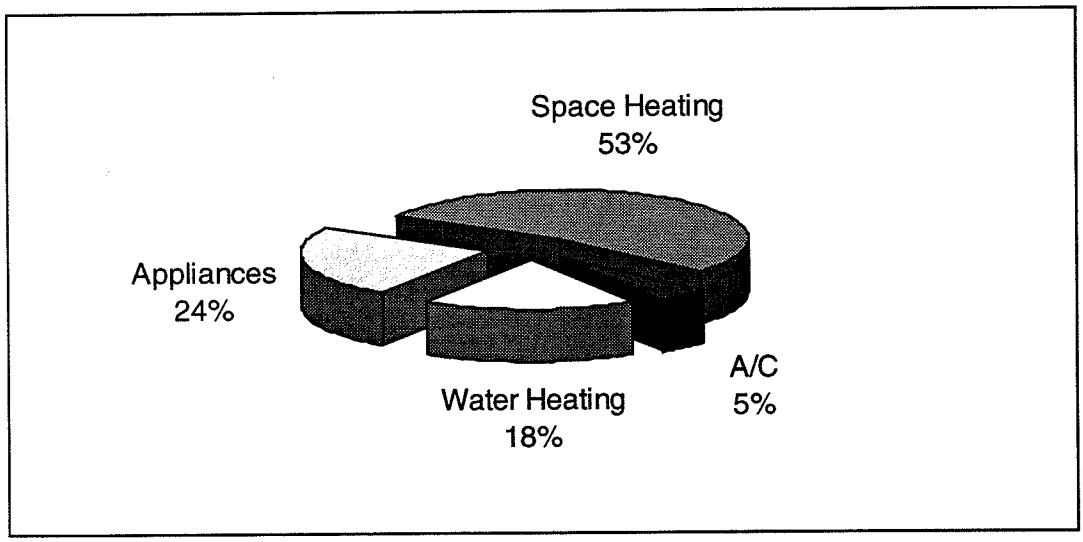

Figure 1.1 Residential sector energy use

Most utilities are summer peaking, meaning that the highest demand is due to cooling loads on the hottest sunniest days. Water needs are generally insensitive to climatic changes rendering solar domestic hot water heating in a good position to alleviate utility energy demands.

Currently, low natural gas prices result in natural gas being the fuel of choice to meet the future demand for electricity. It will be difficult for solar energy to be competitive in areas where natural gas is available. However, there are many regions where natural gas is not accessible.

Solar water heating can be a viable and competitive alternative. The costs of operating and installing different types of water heaters over a life cycle of thirteen years (the average lifetime of a water heater) is presented in Table 1.1. These data are based on the following 1995 fuel costs: $0.52/therm for gas and $0.07kWh for electricity.

Fuel Type	*estimated purchase price installed*	*estimated yearly operating costs*	*estimated life cycle cost, 13 years of operation*
*Gas high-efficiency**	$470	$128	$2,134
*40-gallon gas low efficiency**	$435	$144	$2,307
*Gas side vent**	$850	$134	$2,592
Electric heat pump*	$2000	$123	$3,599
*Electric high-efficiency**	$580	$331	$4,883
*50-gallon electric low efficiency**	$475	$349	$5,012
Solar system #	$2560	$10	$2,690

*Madison Gas and Electric, 1995 #International Energy Agency, 1996.

Table 1.1 Water Heater Life Cycle Costs

The other costs of gas and electricity are often overlooked. Gas and electricity are the culprits producing air pollutants including sulfur dioxide, nitrogen oxides, particulates and heavy metals which impact human health, flora and fauna, building materials, and social assets like recreation and visibility. Greenhouse gases including carbon dioxide, methane, and chlorofluorocarbons are suspected of contributing to global climate change and pose potential impacts on agriculture and human health. Water use and water quality are affected by electricity production, principally through thermal pollution or hydroelectric projects that affect aquatic populations. Land use is also affected by power plant sites and by waste disposal including solid, liquid and nuclear wastes (DOE, 1995).

1.2 SDHW Barriers

There are a number of barriers that have prevented the widespread adoption of solar water heaters by both utilities and homeowners in the past. These have included high capital costs, a reputation for poor system reliability, an inadequate system infrastructure and limited public knowledge of the gains and benefits of current technology (CANMET, 1993).

With deregulation and new competition, utilities are seeking innovative new products and services that will add value and produce customer loyalty. Utilities can experience demand reduction from solar water heating systems during peak times, typically morning and evenings when hot water draws tend to be the greatest. The energy reduction eliminates the need for larger power plant generating capacities and pollution from power plants is reduced as loads decrease. Many electricity-providing utilities are losing customers who are switching to cheaper gas; solar hot water heating may provide a means of retaining customers.

Many utilities are now employing Energy Service Companies (ESCOs). The concept presents the possibility of converting solar water heating from a subsidized Demand Side Management program to a profitable business. The ESCO is typically responsible for the installation, service and maintenance of the solar hot water system. In return for contributing to an increased market size, the ESCO receives a portion of performance savings from the utility. The Utility on the other hand receives a monthly service fee from the homeowner in return for the services the ESCO provides. The homeowner experiences

no first costs and is assured reliability and maintenance of the system. The ESCO concept is demonstrated in Figure 1.2 (Enstar, 1996).

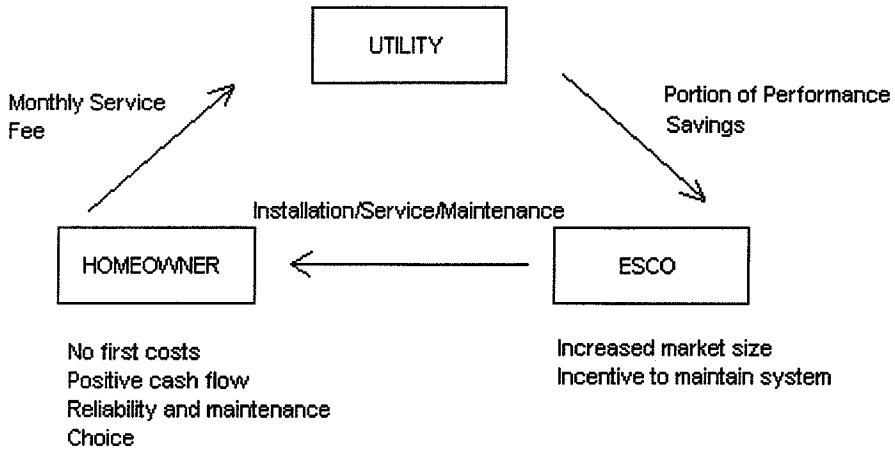

Figure 1.2 Schematic of the ESCO concept

This end-use pricing, which involves the sale of solar heated water itself, rather than the sale or lease of equipment that makes it, is believed to increase market penetration. The increased demand will have a positive effect on the economics of solar water heating (Lyons and Comer, 1997).

1.3 Solar Domestic Hot Water Systems

The primary components in a solar domestic hot water system are a solar collector, a tank, a pump and a controller. The function of the solar collector is to absorb solar radiation by means of an absorber surface, which is usually a black copper plate, and convert it into thermal energy. The thermal energy is then conducted to a flowing fluid by means of

copper tubes welded to the absorber surface. The collector is protected from convective losses with a glass cover that is transparent to incoming long-wave radiation, but prohibits short wave radiation leaving the collector. Insulating material is usually placed along the sides and back of the collector. The tank is the storage media for the heated water. It is common to use retrofitted conventional gas water-heater tanks. A pump is normally controlled by a differential temperature-sensing controller that turns on the pump when the collector outlet temperature is greater than the temperature in the bottom of the tank. Auxiliary heat is usually added by means of a heating element inside the tank or as an external 'zip' heater.

The components above form a direct solar domestic hot water system such as the one shown in Figure 1.3.

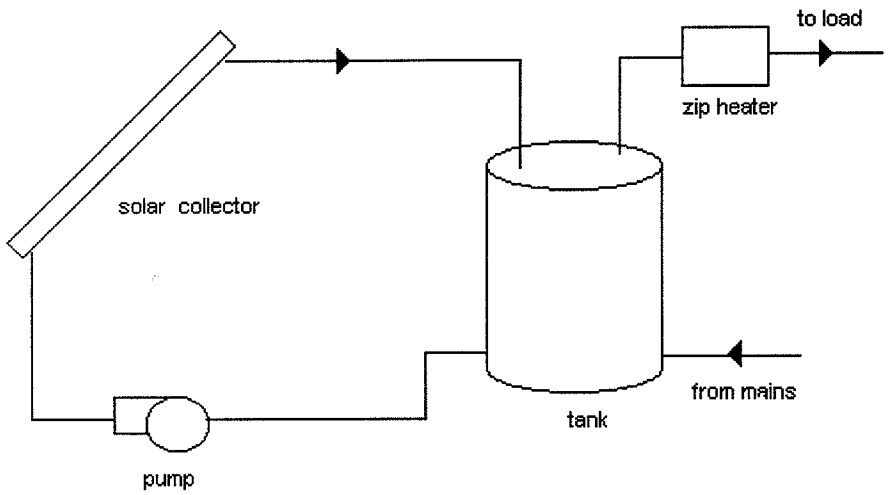

Figure 1.3 Direct solar domestic hot water system (not to scale)

Some form of freeze protection is required in many climates. One method of freeze protection is to use a heat exchanger where antifreeze is circulated in the collector-side loop and water in the tank-side loop. An example of such an indirect solar domestic hot water system is shown in Figure 1.4.

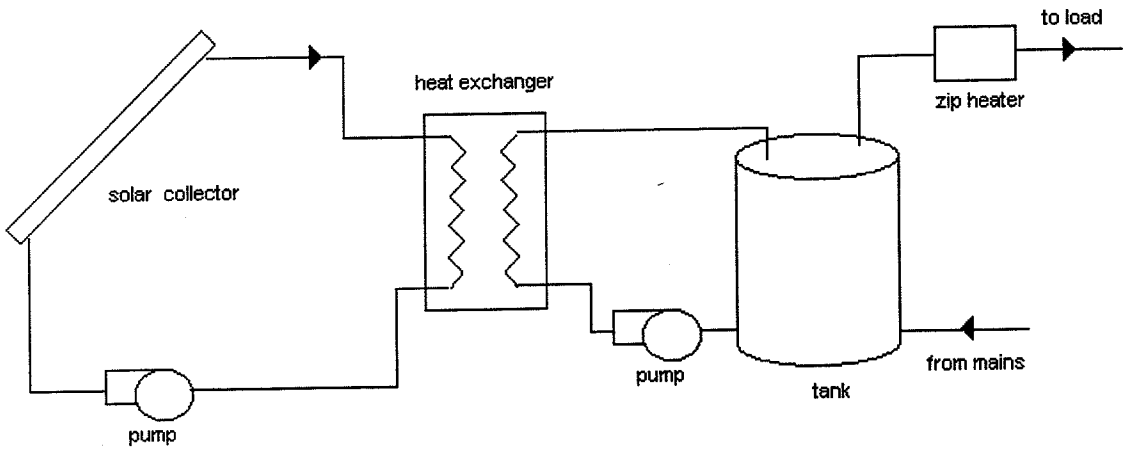

Figure 1.4 Indirect solar domestic hot water system (not to scale)

A means to easily assess the performance of a system is to determine the solar fraction, given by equation 1.1.

$$SF = 1 - \frac{Q_{auxiliary}}{Q_{load}} \qquad (1.1)$$

where $Q_{auxiliary}$ is the auxiliary heat requirement needed to meet the load, given by Q_{load}. The solar fraction is the proportion of the load that is met by solar energy. The difference between the load energy requirement and the auxiliary energy input is the amount of solar energy gained.

Flow rates through solar systems are usually given per unit area of the collector with units of $kg/s.m^2$.

1.4 Simulating Systems

Simulations provide a means of predicting and optimizing a system. System performance is best analyzed with a simulation package, such as TRNSYS, whilst individual system components can be readily analyzed with analytical solutions, equations and numerical methods.

TRNSYS is a transient system simulation program with a modular structure. The system description is specified in a 'deck' in which the user can specify the system components and how they are connected. The program comes equipped with a library of components commonly found in thermal energy systems, as well as component routines to handle input of weather data and output of simulation results. The advantage of using such a program is that its modularity facilitates the addition of mathematical models, referred to as TYPES. One can easily observe the variation of certain parameters on a system, which would be costly to analyze experimentally.

Meteorological information including horizontal surface radiation, tilted surface radiation, wind speed, and ambient temperature are used as inputs describing the environmental conditions specific to each location. Each component, specified by a TYPE, has its own parameters and input and output variables. The components are readily 'linked' together by

combing the output variables of one component to the input variables of another component.

1.5 Load Profile

Hot water usage profiles used in this research were adapted from WATSIM software by Williams (1996). The 8760 hourly water draw profiles were based on the standard water draw specification file provided in the WATSIM program. The 'neutral' household of four draw profile has been chosen. The neutral household of four's water draw lies between water draws of conservative and profligate households. The average daily hot water draw is about 77.2 gallons per day (12.2 kg/hr).

1.6 Thesis Objective

Residential hot water use represents a large proportion of residential energy use. The residential energy use accounts for approximately one third of the total energy use. Utilities can use end-use pricing to target solar domestic hot water heating. This offers many benefits in terms of increased market share and reduced demand at the generation level in an increasingly competitive environment. The development of low-flow solar domestic hot water systems does not only provide a cost-effective alternative in hot water systems, but can also reduce emissions and demand at the generation level. This thesis demonstrates some strategies in designing an optimal low-flow system.

CHAPTER 2: LOW-FLOW SOLAR DOMESTIC HOT WATER SYSTEMS

The conventional strategy in designing solar domestic hot water systems has been to maximize the solar collector heat removal factor (and the heat exchanger energy transfer coefficient for indirect systems) while attempting to minimize parasitic power. The Hottel-Whillier equation (Duffie and Beckman, 1991) given in equation 2.1 defines the efficiency for a solar collector in terms of the collector heat removal factor F_R, given in equation 2.2.

$$\eta_i = \frac{F_R[G_T(\tau\alpha)_{av} - U_L(T_i - T_a)]}{G_T} \qquad (2.1)$$

$$F_R = \frac{\dot{m}C_p}{A_c U_L}\left[1 - exp\left(-\frac{A_c U_L F'}{\dot{m}C_p}\right)\right] \qquad (2.2)$$

where

G_T = the solar radiation (W/m^2)

$(\tau\alpha)_{av}$ = the average transmission-absorption product given by the cover and absorber configuration

U_L = the collector loss coefficient (W/m^2K)

T_I = the temperature of the collector inlet fluid (K)

T_a = the ambient temperature (K).

In Equation 2.2,

$\dot{m}$ = the collector fluid flow rate (kg/s)

C_p = the collector fluid specific heat (J/kg.K)

A_c = the collector area (m^2)

F' = the collector efficiency factor

More details on the collector heat removal factor will be given in chapter 3.

Observing equation 2.1, it can be seen that increasing the mass flow rate will indeed increase the collector heat removal factor, but this does not necessarily mean the collector efficiency given by equation 2.2 will increase. As the collector flow rate is increased the collector inlet temperature may be higher due to tank mixing and therefore the losses will be higher (Van Koppen et al. 1979).

An alternative to maximizing the collector heat removal factor is to increase tank stratification. Increased stratification causes the temperature gradient along the height of the tank to be larger meaning the temperature at the top of the tank is much greater than the temperature at the bottom of the tank.

In the past, the average flow rates have been high and resulted in an average daily collector flow rate that is three or more times greater than the average daily hot water draw (Fanney and Klein, 1988). The tank is usually sized to the average daily load, thus storage fluid is recirculated through the collector loop three or more times a day.

Naturally, the tank will stratify when there is no circulation. When there is solar energy collection, there will be circulation and the tank will become mixed. It has been confirmed experimentally that at lower flow rates higher stratification exists (Fanney and Klein, 1988). The optimum flow rate is found to be approximately 10 to 33% of that typically used in forced circulation direct systems (Fanney and Klein, 1988). Wuestling, Klein and Duffie (1985) found the optimum performance for a system without a heat exchanger is achieved when the monthly average daily total water circulated through the collector array is approximately equal to the average daily total load.

Fanney and Klein (1988) performed side by side tests on identical SDHW systems. One system had a 0.020 kg/s.m^2 collector array flow rate, which was in accordance with manufacturer's recommendations. The other system was based on observations of tank stratification given by Van Koppen et al (1979) and Wuestling (1983) with a 0.0033 kg/s.m^2 collector array flow rate. The system with the lower collector flow rate resulted in an 8% increase in solar energy delivered to the storage tank and a 10% decrease in auxiliary energy consumption.

2.1 Simulating Tank Stratification

Stratified tank models fall into two main categories, the multi-node approach and the plug flow approach. The multi-node approach involves dividing the tank into N sections or nodes and performing an energy balance for each node. The plug flow approach assumes

that segments of liquid at various temperatures move through the tank in plug flow; the model keeps track of the size, temperature and position of the segments.

TRNSYS Type 60 simulates a stratified fluid storage tank using the multi-node approach. The tank is assumed to contain equal volume segments or nodes (however, there is an option to use unequal size nodes). Using one node simulates a fully mixed tank. Increasing the number of nodes decreases internal mixing and a higher degree of thermal stratification is achieved. It is important to determine the sensitivity of the number of nodes chosen. Up to 100 nodes may be chosen, but increasing the number of nodes substantially increases the computing time. It is necessary to find the minimum number of nodes to reasonably model the effects of stratification. Figures 2.1 and 2.2 show the effects of the solar fraction for the number of nodes for two locations, Madison, Wisconsin and Miami, Florida. The flow rate is given per collector area, rendering the plots independent of collector area.

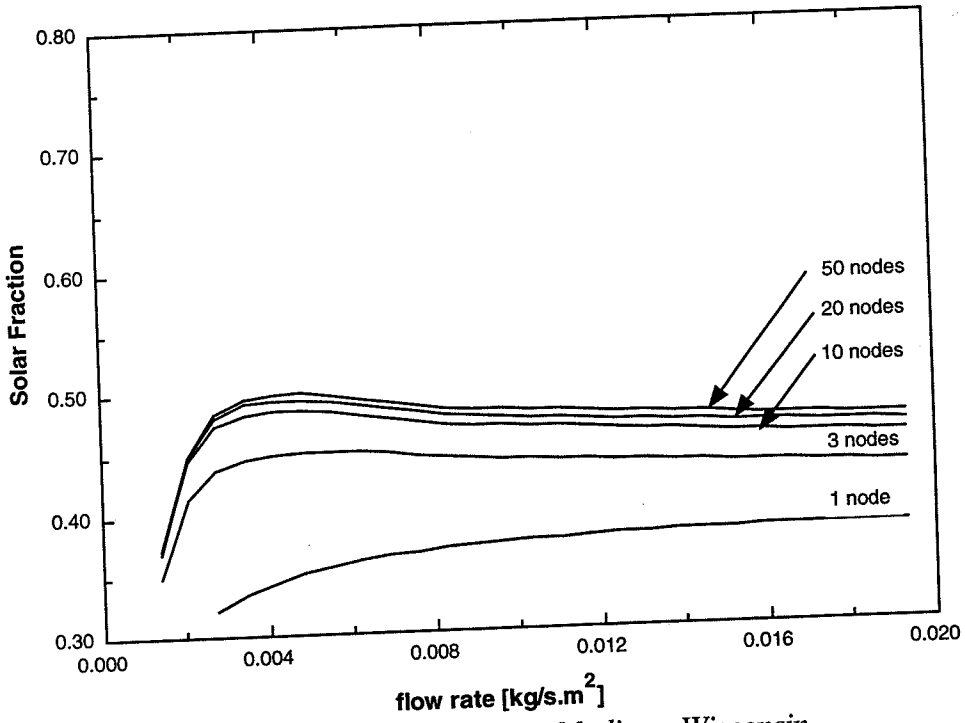

Figure 2.1 Sensitivity to the number of nodes for Madison, Wisconsin

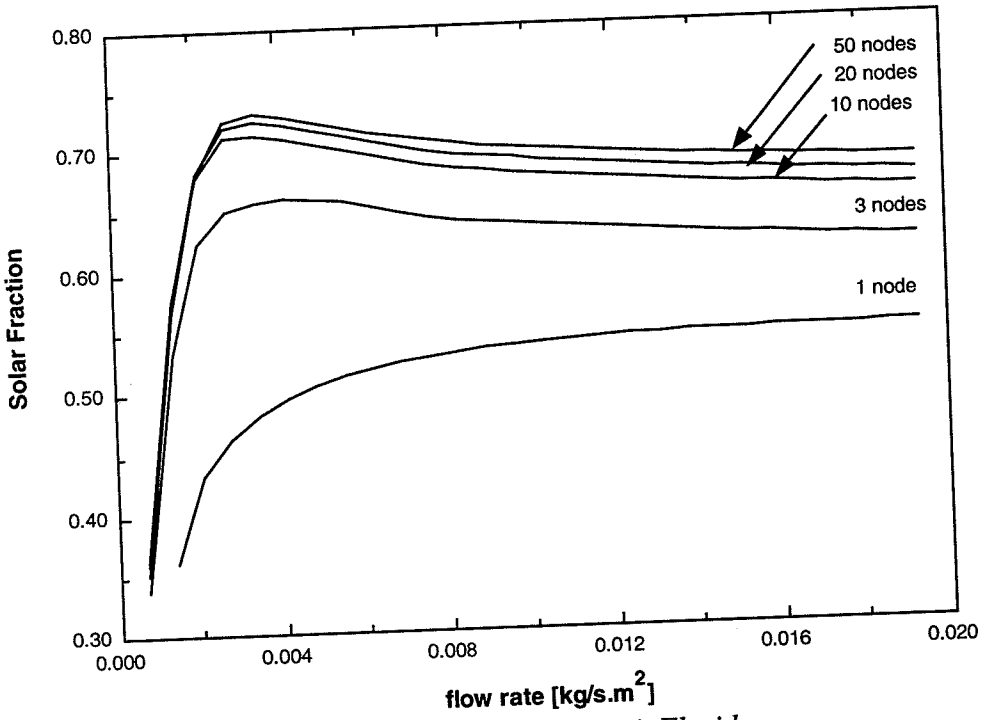

Figure 2.2 Sensitivity to the number of nodes for Miami, Florida.

Increasing the nodes and hence the degree of stratification increases the solar fraction. At low collector flow, the simulation results obtained for maximum stratification agree well with the experimental results (Fanney and Klein, 1988). It can be seen that the difference between 20 and 50 nodes is very small. Since 50 nodes require too much computing time, 20 nodes will be used in this research for all simulations.

The optimum collector flow can be shown independent of location and the time of the year by comparing Figure 2.1 and Figure 2.2. The average daily load draw is 0.0035 kg/s.m^2. The average daily load was found by averaging the hourly loads of the load profile over the year for the hours of sunshine, approximately 8 hours each day. This value is close to the optimum flow rate for both locations.

Another important factor is the tank storage size. An undersized tank will force recirculation, whereas an increased tank size will incur additional material costs and increase convection losses to the environment through the increased surface area. Figure 2.3 demonstrates the effect of the variation of tank volume on solar fraction. The tank losses have been assumed negligible; if they were included, increasing the volume would increase the losses to the environment and therefore the solar fraction would decrease.

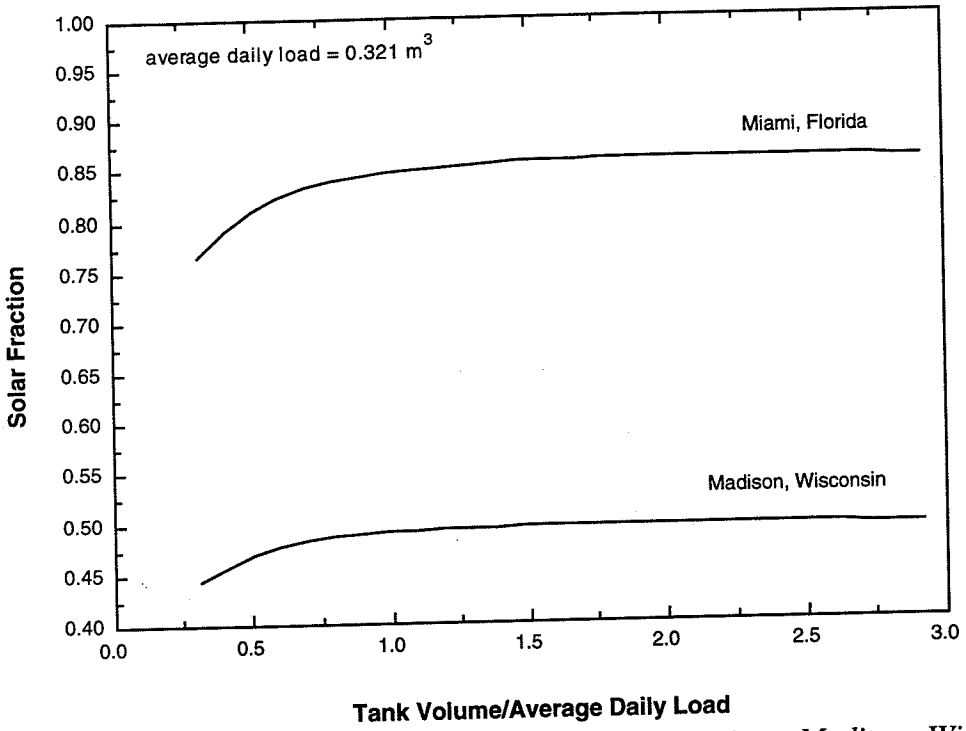

Figure 2.3 Effects of variation of tank volume for two locations, Madison, Wisconsin and Miami, Florida.

Figure 2.3 demonstrates the optimal tank volume is independent of location. A tank volume of about 0.4 m^3 is the optimal for the given load. Decreasing the storage volume will not allow the tank to fully stratify. Further increasing the tank volume will have little effect on the solar fraction until a volume is reached were convective losses to the environment are so large that the solar fraction is reduced. A tank volume of 0.4 m^3 will be used for all simulations in this research.

2.2 Conclusions

Reducing the flow rate can significantly improve solar gains as tank stratification is improved. However, the storage tank volume, daily load, and load distribution have a direct

effect on the optimum fixed flow rate because they directly contribute to the amount of tank recirculation. Careful selection of tank size and number of nodes need to be considered. For the given load profile 20 nodes model maximum tank stratification without drastically increasing the computing time. A tank volume of about 0.4 m^3 is about the optimal size in terms of material savings and maximum stratification.

CHAPTER 3: COLLECTOR PERFORMANCE

Solar collectors function as heat exchangers; they receive solar radiant energy and transfer it to the flowing fluid. The useful energy gain of the collector determines the temperature rise of the flowing fluid in terms of design and operational variables.

Equation 3.1 (Duffie and Beckman, 1991) expresses the useful energy gain of a solar collector in the following form.

$$Q_u = A_c F_R [G_T(\tau\alpha) - U_L(T_i - T_a)] \qquad (3.1)$$

where F_R is the collector heat removal factor, $(\tau\alpha)$ is the transmittance absorptance product, U_L (W/m^2.K) is the overall loss coefficient, A_c (m^2) is the collector area, G_T (W/m^2) is the incident radiation and T_i (K) and T_a (K) are the fluid inlet and ambient temperatures respectively.

The collector heat removal factor, F_R, is the ratio of actual useful energy gain of a collector to the useful gain if the whole collector surface were at the fluid inlet temperature, equation 3.2.

$$F_R = \frac{\dot{m}C_p(T_o - T_i)}{A_c[G_T(\tau\alpha) - U_L(T_i - T_a)]} \qquad (3.2)$$

In equation 3.2, $\dot{m}$ is the mass flow rate, C_p (J/kg.K) is the specific heat of the collector fluid and T_o (K) is the fluid outlet temperature. F_R is analogous to the heat exchanger effectiveness.

Radiation passes through the cover system and is incident on the absorber plate. Some radiation is reflected back to the cover system, which again may be partly absorbed and reflected by the plate. The transmittance-absorptance, ($\tau\alpha$), represents the overall effect of a cover-absorber combination rather than the product of the two properties.

Energy is transferred to the surroundings from the top, sides and bottom of the collector. This energy transfer rate is given in terms of the overall loss coefficient, U_L (W/m^2.K). A relation for U_L (Duffie and Beckman, 1991) is given in equation 3.3.

$$U_L = U_{top} + U_{edge} + U_{back} \qquad (3.3)$$

where an approximate relation for U_{top} (W/m^2.K) given by Klein (1975) is shown in equation 3.4, and U_{edge} (W/m^2.K) and U_{back} (W/m^2.K) are the losses from the edge and back of the collector respectively.

$$U_{top} = \frac{1}{\dfrac{N_G}{\dfrac{C}{T_{pm}}\left[\dfrac{(T_{pm}-T_a)}{N_G+f}\right]^{0.33}+\dfrac{1}{h_w}}} + \frac{\sigma\left(T_{pm}^{\,2}+T_a^{\,2}\right)\left(T_{pm}+T_a\right)}{\dfrac{1}{\varepsilon_p+0.05N_G\left(1-\varepsilon_p\right)}+\dfrac{2N_G+f-1}{\varepsilon_g}-N_G} \qquad (3.4)$$

where

N_G = number of glass covers

$f = \left(1+0.04h_w+0.0005h_w^{\,2}\right)\left(1+0.091N_G\right)$

$C = 365.9\left(1-0.00883\beta+0.0001298\beta^2\right)$

β =collector tilt (degrees)

ε_g = emittance of glass

ε_p = emittance of plate

T_a = ambient temperature (K)

T_{pm} = mean plate temperature (K)

$$T_{pm} = T_i + \frac{Q_u/A_c}{F_R U_L}\left(1-F_R\right)$$

h_w = wind heat transfer coefficient (W/m^2.C)

It can readily be determined from equation 3.2 that the heat removal factor is heavily dependent on flow rate at low flow rate values. At high flow rates, F_R becomes independent of flow rate. Reducing the collector flow rate is detrimental to the collector

heat removal factor. It is pertinent to find the configuration and geometry that is most appropriate in terms of pumping power and collector efficiency (defined in equation 2.1). In this analysis the popular header-riser flat-plate collector and the serpentine flat-plate collector will be analyzed and compared.

3.1 Header/Riser Flat-plate Collector

The header-riser flat-plate collector consists of two horizontal headers and a series of parallel, vertical risers as shown in Figure 3.1.

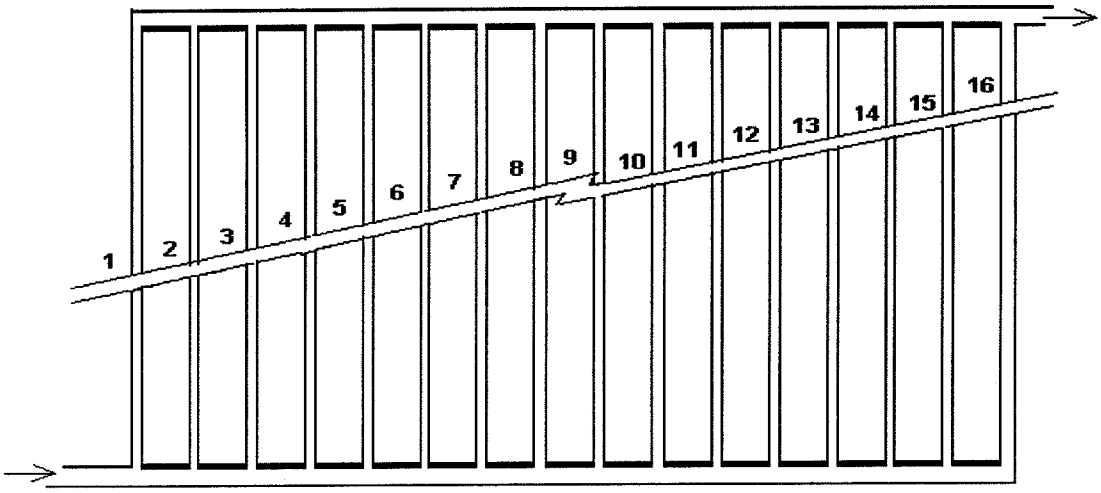

Figure 3.1 Conventional flat-plate collector

The analysis of the header-riser flat-plate collector makes many assumptions (Duffie and Beckman, 1991). These include the following:

- Headers can be neglected since they cover a small area.
- The headers provide uniform flow to tubes.
- Heat flow through the cover is one-dimensional.

- Temperature gradients around the tubes can be neglected.
- The temperature gradients in the direction of flow and between the tubes can be treated independently.

One primary concern is how these assumptions hold for low flow. It will be shown that the flat-plate collector does not have equal flow rates through the risers. The pressure drops from the bottom to the top of the risers are greater at the ends than the center of the collector. This leads to higher flows in the end risers and lower flows in the center risers.

3.1.1 Pressure Distribution

Fanney and Klein (1985) experimentally found that for low flow rates (less than 0.0025 kg/sm^2 compared to the manufacturer's recommended flow rate of 0.020 kg/sm^2) there was an imbalance in the flow through a collector array. The flow was not divided equally between three individual collectors. The imbalanced flow condition was detected by monitoring thermocouples attached to the absorber plates. However, the individual collectors were not examined for flow imbalances.

Dunkle and Davey (1970) state that the efficiency of large solar water heating installations is reduced if flow is not uniformly distributed through the absorber. They found that flow is "short circuited" through the first and last few risers leaving a dead zone of low flow near the center of the bank. In these regions of low flow rates, there are higher heat losses and lower thermal efficiency due to the higher temperatures in these areas. Temperature

distribution is the worst at the highest flow rate. Dunkle and Davey also state that free convection forces counterbalance the "short circuit" effect when the absorbers are inclined.

A model of the pressure distribution was developed by using mass balances and momentum balances at each node. A node is defined at each bend or pipe intersection of the collector. For each node, the mass flowing in and out was determined and the pressure was found from the head loss and the preceding node pressure. Figure 3.2 represents a simplified collector with two risers.

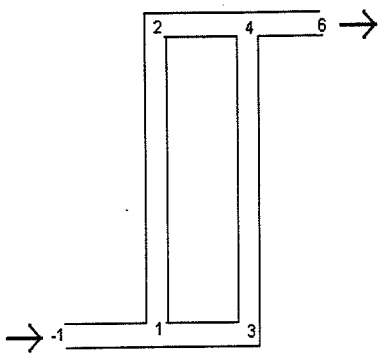

Figure 3.2 Simplified collector with two risers

For the above Figure, the momentum balance is represented in equations 3.5.

$$
\begin{aligned}
P_{-1} &= P_1 + \left[\rho f \frac{L\vec{v}^2}{2D_i}\right]_{-1,1} \\
P_1 &= P_2 + \left[\rho f \frac{L\vec{v}^2}{2D_i}\right]_{1,2} \\
P_1 &= P_3 + \left[\rho f \frac{L\vec{v}^2}{2D_i}\right]_{1,3} \\
P_2 &= P_4 + \left[\rho f \frac{L\vec{v}^2}{2D_i}\right]_{2,4} \\
P_3 &= P_4 + \left[\rho f \frac{L\vec{v}^2}{2D_i}\right]_{3,4} \\
P_4 &= P_6 + \left[\rho f \frac{L\vec{v}^2}{2D_i}\right]_{4,6}
\end{aligned}
\qquad (3.5)
$$

In equations 3.5, ρ (kg/m^3) is density, f is the friction factor evaluated from the Moody Chart, L (m) is the length of each header or riser segment, $\vec{v}$ (m/s) is the velocity, which is found from the mass flow rate, and D_i (m) is the inner diameter of the tube. The mass balance is given in equations 3.6, where $\dot{m}$ (kg/s) is the mass flow rate through each segment.

$$
\begin{aligned}
\dot{m}_{-1,1} &= \dot{m}_{1,3} + \dot{m}_{1,2} \\
\dot{m}_{4,6} &= \dot{m}_{3,4} + \dot{m}_{2,4} \\
\dot{m}_{1,2} &= \dot{m}_{2,4} \\
\dot{m}_{1,3} &= \dot{m}_{3,4}
\end{aligned}
\qquad (3.6)
$$

Gerhart and Gross (1985) give loss coefficients for Tee joints that were used at the header and riser joints. The collector is arranged in such a way that the headers form the line flow of the tee joint and the risers form the branch flow. The loss coefficients for the branch and

line flow used were estimated from the data given by Gerhart and Gross. Loss coefficients are used to find an equivalent length that is added to length of the header or riser when calculating the pressure loss. The equivalent length is found using equation 3.7, where K is the loss coefficient, D (m) is the pipe diameter and f is the friction factor.

$$L_{equivalent} = \frac{KD}{f} \tag{3.7}$$

The technical data for the Alta Energy Liquid Flat-plate Collector Model ATL 100-1 recommends flow rates of 0.75 gpm to 1.5 gpm that result in pressure drops of 0.01 to 0.04 psi. The Alta Energy collector has a net area of 22.1 ft^2. The risers comprise of 3/8-inch copper tubes spaced 2 inches apart from the centers and the headers are one inch in diameter. The pressure drops calculated for the Alta Energy collector geometry agree with the specified pressure drops given by the manufacturer as shown in Figure 3.3.

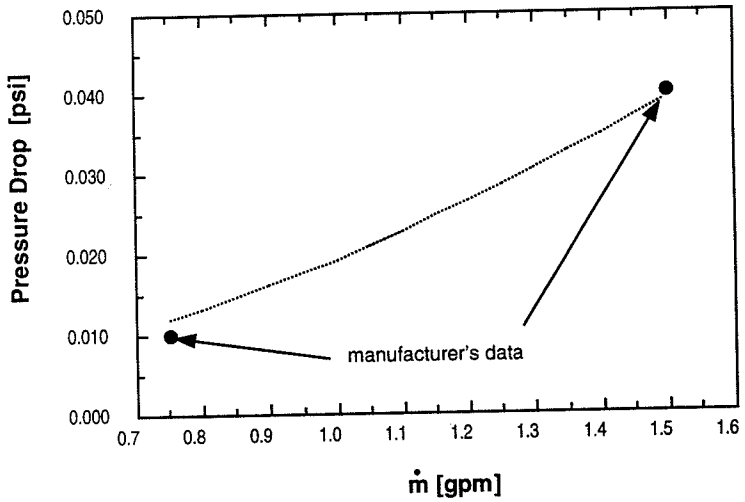

Figure 3.3 Flow rates and corresponding pressure drops

Flow through the flat-plate collector becomes more evenly distributed as the flow rate is reduced. Figure 3.4 shows the dimensionless flow rate through the collector, that is, the flow rate through the riser divided by the flow rate entering the collector as a function of riser number. As the mass flow rates increase, the relative flow through the outer risers increases while the relative flow rates in the inner risers decreases.

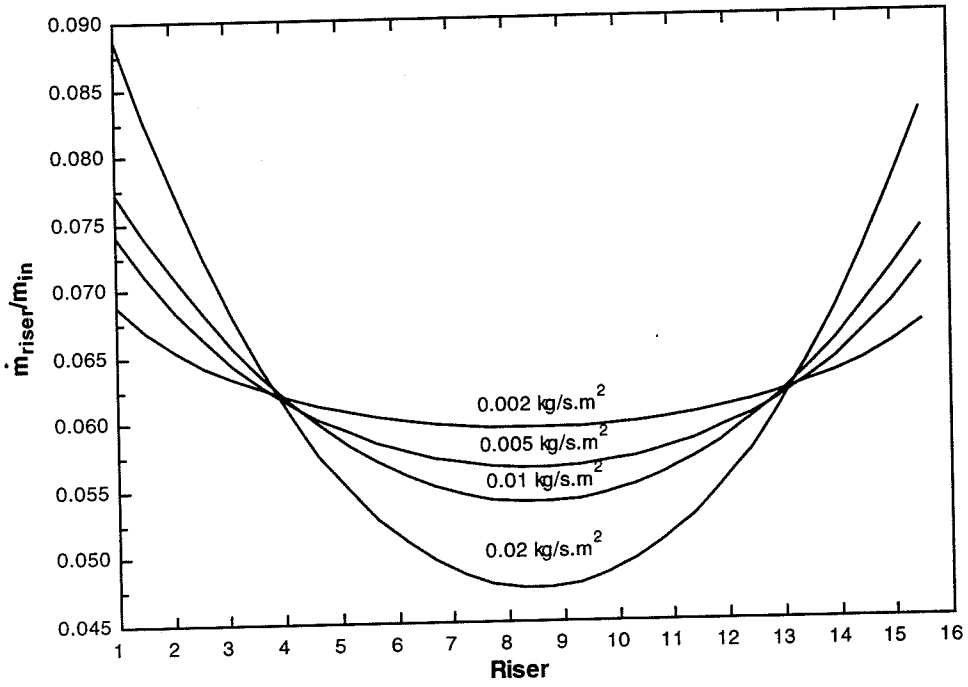

Figure 3.4 Flow distribution through a collector with varying flow rates

The imbalance found by Fanney and Klein is at odds with the above analysis which indicates that flow imbalance should decrease with decreasing flow rate. The reason that Fanney and Klein's results differ may be because they were measuring temperature and not flow.

In order to verify, that the discrepancy was not based on the loss coefficients at the joints, the collector was modeled with varying loss coefficients. The loss coefficients were randomly chosen. The coefficients for the headers vary from 1.45 to 2.7. The loss coefficients for the risers vary from 0.8 to 1.5. It was still found that the low-flow model had the most evenly distributed flow.

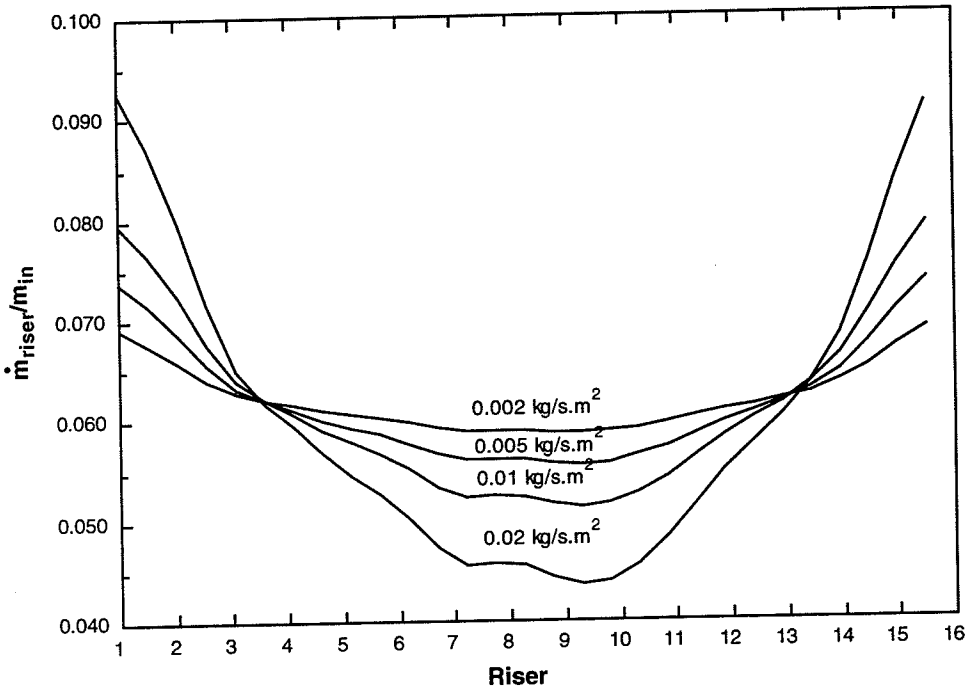

Figure 3.5 Flow distribution for varying the loss coefficients

The pressure drop along the headers for the common situation of water entering the bottom header on one side of the collector and leaving the top header on the other side was also determined. Figure 3.6 demonstrates the dimensionless pressure through the headers.

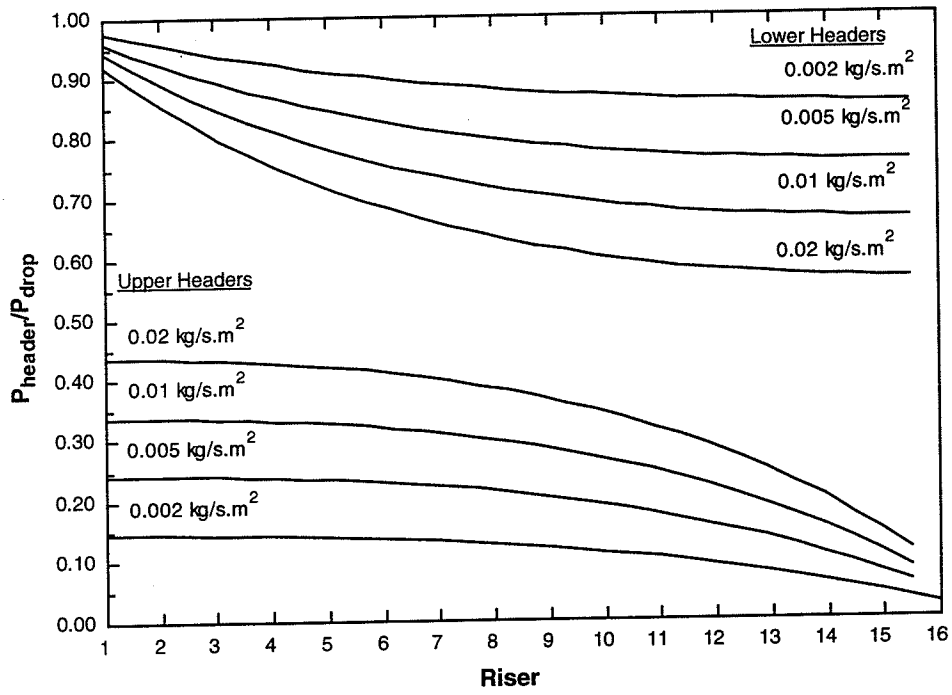

Figure 3.6 Pressure distribution through a collector with varying flow rates

Again, these results are in agreement with Dunkle and for flow distribution through arrays of flat-plate collectors.

Lowering the flow rate has the positive effects of a more even flow distribution and pressure drop across the bank of risers.

3.1.2 Collector Heat Removal Factor

For a header-riser flat-plate collector, the collector heat removal factor can be expressed as shown in equation 3.8 (Duffie and Beckman, 1991).

$$F_R = \frac{\dot{m}C_p}{A_c U_L}\left[1 - exp\left(-\frac{A_c U_L F'}{\dot{m}C_p}\right)\right] \qquad (3.8)$$

where F' is the collector efficiency factor shown in equation 3.9.

$$F' = \frac{1/U_L}{W\left[\frac{1}{U_L[D+(W-D)F]} + \frac{1}{C_b} + \frac{1}{\pi D_i h_{fi}}\right]} \qquad (3.9)$$

In equation 3.9, W (m) represents tube spacing, C_b (W/m.K) is the contact resistance, h_{fi} (W/m^2.K) is the internal fluid heat transfer coefficient and F is the standard fin efficiency, given in equation 3.10.

$$F = \frac{tanh[m(W-D)/2]}{m(W-D)/2} \qquad (3.10)$$

Further details of the standard fin efficiency and the internal fluid heat transfer coefficient will be given in section 3.4.

It can be seen from this equation that increasing the flow rate will indeed increase the heat removal factor. In the past, this has led to the conclusion that higher flow systems will yield better results. However, low flow rates have the advantage of allowing the storage tank to stratify. This means that the temperature gradient along the height of the tank will be high. Hotter fluid will be available to meet the load and colder fluid will circulate through the collector loop. The temperature rise across the collector will be higher due to the lower flow rates. An added advantage is the decreased cost associated with pumping the fluid. Since low-flow systems may give an overall better system performance, the best collector design must be determined. The serpentine collector design is a viable alternative, as the

flow rates are low, the higher-pressure drops through the serpentine collector are of little concern. It has already been shown that for low flow the header-riser flat-plate collector will have an even flow distribution, but the lower flows through each riser may adversely affect the heat transfer coefficients and hence performance.

3.2 Serpentine Flat-plate Collector

Serpentine collectors consist of a flow duct that is bonded to the absorber plate in a serpentine or zigzag fashion. A serpentine collector is shown in Figure 3.7.

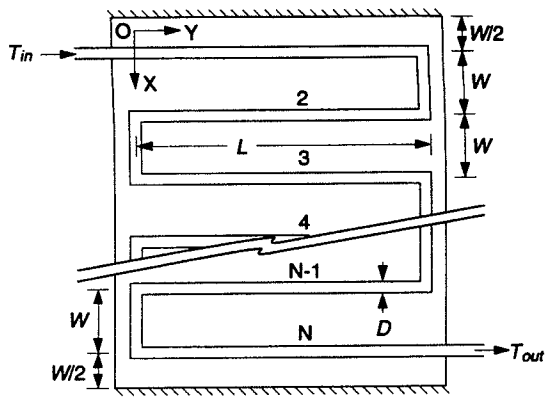

Figure 3.7 Serpentine flat-plate collector

3.2.1 Pressure Distribution

The pressure drop for a serpentine collector is easily calculated from equation 3.11.

$$P = \rho f \frac{L_{total} \vec{v}^2}{2D_i} \qquad (3.11)$$

In equation 3.11, L_{total} (m) is the tube length plus the equivalent length for the losses at the bends. Clearly, the pressure drop increases with increasing flow rate and with total length.

3.2.2 Collector Heat Removal Factor

The heat removal factor for a serpentine collector is much more difficult to determine than for a conventional flat-plate collector. Unlike the analysis for the header-riser flat-plate where the fins between the tubes are assumed adiabatic at the center of the tube spacing, there is heat transfer between the tubes for a serpentine collector.

Abdel-Khalik (1976) analyzed the heat removal for a flat-plate solar collector with a serpentine tube. This analysis produced graphical results to obtain the heat removal factor. Figure 3.8 represents the generalized chart for estimating the heat removal factor, F_R, for flat-plate collectors with serpentines of arbitrary geometry and number of bends. The parameters F_1 and F_2, given in equations 3.12 and 3.13 respectively, are functions of physical design parameters, including plate thickness, conductivity and tube spacing.

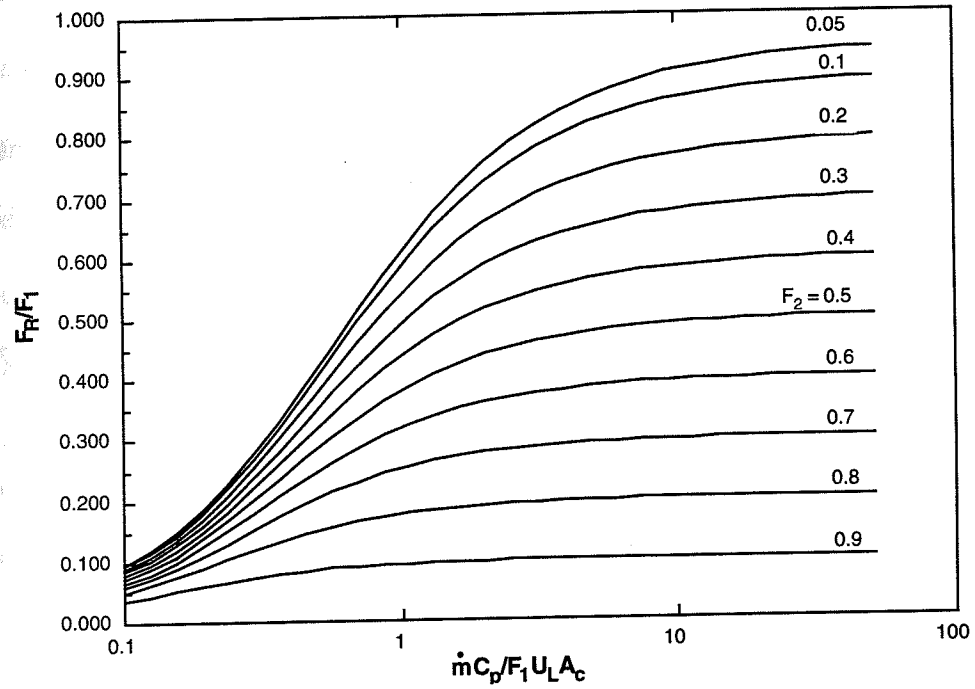

Figure 3.8 Generalized chart for estimating the heat removal factor by Abdel-Khalik

$$F_1 = \frac{N\kappa L}{U_L A_c} \frac{\kappa R(1+\gamma)^2 - 1 - \gamma - \kappa R}{[\kappa R(1+\gamma) - 1]^2 - (\kappa R)^2} \tag{3.12}$$

$$F_2 = \frac{1}{\kappa R(1+\gamma)^2 - 1 - \gamma - \kappa R} \tag{3.13}$$

where

$$\kappa = \frac{k\delta m}{(W-D)\sinh m} \tag{3.14}$$

$$\gamma = -2\cosh m - \frac{DU_L}{\kappa} \tag{3.15}$$

$$m = (W-D)\sqrt{\frac{U_L}{k\delta}} \tag{3.16}$$

In the above equations, D (m) is the outer tube diameter, k (W/m.K) represents the plate conductivity, δ (m) is the plate thickness, R (m.K/W) is the resistance between the tube and the plate and N is the number of turns in the serpentine collector minus one. R is a thermal resistance defined by equation 3.17.

$$R = \frac{1}{C_b} + \frac{1}{\pi D_i h_{fi}} \qquad (3.17)$$

Abdel-Khalik states that the differences in the values of F_R/F_1 for one turn, (N=2) and those obtained numerically for higher values of N are less than 5 %. These differences vanish completely for $\dot{m}c_p / F_1 U_L A_c$ greater than unity. In other words, the graphical results are valid within 5% for all practical situations.

Zhang and Lavan (1985) argue that this is not the case. Zhang and Lavan present an analytical solution to Abdel-Khalik's analysis for N=2 or for the case where the parameter, $\dot{m}c_p / F_1 U_L A_c$ is greater than unity. They also provide analytical solutions for N=3 and N=4, however these are in matrix form and difficult to implement.

Zhang and Lavan state that the heat removal factor, F_R, is generally a maximum at N=1 and is generally a minimum at N=2. As N increases, F_R increases, but at a decreasing rate. For $N \rightarrow \infty$, F_R seems to approach the value for F_R at N=1. As the number of turns increases, the tube length increases for a given area. The surface area exposed to solar radiation increases and F_R increases. When N=1 the serpentine collector acts as a header-riser flat-plate and F_R is the largest since there is no heat transfer between tubes.

Lund (1989) also finds the heat removal factor independently of the methods above. In his analysis, he expresses serpentine performance in terms of an effectiveness-NTU relationship. Lund couples conduction and transport equations that are rendered in non-dimensional form using a shape factor. The shape factor is determined by duct shape and conduction through the duct from the absorber plate. Lund's analysis seems to be most useful for turbulent flow because heat transfer is increased for turbulent flow. In this flow regime, for N=2 the results are consistent with those obtained by Zhang and Lavan.

Chiou and Perera (1986) also analyzed the serpentine collector for any number of turns. The results are presented in awkward matrix forms. They show that the thermal efficiency of the solar collector for a serpentine tube arrangement is less than that for a header-riser configuration for most of the day. During the morning hours and late afternoon, the serpentine collector performs better in terms of the heat removal factor. The flow rate used is 0.0555 kg/s. Chiou and Perera conclude there are two possible reasons for this. First, there is a higher-pressure drop associated with the serpentine collector that may create flow imbalances; therefore, the flow imbalances will cause poor heat transfer. Second, the heat transfer between the fluid and the plate reduces toward the outlet of the serpentine collector. The difference is most likely due to an overall lower collector-plate temperature for the header-riser flat-plate collector and therefore decreased thermal losses.

For practical applications, serpentine collectors have many turns, and therefore it is necessary to calculate F_R with a simple method. The matrix solutions are cumbersome to implement.

3.3 Finite difference technique

A finite difference technique was developed. Abdel-Khalik presents analytical equations for heat flow per unit length entering the base of the tube, given in equations 3.17. In these equations, m is given by equation 3.15 and T_{bi} (K) is the temperature at the base of the plate for the segment i.

$$\begin{aligned} q_i^+ &= \kappa[\theta_{i-1} - \theta_i \cosh m] \quad (2 \le i \le N) \\ q_i^- &= \kappa[\theta_{i+1} - \theta_i \cosh m] \quad (1 \le i \le N-1) \\ q_1^+ &= \kappa\theta_1(1 - \cosh m) \\ q_N^- &= \kappa\theta_N(1 - \cosh m) \end{aligned} \tag{3.18}$$

where

$$\theta_i = T_{bi} - T_a - \frac{G_T}{U_L} \tag{3.19}$$

The useful energy gain to the tubes is given by equations 3.20.

$$q_{useful} = q_i - DU_L\theta_i$$

$$q_{useful} = \frac{(T_{bi} - T_{fi})}{R} \tag{3.20}$$

where the quantity $[-DU_L\theta_i]$ is the energy collected per unit time and per unit length above the tube.

Below is a representation of the finite difference technique. The values of q represent useful energy, given by equations 3.20, transferred to the tube from the upper and lower parts of the absorber plate and γ is an intermediate temperature.

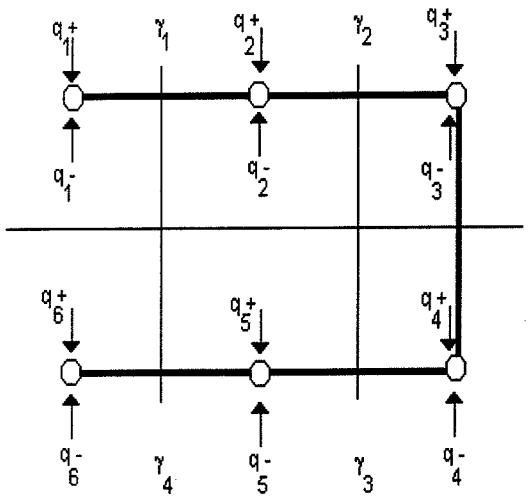

Figure 3.9 Representation of the finite difference technique

The heat transferred to each node is represented in equations 3.21.

$$\begin{aligned}
\dot{m}C_p(\gamma_1 - T_1) &= q_1\frac{\Delta Y}{2} \\
\dot{m}C_p(\gamma_2 - \gamma_1) &= q_2\Delta Y \\
\dot{m}C_p(\gamma_3 - \gamma_2) &= (q_3 + q_4)\Delta Y \\
\dot{m}C_p(\gamma_4 - \gamma_3) &= q_5\Delta Y \\
\dot{m}C_p(T_6 - \gamma_4) &= q_6\frac{\Delta Y}{2}
\end{aligned} \qquad (3.21)$$

where

$$\frac{\gamma_1+\gamma_2}{2}=T_2$$

$$\frac{\gamma_2+\gamma_3}{2}=T_3=T_4$$

$$\frac{\gamma_3+\gamma_4}{2}=T_5$$

Special care was taken in the algorithm to ensure the boundary conditions at each turn were met. The boundary condition in the above example is T_3=T_4.

This finite difference algorithm was implemented in an EES program, appendix C. EES, Engineering Equation Solver (Klein and Alvarado, 1997), is a computer program that solves sets of equations using matrix techniques. The program was set up in order to enable any number of turns and any number of nodes.

The main advantage of this finite difference technique is that no assumptions were made that implied that the technique would only work under certain flow or geometry conditions, such as $\dot{m}c_p / F_1U_LA_c$ being greater than unity.

When using a finite difference technique, the major concern is the grid size. In this case, the concern was ensuring that the number of nodes was sufficient to accurately model the problem. Sensitivity of the results to the number of nodes was determined for N=4 and N=10 ; the results are presented in Figure 3.10.

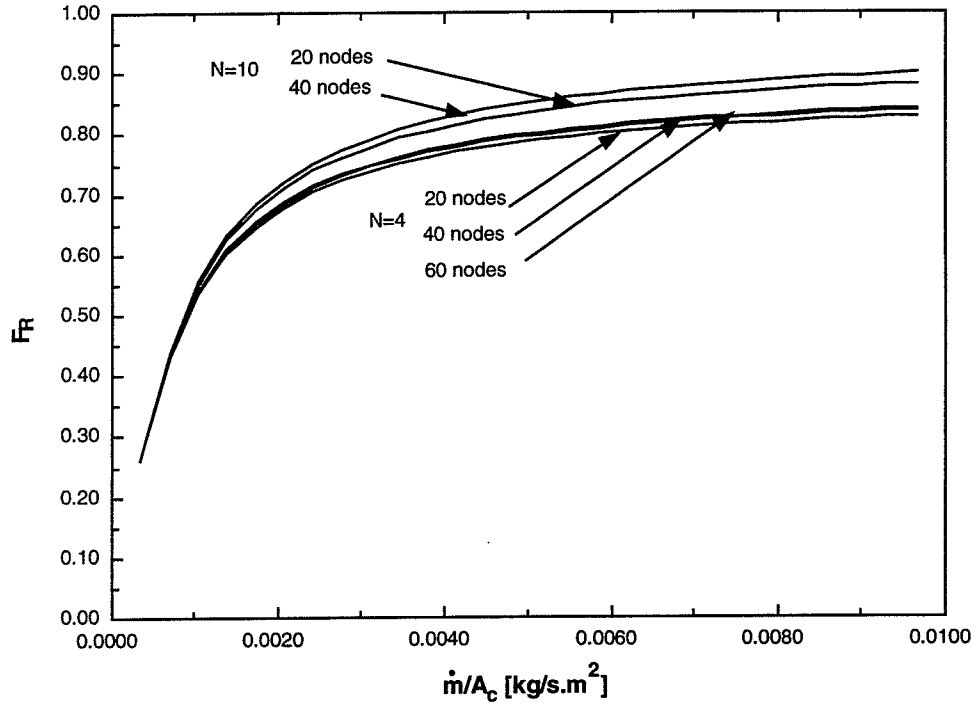

Figure 3.10 Sensitivity to the number of nodes in the finite difference technique.

It can be seen that the finite difference technique is sensitive to the number of nodes. For the *N*=4 serpentine collector, 20, 40 and 60 nodes were used. The sensitivity is more marked for the higher flow rates. Little difference was seen between the 40 and 60 node solution. In the case of the *N*=10 serpentine collector only 20 and 40 nodes were tested. A higher number of nodes was not feasible in terms of computational requirements. Again, the largest discrepancy between the number of nodes was seen at the higher flow rates.

The finite difference technique was compared to the solution given by Abdel-Khalik. Figure 3.11 represents the comparison between the methods. The collector was chosen to have a constant area of one square meter, thus varying the number of turns changed the tube

spacing. Constant values for the fluid heat-transfer-coefficient, h_{fi}, of 1500 W/m^{2}K and heat loss coefficient, U_L of 5 W/m^{2}K were used.

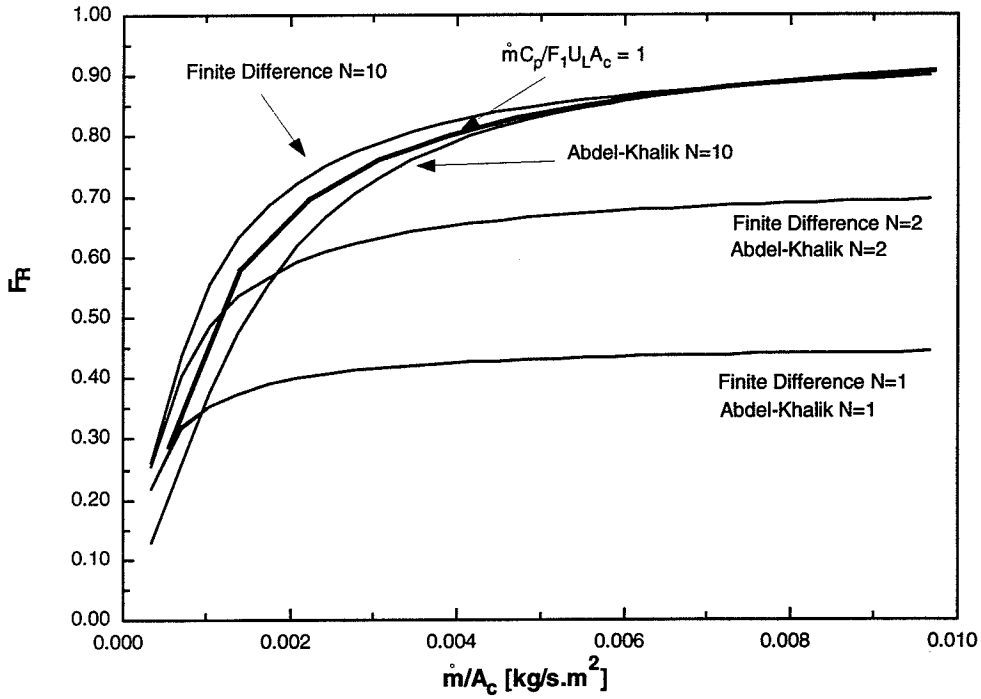

Figure 3.11 Comparison of the finite difference and Abdel-Khalik model

The locus of $\dot{m}c_p / F_1U_LA_c$ equal to unity was also plotted. For values of $\dot{m}c_p / F_1U_LA_c$ greater than unity, the Finite Difference and Abdel-Khalik model compare favorably. At all flow rates, the two methods for one and two turns yield identical results. For N=4 the values for the collector heat removal factor compare reasonably within 4% with the largest discrepancies occurring when $\dot{m}c_p / F_1U_LA_c$ is less than unity. The parameter $\dot{m}c_p / F_1U_LA_c$ is equal to unity at a flow rate per unit area of about 0.06 kg/sm^2 with a serpentine model of N=10. Unfortunately, for the region of interest, at low flow rates and

high values of the collector heat removal factor, the parameter $\dot{m}c_p / F_1 U_L A_c$ is less than unity and Abdel-Khalik's analysis does not hold for $N > 2$. At a flow rate of 0.002 kg/s.m^2 the percentage difference in the values of F_R for the finite difference and Abdel-Khalik's analysis is about 15 %.

The results of Figure 3.11 do not reveal how the collector heat removal factor is dependent on tube spacing. Figure 3.12 gives an indication of the effects of tube spacing.

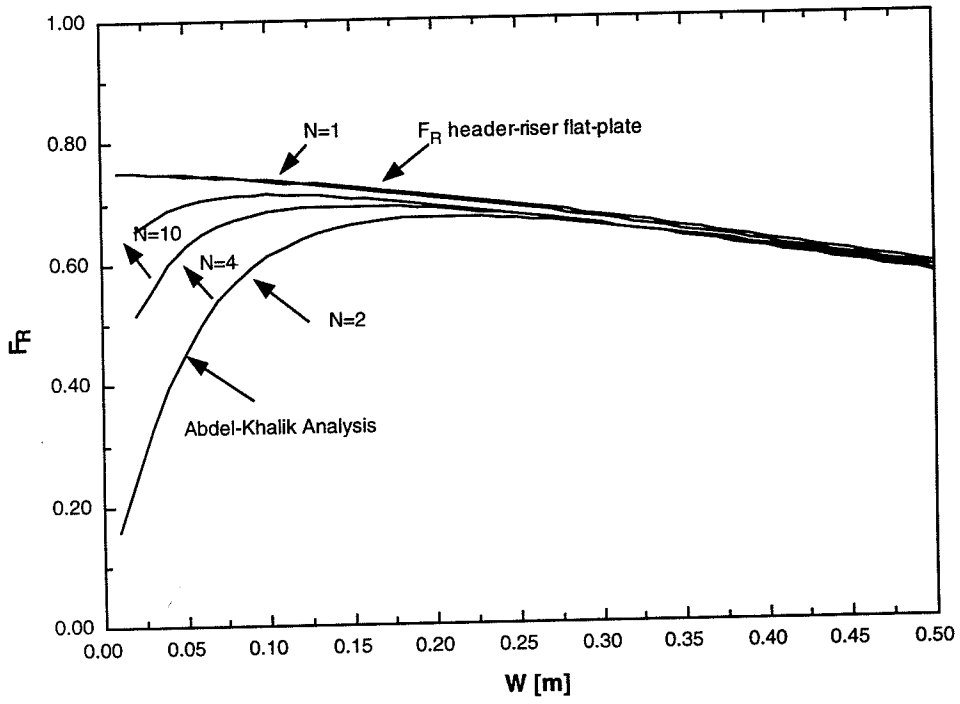

Figure 3.12 Variation of tube spacing and number of turns

There is an asymptote for F_R at a tube spacing of about 1 cm. The Figure reveals that the minimum value for F_R occurs when N=2 and the maximum value occurs when N=1. As the number of turns increases, the values of F_R approach the values of F_R for N=1, therefore it

can be postulated for $N=\infty$ the values of F_R equal the values of F_R at $N=1$. This agrees with the results obtained by Zhang and Lavan. The effect of the number of turns for a given tube spacing of 10 cm is shown in Figure 3.13.

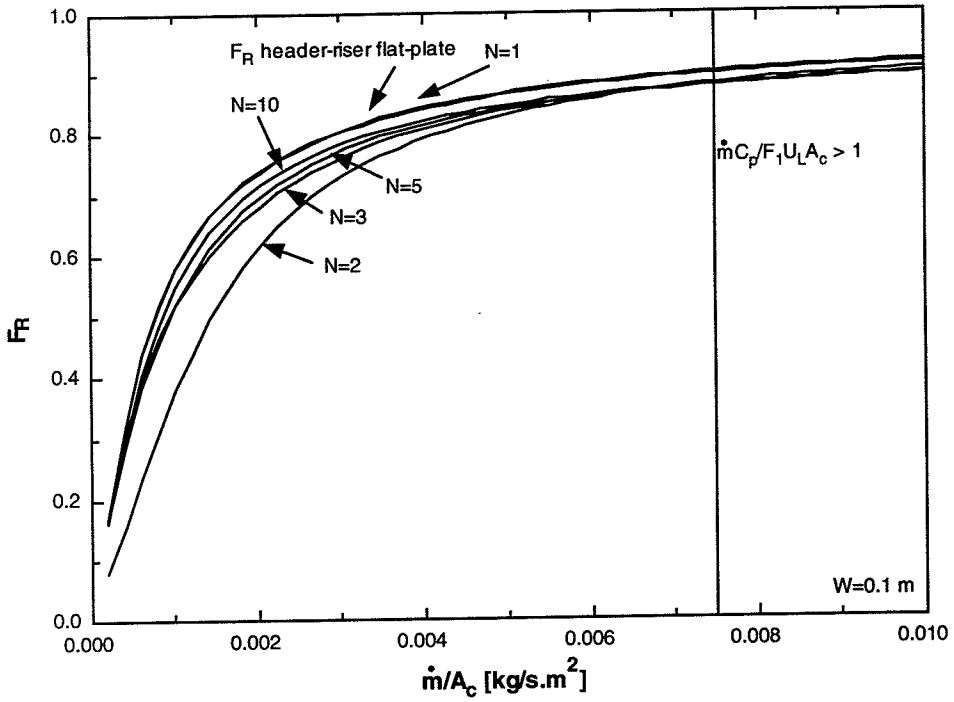

Figure 3.13 Effect of the number of turns on collector performance

The results are also presented as the ratio of F_R to $F_{R,flat}$ (for various numbers of turns), shown in Figure 3.14.

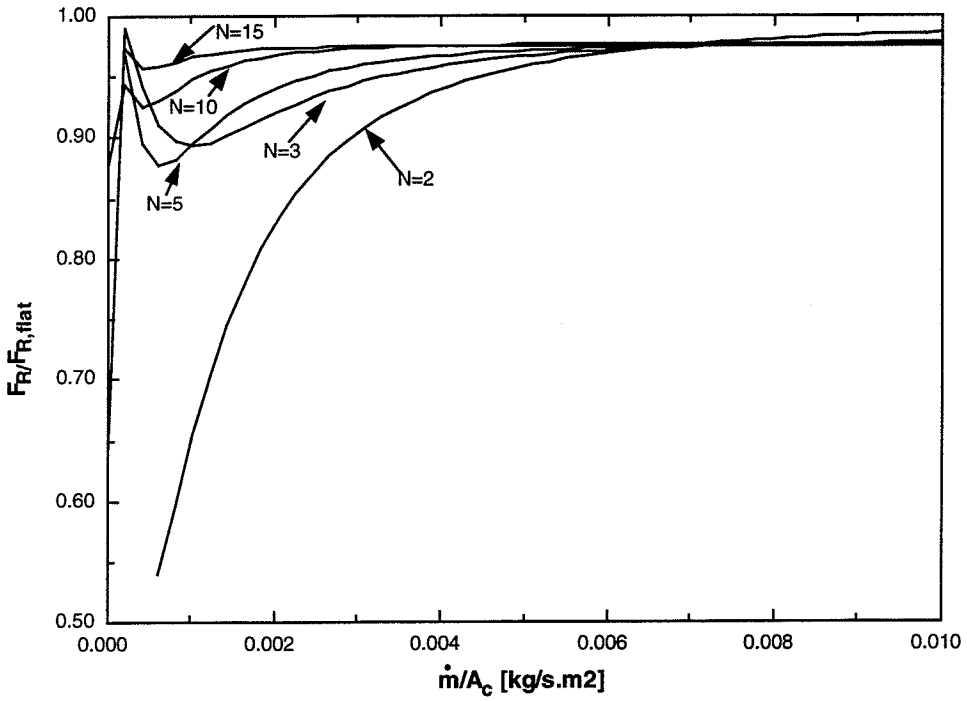

Figure 3.14 Comparing the number of turns of the serpentine collector to the one turn collector

The difference for F_R between the 15 turn serpentine collector and the flat-plate collector is at worst less than five percent for a flow rate of 0.004 kg/s.m^2. This flow rate is well below the expected operating range. For a flow rate of 0.002 kg/s.m^2 the difference between the models is less than 3 percent.

A serpentine collector may have more than 15 turns. In this case, the analysis for a long straight collector with no turns will hold. Therefore, the model is very close to the model for the flat-plate collector, with the exception being that the internal heat transfer coefficient will be different. A collector of N=1 could also be made by using a conventional collector with many turns and creating long cuts between the tubes, effectively decoupling the collector tubes.

The internal heat transfer coefficient is dependent on the flow rate through the tubes, the diameter of the tubes, the length of the tubes and the flow regime, that is, whether it is laminar or turbulent.

For laminar flow (Reynolds numbers less than 2100), the Nusselt number is given by equation 3.21, developed by Heaton et al (Incropera and DeWitt, 1990) for the case of constant heat rate.

$$Nu = 3.7 + \frac{0.0534(\mathrm{Re}\,\mathrm{Pr}\,D_i/L)^{1.15}}{1+0.0335(\mathrm{Re}\,\mathrm{Pr}\,D_i/L)^{0.82}} \qquad (3.22)$$

where Re is the Reynolds numbers, Pr, is the Prandtl number, D_i (m) is the tube diameter and L (m) is the tube length.

In the turbulent flow regime, Reynolds numbers greater than 2100, the Nusselt number is given by Gnielinski's modification of the Petukhov equation (Incropera and DeWitt, 1990) for Reynolds numbers between 3000 and 5 x10^6, shown in equation 3.22.

$$Nu = \frac{\left(\frac{f}{8}\right)(\mathrm{Re}-1000)\,\mathrm{Pr}}{\left(1+12.7\left(\frac{f}{8}\right)^{1/2}\left(\mathrm{Pr}^{2/3}-1\right)\right)} \qquad (3.23)$$

In the above equation, f, represents the friction factor from the Moody chart.

3.4 Design Considerations

Many design parameters need to be optimized. The fin efficiency gives an indication of the ratio of the heat transfer rate from a fin to the heat transfer rate that would be obtained if the entire fin surface area were to be maintained at the same temperature as the primary surface. The fin efficiency assumes that there is no contact resistance at the fin base. Figure 3.12 gives an example of the effect that the variation of tube spacing had on the collector heat removal factor. The increasing value for F_R at decreasing values of tube spacing is related to the fin efficiency as the fin length approaches zero the fin efficiency approaches 100 %. In this region of the curve, there are no losses, but at the same time, the area subject to incident radiation has been greatly reduced. Figure 3.15 shows the fin efficiency curve.

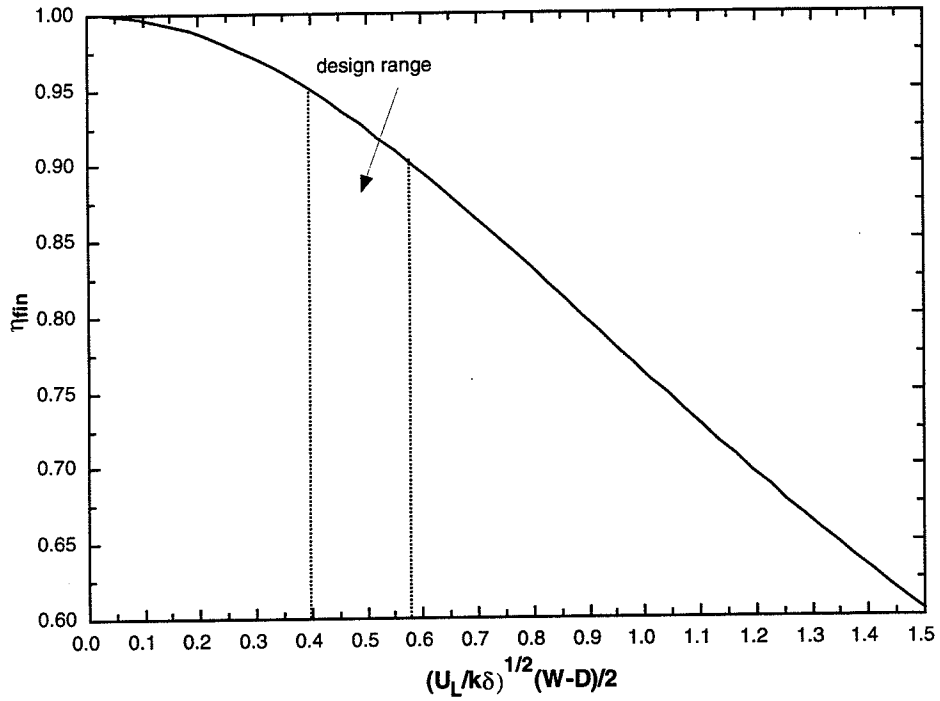

Figure 3.15 Fin efficiency curve

A general rule of thumb is that the fin efficiency should be about 90 to 95 %. Higher efficiencies do not tend to be cost effective for this increased efficiency. The above Figure is in terms of the design parameter, $\left(\frac{U_L}{k\delta}\right)^{1/2}\frac{(W-D)}{2}$, where U_L (W/m^{2}K) is the loss coefficient, W (m) is the tube spacing, D (m) is the tube diameter, k (W/m.K) is the plate conductivity and δ (m) is the plate thickness. The fin efficiency has been represented for the case of one turn.

Figure 3.16 represents the effect of tube diameter for a given flow rate of 0.002 kg/s.m^2. It can be seen that the tube diameter plays little importance in the collector heat removal factor

for the header-riser flat-plate collector. However, the tube diameter is very important in serpentine collectors. In order to promote turbulent flow, the tube diameter should be small.

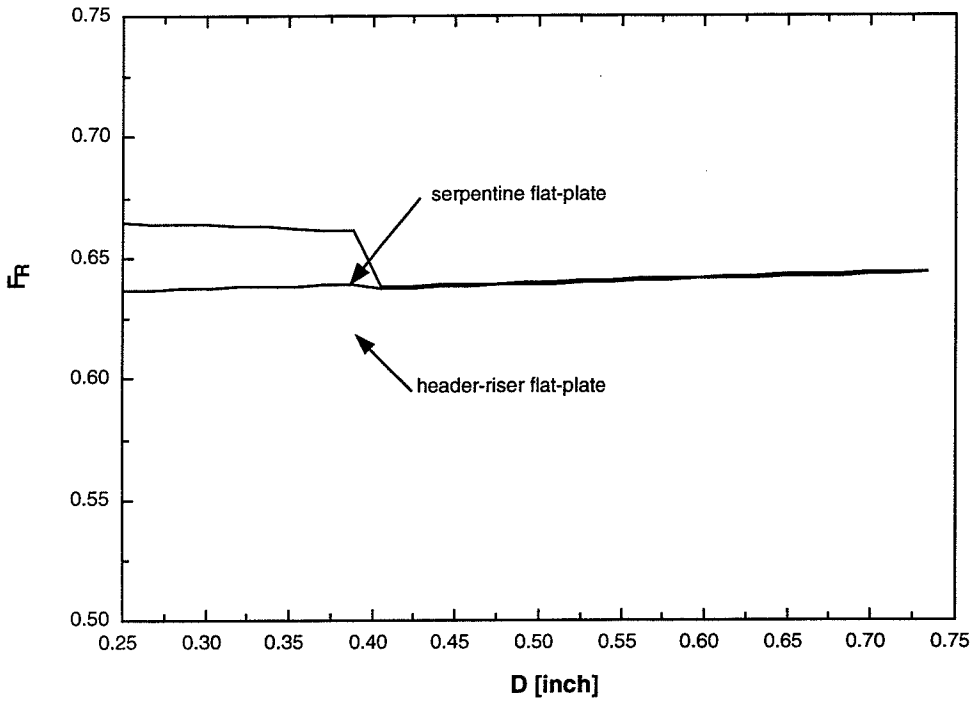

Figure 3.16 Effect of tube diameter on collector performance

The fin efficiency was plotted against the tube spacing for plate thicknesses of 0.0002 m and 0.0003 m in Figure 3.17. The copper tubing chosen has an outer diameter of 1/4 inch and an inner diameter of 0.194 inches. The plate conductivity is 385 W/m.K.

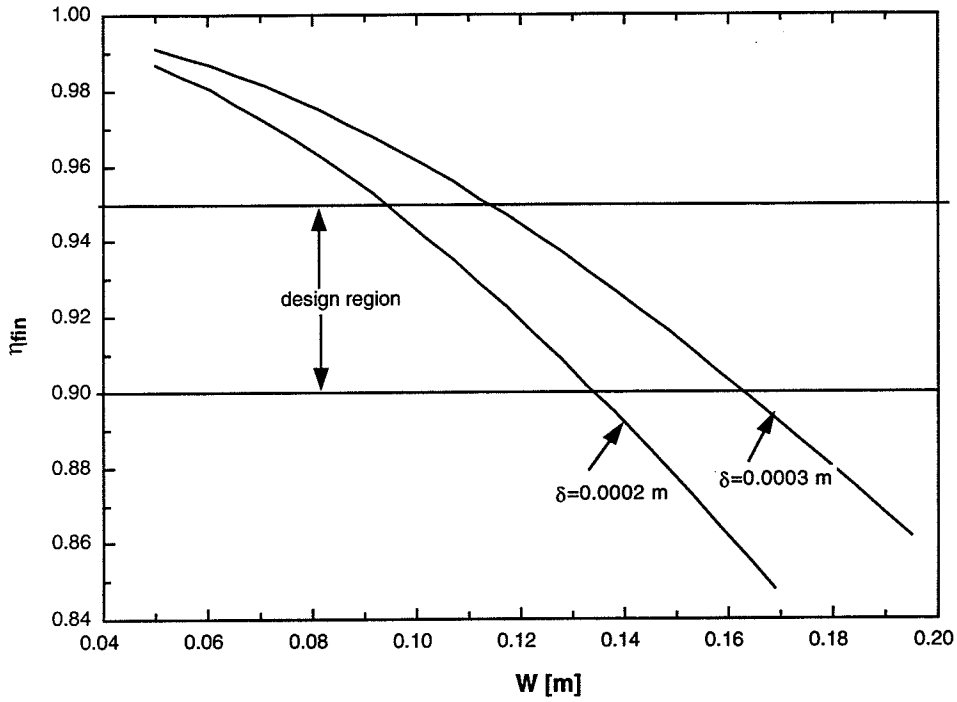

Figure 3.17 Optimisation of the plate thickness and tube spacing for 1/4 inch diameter tube

The serpentine collector needs to be optimised in terms of the plate thickness, tube spacing and tube diameter. As stated earlier, increasing the number of turns will increase the collector heat removal factor. A tube spacing of 10 cm was chosen with a plate thickness of 0.2 mm.

Solar collector designs seem to be dictated by the size of the glass cover. In order to decrease costs standard sizes are chosen. Consequently, a 60"x 84" sheet of glass will be used, which is aproximately the size of a patio door, and it is about the maximum size that can be comfortably handled.

The serpentine collector model was tested under two configurations: with the tubing parallel to the long side of the collector and parallel to the short side of the collector. The finite

difference model was used to asses the two configurations. The model was tested for the same surface area of 0.8 m^2. Three turns were used for the configuration with the tubes running parallel to the short side and one turn for the configuration with the tubes parallel to the long side. These were both compared to the model with no turns shown in Figure 3.18. There was very little difference between the two configurations, however for low flow rates the configuration with three turns outperformed the one turn model.

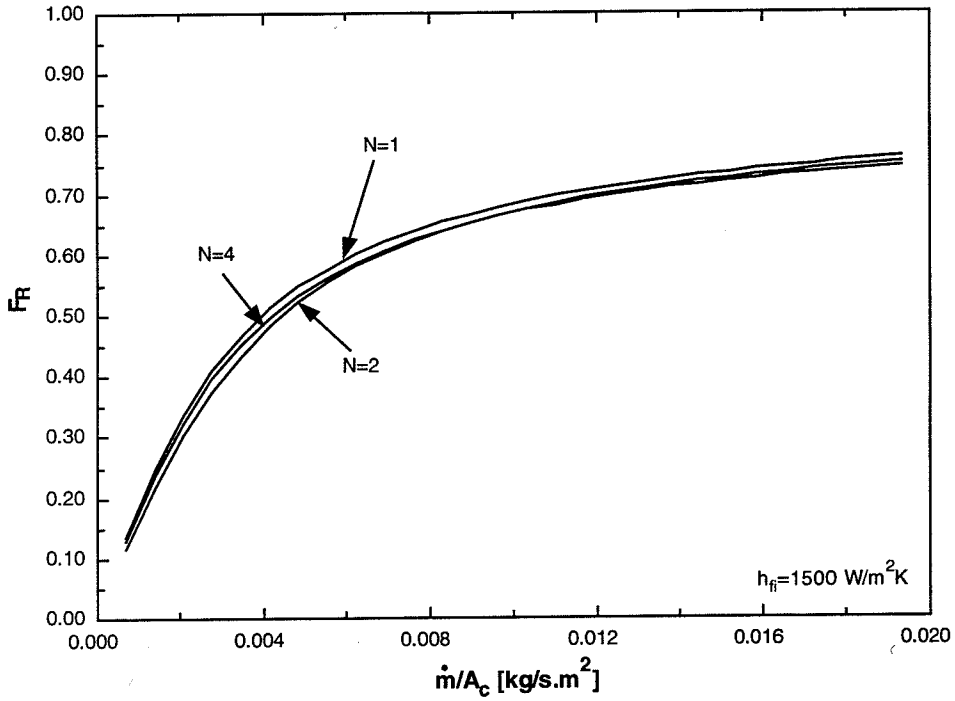

Figure 3.18 Dependence on collector orientation, tube lengths and number of turns

For the collector dimensions of 60"x 80", the collector should have 19 tubes in parallel with 18 turns for optimal low-flow performance. The flat-plate model can readily be used for this number of turns.

The serpentine collector was compared to the conventional header-riser flat-plate, Figure 3.19. The serpentine collector has better performance due to the higher heat transfer coefficient at collector flow rates greater than approximately 0.001 kg/s.m^2. The flow through the serpentine collector is 19 times greater than the flow through each riser of the conventional collector.

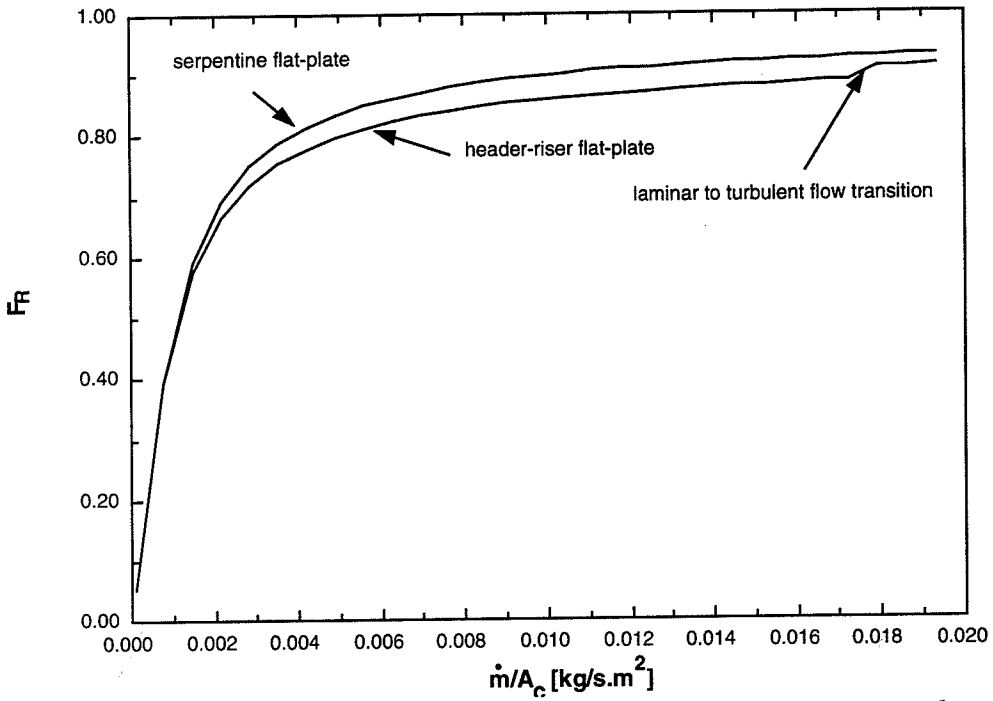

Figure 3.19 Comparison of the heat removal factor for the header-riser and serpentine flat-plate collectors

The reason why serpentine collectors have been disregarded in the past is because of the belief that the pressure drop would be too large. Figure 3.20 represents the pressure drop across the collectors.

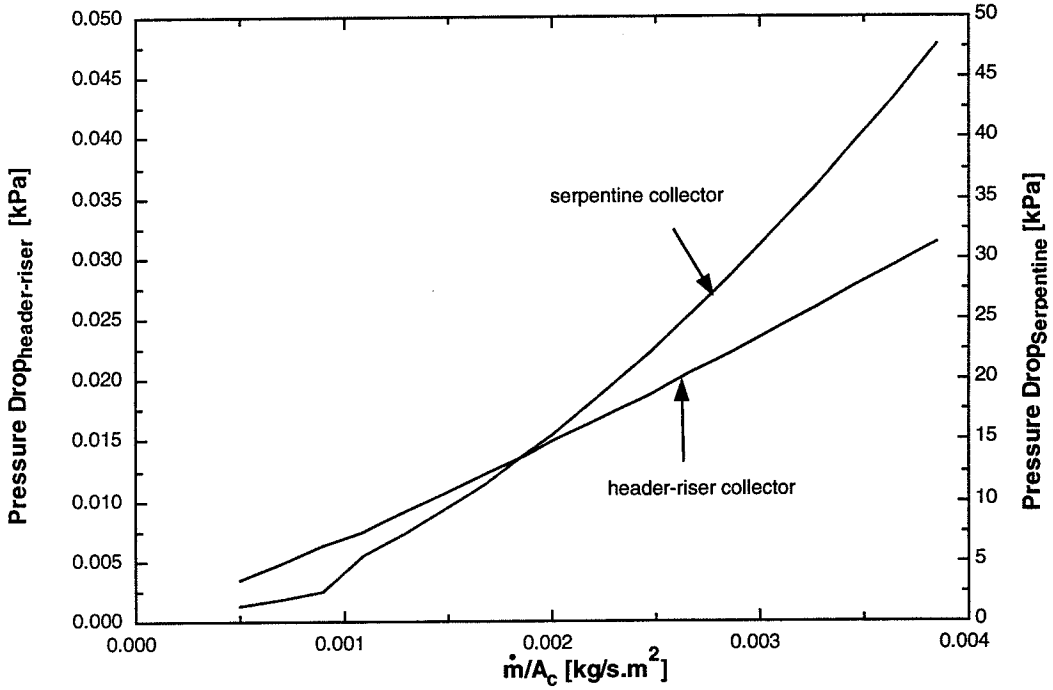

Figure 3.20 Comparison of the pressure drop across header-riser and serpentine flat-plate collectors

The pressure drop for the serpentine collector is much higher, however for a flow rate of 0.002 kg/s.m^2, the pressure drop of the serpentine collector is approximately 15 kPa. This pressure drop is equivalent to a head of 1.45 m of water. Figure 3.21 represents the pumping power requirements for the serpentine collector.

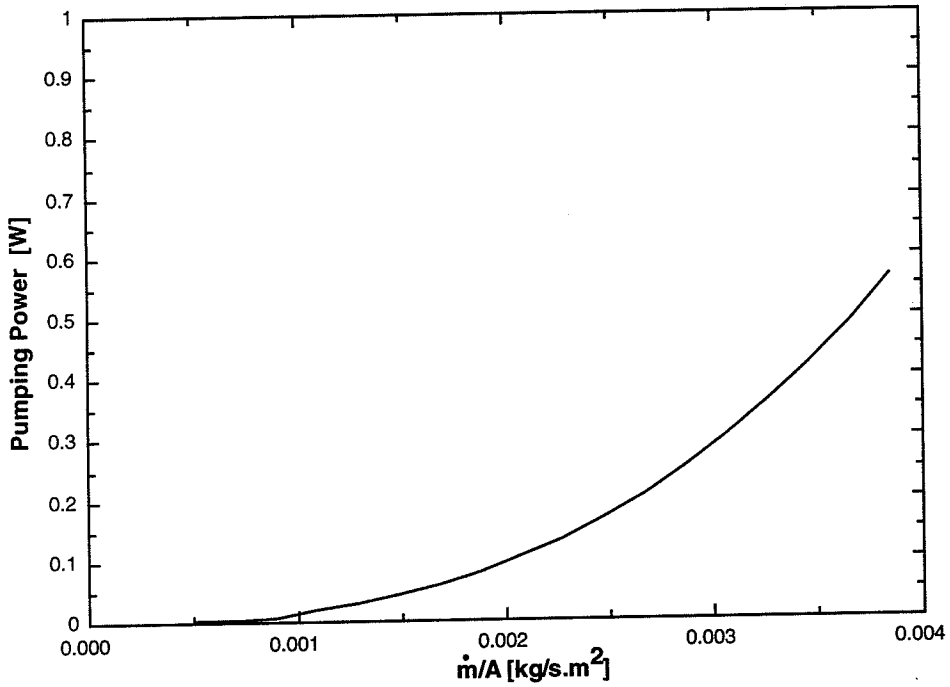

Figure 3.21 Pumping power requirements for the serpentine collector

The pumping power requirement for a flow rate of 0.002 kg/s.m^2 is approximately 0.1 W. The fluid through the collector could be driven by a PV powered pump.

3.5 TRNSYS Component

In order to calculate the system performance, a TRNSYS model of the serpentine collector was made. The model uses the assumption that it can be modeled as a long collector, with no bends. This is essentially the model for the conventional header-riser flat-plate collector, however the internal heat coefficient has been modified to account for the higher flow rate and longer tube. A complete description of this TRNSYS component for a serpentine collector, TYPE 86 is provided in appendix A.

Using a simple TRNSYS deck (appendix B), the header-riser collector was compared to the performance of the serpentine collector. Figure 3.22 represents the performance of the serpentine collector and the header-riser collector for various flow rates.

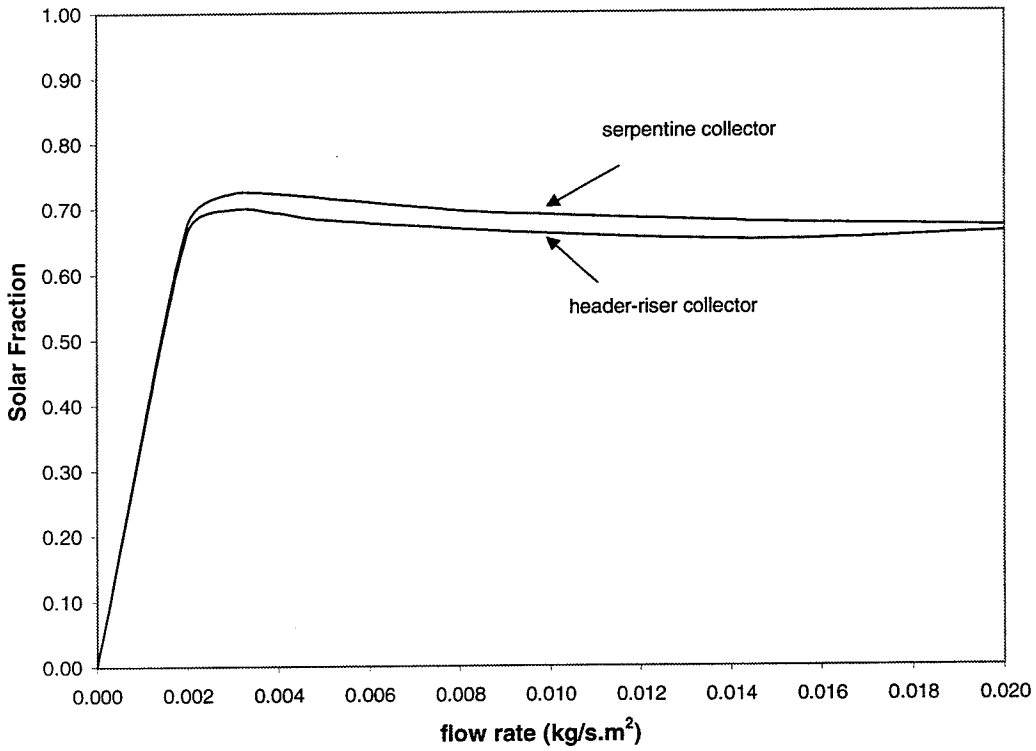

Figure 3.22 Comparison of yearly performance of serpentine and header-riser flat-plate collectors for various flow rates.

3.6 Serpentine Collectors Connected in Parallel

In order to reduce the pressure drop across a serpentine collector it may be necessary to add collectors in parallel. It can be shown that the addition of collectors in parallel will have little effect on the collector heat removal factor given that the total area remains the same. This is shown in Figure 3.23 for a single collector and two and three collectors in parallel

for the same total area. The collectors have the same area, the same number of turns and the same spacing between turns; the only difference is the collector width has been changed.

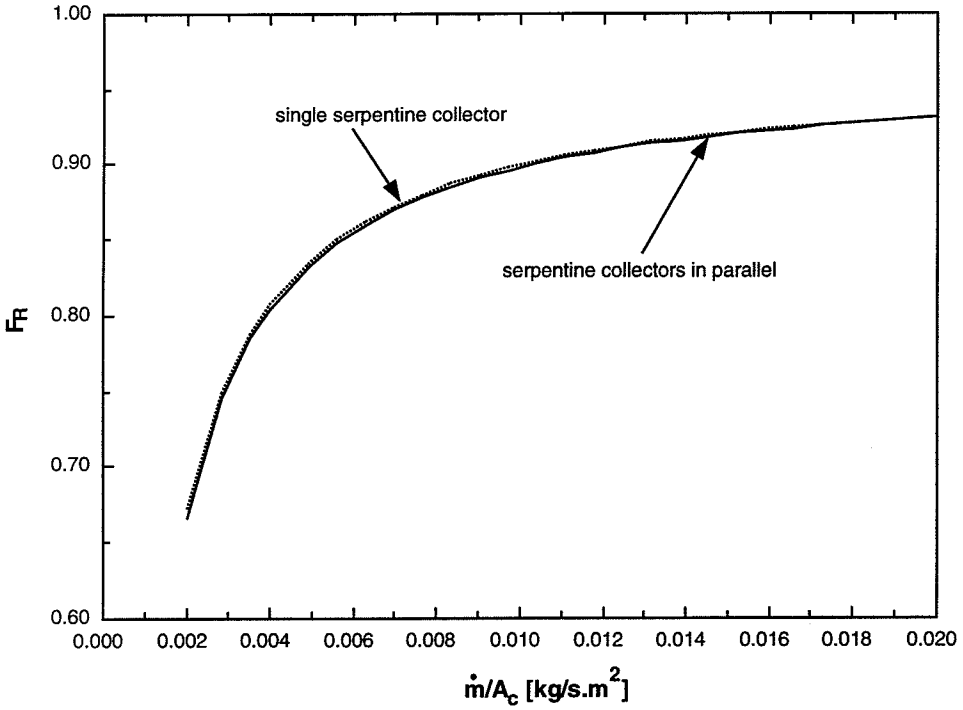

Figure 3.23 Addition of serpentine collectors in parallel

3.7 Conclusions

The flow distribution through a header-riser flat-plate collector becomes more even as flow rate is reduced and flow imbalances are reduced. However, the header-riser suffers from decreased useful energy gain as the flow rate is reduced. Serpentine collectors perform slightly better than a header-riser collector with the same area, tube spacing and tube diameter. The serpentine collectors perform better due to the earlier onset of turbulent flow, which enhances the internal heat transfer coefficient. The onset of turbulent flow is a

function of the tube diameter and flow rate. However, as soon as the flow becomes turbulent, the pumping power increases substantially.

CHAPTER 4: PV DRIVEN PUMP

Many solar domestic hot water systems require an auxiliary electric source to operate a pump in order to circulate fluid through the solar collector. Alternatively, thermosyphon systems use the buoyant forces associated with warmer fluids to circulate fluid through a system. The disadvantage with the thermosyphon systems is that they require the tank to be elevated with respect to the collector. In the case of the forced circulation system, the collector circulating fluid is pumped at a constant rate and it is commonly controlled by an ON/OFF differential temperature-sensing controller.

A photovoltaic powered pump can be used to replace the standard electrical pump. The PV driven pump provides some distinct advantages. First, the PV pumping system can eliminate the need for a controller since the PV pump will only respond to solar radiation and will only pump at times the solar collector is receiving radiation. The controller is usually the most problematic component in solar domestic hot water systems since it does not always function as designed (Al-Ibrahim, 1997). The conventional control strategy uses a differential temperature-sensing controller to activate pumps that circulate the heat transfer fluids at a fixed flow rate. The controller generally turns on if the water inlet to the collector is less than the collector fluid outlet temperature by some dead band. Sometimes, fluid will circulate when there is little or no radiation causing colder water to enter the tank and destroy tank stratification.

The PV pump also eliminates the need for an auxiliary power source. This is particularly important when auxiliary power sources are not readily available. The reduction of parasitic pumping power can also reduce on-peak utility demand since it will work well during the middle of the day, which is typically the time of peak electricity demand for many utilities. Although the energy demand of an individual pump may seem low, the combined effect of all the utility driven pumps in the utility district drawing energy at the same time will influence the peak load the utility must meet.

Many different types of photovoltaic pumping systems exist. These include a PV directly coupled to a DC motor and pump, a battery buffered pumping system where a battery is connected across the PV array to feed the DC motor driving a pump, and a maximum power point tracker where the system will always operate at the PV panel's maximum power point (Kou, 1996).

Directly coupling the PV array to a DC motor and pump is the most appropriate for the purpose of solar domestic hot water systems. Figure 4.1 represents a schematic of the system (Kou, 1996).

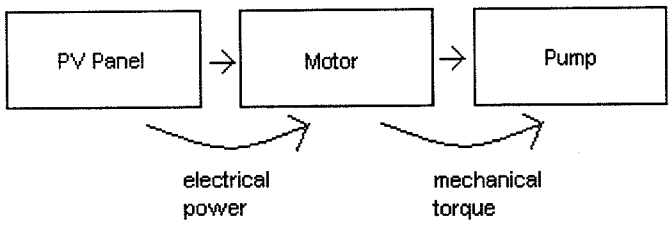

Figure 4.1 Schematic of PV pumping system

The PV pumping performance is a function of radiation level, array area, conversion efficiency, slope of the PV array, ambient temperature and the pump-motor-hydraulic system characteristics.

Before discussing PV driven pumps, a brief overview of photovoltaic cells is presented.

4.1 Photovoltaic Cells

Photovoltaic cells function by converting solar radiation into electrical energy. Photovoltaic cells are made of a semiconductor material such as single-crystal silicon or amorphous (non-crystalline) silicon. Semi-conductors normally behave electrically like an insulator that inhibits the transfer of electrical energy. However, when sufficient energy, such as sunlight is incident on these materials they act like electrical conductors. When two dissimilar semiconductors are placed in contact, a potential barrier forms allowing the generation of current with incident solar radiation. Electrical connectors are attached to the two semiconductors to form either a grid on the top surface or a thin metallic coating on the back.

The potential barrier is formed by doping the silicon atoms with small amounts of boron on one side of the cell creating p-silicon, which has a deficiency of electrons in the outer shell forming 'holes'. The other side is made by doping the silicon with phosphorus to form n-silicon, which has an excess of electrons in its outer shell. The two doped layers are joined forming a p-n junction. A barrier is formed at the junction as electrons from the n-silicon cross the p-n junction to the p-silicon, while the 'holes' of the p-silicon cross over to the n-

silicon until an equilibrium state of an excess of negative charges on the p-silicon side of the junction and an excess of positive charges on the n-silicon side of the junction is formed. After the barrier is formed, electrons are repelled from crossing the junction from the n-silicon side and similarly 'holes' cannot cross the junction from the p-silicon side, a schematic of the junction is shown in Figure 4.2 (SERI, 1988).

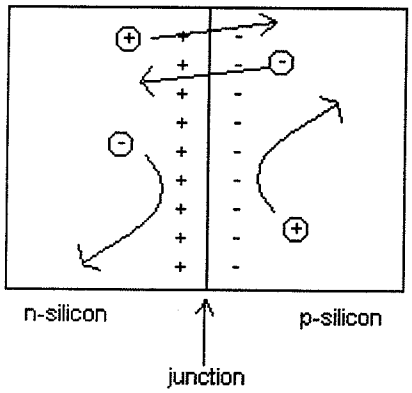

Figure 4.2 Schematic of the p-n junction of a silicon photovoltaic cell.

Solar radiation is composed of discrete energy units called photons. If these photons have sufficient energy, an electron from the outer shell of the n-silicon atom is freed leaving a 'hole' and a free electron. The free electrons, if connected by an external circuit, will flow to the p-silicon creating an electrical current. There is a minimum energy level, corresponding to a maximum wavelength (1.15 μm for silicon), of photons that can produce a hole-electron pair. Some photons have insufficient energy to create a hole-electron pair and others have energy levels higher than that needed to produce a hole-electron pair and thereby heat the cell. The maximum theoretical efficiency of silicon cells is 23% (Duffie and Beckman, 1991).

The photovoltaic cell, module or array can be modeled by the equivalent circuit shown in Figure 4.3 (Duffie and Beckman, 1991).

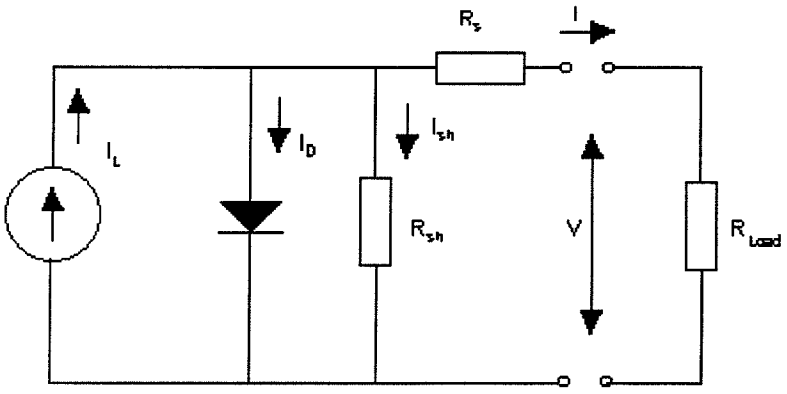

Figure 4.3 Equivalent circuit for a photovoltaic cell

The photovoltaic circuit consists of five parameters: the light current, I_L, the diode reverse saturation current, I_o, the series resistance, R_s, the shunt resistance, R_{sh}, and the thermal voltage, a. The thermal voltage is a parameter that varies with temperature. At a fixed temperature and solar radiation, the current-voltage characteristic of this model is given by equation 4.1.

$$I = I_L - I_D - I_{sh} = I_L - I_o\{\exp[(V + IR_s)/a] - 1\} - \frac{V + IR_s}{R_{sh}} \qquad (4.1)$$

where

I_L =light current (A)

I_D =diode current (A)

I_{sh} =shunt resistance current (A)

I_o =dark current (A)

I =operation current (A)

V =operation voltage (V)

R_s =series resistance (Ω)

R_{sh} =shunt resistance (Ω)

a =thermal voltage (V)

The model can be simplified to four parameters by neglecting the shunt resistance because it tends to be very large compared with the series resistance for modern photovoltaic cells. Equation 4.2 becomes

$$I = I_L - I_D - I_{sh} = I_L - I_o\{\exp[(V + IR_s)/a] - 1\} \qquad (4.2)$$

Four parameters are now needed to accurately model the photovoltaic cell. The following assumptions can be made to determine the remaining parameters.

The short circuit current is equal to the light current at short circuit conditions since the diode current is very small, this is shown in equation 4.3

$$I_L = I_{sc} \qquad (4.3)$$

where I_{sc} is the short circuit current (A).

The current is zero at open circuit conditions and the following approximation shown in equation 4.4 can be derived from equation 4.2 assuming that the *1* is small compared to the *V/a* term.

$$I_0 = I_L \exp(-V_{oc}/a) \tag{4.4}$$

where V_{oc} is the open circuit voltage (V).

Photovoltaic cell manufacturers often provide the maximum power conditions for current and voltage and therefore the series resistance can be found from equation 4.5.

$$R_s = \frac{a \ln\left(1 - \frac{I_{mp}}{I_L}\right) - V_{mp} + V_{oc}}{I_{mp}} \tag{4.5}$$

where I_{mp} is the maximum power point current (A), and V_{mp} is the maximum power point voltage (V).

The cell performance and therefore the cell parameters, with the exception of the series resistance vary with temperature. The module efficiency decreases at higher temperatures. Townsend (Duffie and Beckman, 1996) showed that the following equations 4.6-4.7 could be used to approximate these temperature variations in the PV model parameters.

$$\frac{a}{a_{ref}} = \frac{T_c}{T_{c,ref}} \tag{4.6}$$

where a and a_{ref} are the thermal voltage and reference thermal voltage (V) respectively and T_c and $T_{c,ref}$ are the cell temperature and reference cell temperature (K) respectively. The thermal reference voltage is given by equation 4.7.

$$a_{ref} = \frac{\mu_{V,oc} T_{c,ref} - V_{oc,ref} + \varepsilon N_s}{\frac{\mu_{I,sc} T_{c,ref}}{I_{L,ref}} - 3} \tag{4.7}$$

where $\mu_{V,oc}$ is the temperature coefficient for the open circuit voltage (V/K) given in equation 4.8 and $\mu_{I,sc}$ is the temperature coefficient of the short circuit current (A/K) shown in equation 4.9.

$$\mu_{I,sc} = \frac{dI_{sc}}{dT} \tag{4.8}$$

$$\mu_{V,oc} = \frac{dV_{oc}}{dT} \tag{4.9}$$

The light current is then given by equation 4.10.

$$I_L = \frac{G_T}{G_{T,ref}} \left[I_{L,ref} + \mu_{I,sc} \left(T_c - T_{c,ref} \right) \right] \tag{4.10}$$

where I_L and $I_{L,ref}$ are the light current and the reference light current (A), G_T and $G_{T,ref}$ are the solar radiation and reference solar radiation respectively (W/m^2.K). The dark current is given by equation 4.11.

$$\frac{I_o}{I_{o,ref}} = \left(\frac{T_c}{T_{c,ref}}\right)^3 \exp\left[\frac{\varepsilon N_s}{a_{ref}}\left(1 - \frac{T_{c,ref}}{T_c}\right)\right] \qquad (4.11)$$

where ε is the material bandgap energy, 1.12 eV for silicon, and N_s is the product of the number of cells in series in a module and the number of modules in series.

Figure 4.4 demonstrates the relation between current, voltage and power for a photovoltaic cell. Recall that power is defined as the product of current and voltage as shown in equation 4.12.

$$P = IV \qquad (4.12)$$

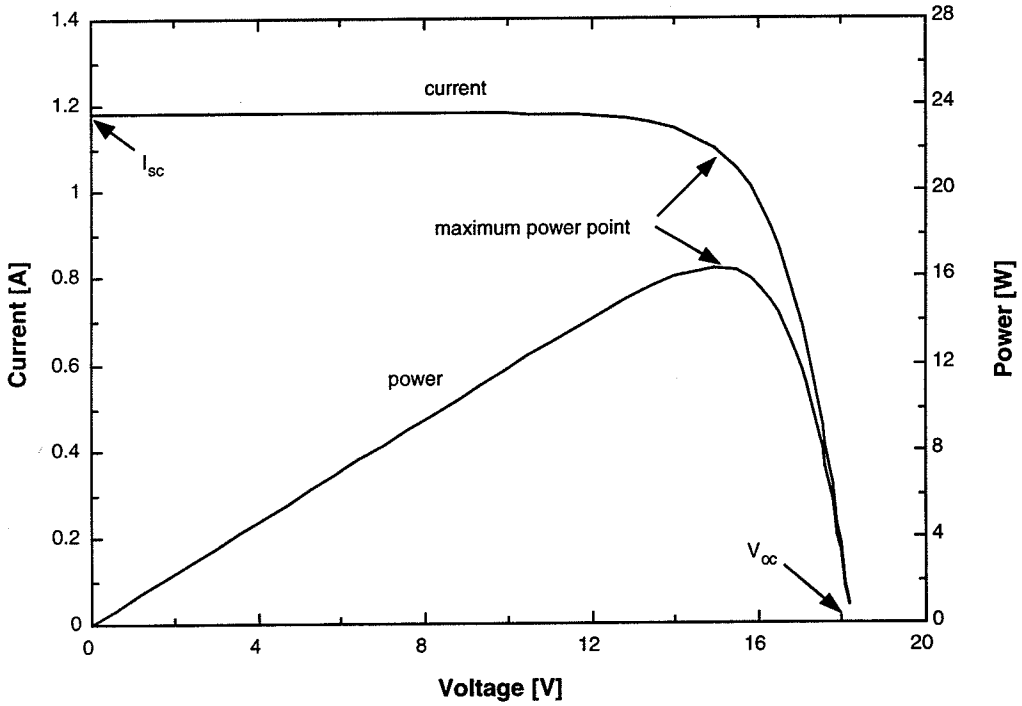

Figure 4.4 Relationship between current, voltage and power for a photovoltaic cell.

Two photovoltaic panels combined in parallel double the current while two photovoltaic cells combined in series will double the voltage. These rules apply to many panels combined in parallel and series to form arrays.

Operating at the maximum power point ensures that the PV will operate at its maximum efficiency. The maximum power point is unique for a given solar radiation and ambient temperature.

4.2 PV and Pump System

Ideally, the operating point for the PV pump should lie at the maximum power point for the photovoltaic panel. However, as radiation and ambient temperature vary the maximum power point voltage and current will change. Thus, as radiation and temperature change the flow rate will vary. Optimizing the PV pumping system is complex due to the many non-linear equations involved. In order to achieve maximum efficiency the components must be well matched.

PV pumping systems require a minimum radiation to start the pumping. The minimum radiation is called the threshold radiation and it is dependent on the characteristics of the system components. As the radiation increases, the PV pump will circulate fluid at an increasing rate.

Al-Ibrahim (1997) presented a unique method for optimizing the PV pumping system. Instead of optimizing, the individual components which increases computing time he

developed a generalized flow profile. Equation 4.13 represents the flow profile, which for at a given radiation, G, one can solve for the flow, $\dot{Q}$.

$$G = a\dot{Q}^2 + b\dot{Q} + c \qquad (4.13)$$

where a represents the flow at noon when radiation is at a maximum, b is the reciprocal of the rate of increase of flow rate as a function of threshold radiation and c is the threshold radiation level.

Al-Ibrahim's method allows the formulation of a PV pumping system profile with flow rate as a function of solar radiation based on the optimization of a function in terms of a, b and c to maximize the solar fraction. The advantage of this method is that the profile that maximizes the SDHW system is found and then the components of the PV pumping system are selected. According to Al-Ibrahim, the decoupling considerably eases the optimal search. However, this approach will not be taken in this analysis because the individual components will be examined separately.

Chapter 3 presented the flow rates at which optimal performance was found for the solar domestic hot water system using a flat-plate collector and serpentine collector. Using a serpentine collector, the optimal flow rate is about 0.004 kg/s.m^2, with this in mind the PV system will be designed in order to take advantage of this optimal flow rate.

4.2.1 PV Driven Pump Design and Selection

Centrifugal pumps require less torque to start and produce more head than other pumps. Simplicity, low cost, low maintenance and availability of designs for a wide range of flow rates and heads make centrifugal pumps an appropriate choice for solar domestic hot water systems. A centrifugal pump operated at constant speed delivers any capacity from zero to the pump's maximum. Characteristic curves show the interrelation of pump head, capacity, power and efficiency for a specific impeller diameter and casing size (Hicks,1957).

The solar domestic hot water systems under consideration have no static head since they form a loop of pressurized water. The pump only needs to supply a dynamic head. Increasing the dynamic head decreases the flow rate.

The dynamic head in a closed loop system is given in equation 4.14, (Gerhart and Gross,1985).

$$h = \frac{fL}{D}\frac{\vec{v}^2}{2g} \qquad (4.14)$$

Using the serpentine collector of chapter 3 and system piping of 10 meters with four bends and a diameter of 5 mm, the pressure drop across the serpentine collector accounts for almost 80 % of the dynamic head of 21.6 feet. In order to reduce the dynamic head requirement, two serpentine collectors were placed in parallel with half the flow rate in each. It was also shown in chapter 3 that this configuration has little effect on the collector heat removal factor. Under this new configuration, the serpentine collector head is reduced to less than 40 % of the total. The total head is 8.7 feet.

The closed loop system and the pump can be coupled by non-linear equations to obtain the pump operating point. The pump flow rate is a function of the dynamic head, while the dynamic head for the system is dependent on flow rate therefore a unique point exists where these converge.

As discussed in chapter 3, the optimal flow rate was 0.004 kg/s.m^2. Unfortunately, since each pump has a unique set of curves for flow rate as a function of head for different voltages, and no real mathematical model exists for actual pump performance, it was necessary to utilize the characteristics of an existing pump. Pump curves for the Hartell HEH motor were used. Technical data for the pump is given in Appendix D. The pump was then coupled to the system. Figure 4.5 depicts the Hartell pump coupled to a system.

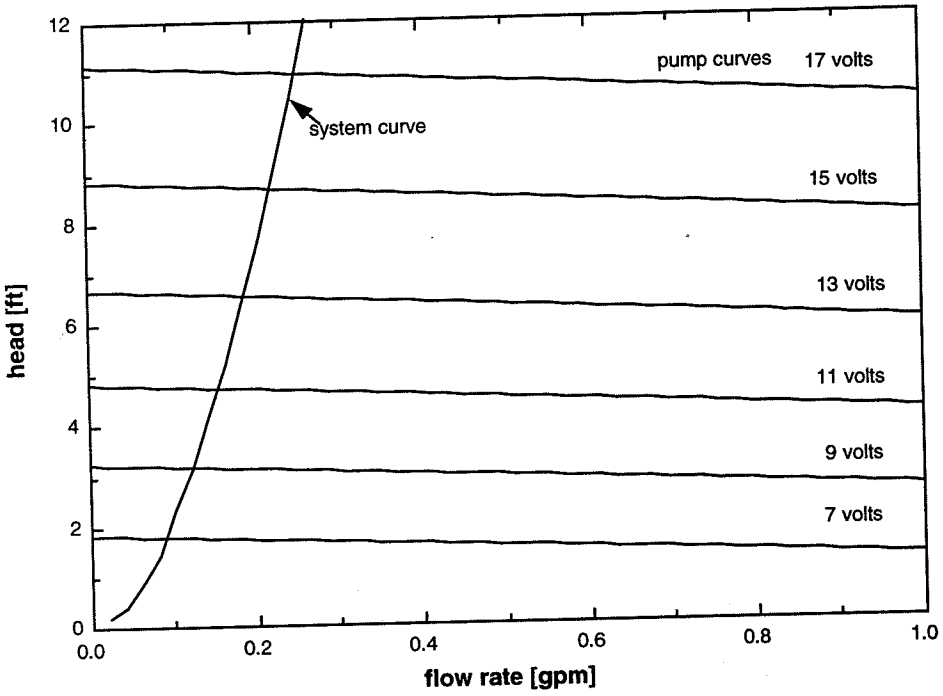

Figure 4.5 Operating point for the Hartell pump and system

The next step in designing the photovoltaic system is to curve fit the pump data that is usually given as flow rate as a function of head for varying voltages and current at maximum head and maximum flow rate. A third order linear regression with cross terms was used in the form shown in equation 4.15. A second order linear regression was used to provide an equation for current in terms of head and voltage of the form shown in equation 4.16. Further details on obtaining the curve fit are given in Appendix D.

$$flowrate = a + b \cdot Head + c \cdot Head^2 + d \cdot Head^3 + e \cdot Voltage + f \cdot Voltage^2 + g \cdot Voltage^3 + h \cdot Head \cdot Voltage + i \cdot Head \cdot Voltage^2 + j \cdot Head^2 \cdot Voltage + k \cdot Head^2 \cdot Voltage^2 \quad (4.15)$$

$$Current = l + m \cdot Voltage + n \cdot Voltage^2 + o \cdot Head + p \cdot Head^2 \quad (4.16)$$

The PV panel and the pump-motor are directly coupled. Motor-pump coupling losses are neglected and motor torque is assumed equal to pump torque. Therefore, PV and motor voltage and current are assumed equal. The pump efficiency for the Hartell HEH motor pump is approximately 2 %.

A new TRNSYS type, TYPE 71, was written for the hydraulic system and pump. The equations that are used to find the operating point of the pump and the hydraulic system may diverge. To ensure convergence the Bisection Solution Method (Murphy et al, 1988) was used. Type 71 requires information about the hydraulic system, the pump curve

coefficients and voltage input. Appendix A includes the code and more details for TYPE 71.

From type 71, the current can be found from the voltage input. The voltage input is obtained from the photovoltaic cell. The photovoltaic cell should ideally operate at the maximum power point. Given the range of desired operating flow rates of 0.0035 kg/s.m^2 to 0.0045 kg/s.m^2, the range of desired operating voltages and currents can be found for the system. A photovoltaic array can then be designed with a maximum power point in this region for 800 W/m^2 and an ambient temperature of 25°C. Many locations will reach maximum daily radiation levels of 800 W/m^2 or higher. Figure 4.6 represents flow rate as a function of voltage and the pump and PV panel as a function of current and voltage. It can be seen that at 800 W/m^2 the flow rate is 0.0045 kg/s.m^2.

coefficients and voltage input. Appendix A includes the code and more details for TYPE 71.

From type 71, the current can be found from the voltage input. The voltage input is obtained from the photovoltaic cell. The photovoltaic cell should ideally operate at the maximum power point. Given the range of desired operating flow rates of 0.0035 kg/s.m^2 to 0.0045 kg/s.m^2, the range of desired operating voltages and currents can be found for the system. A photovoltaic array can then be designed with a maximum power point in this region for 800 W/m^2 and an ambient temperature of 25°C. Many locations will reach maximum daily radiation levels of 800 W/m^2 or higher. Figure 4.6 represents flow rate as a function of voltage and the pump and PV panel as a function of current and voltage. It can be seen that at 800 W/m^2 the flow rate is 0.0045 kg/s.m^2.

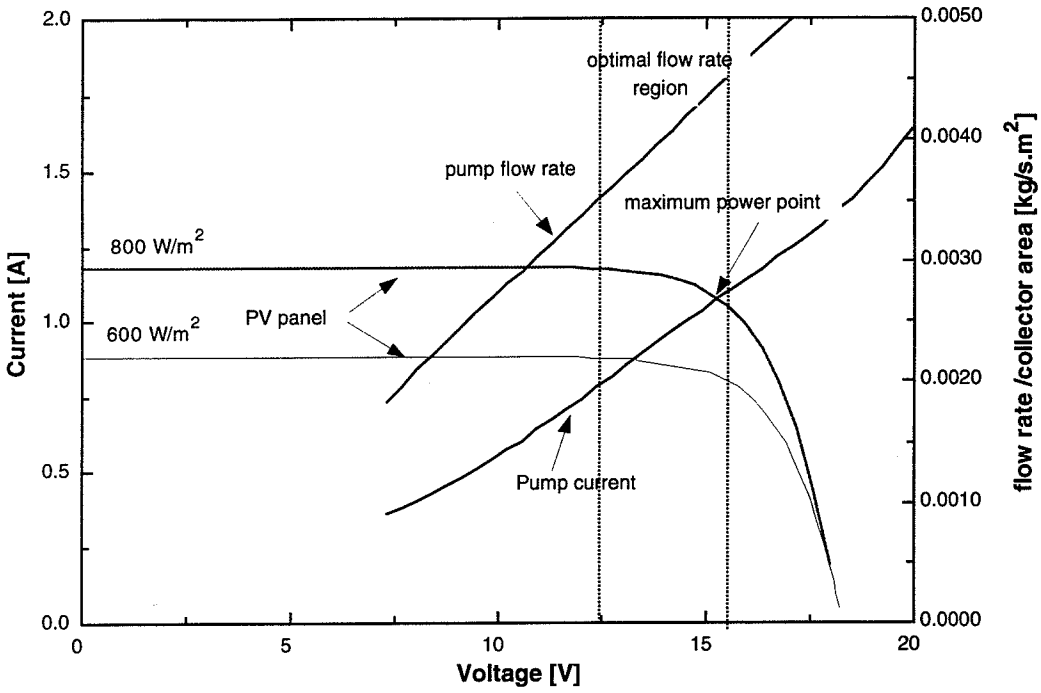

Figure 4.6 PV and Pump System

Figure 4.7 shows that at 800 W/m^2 the operating point for the PV pump lies at the maximum power point.

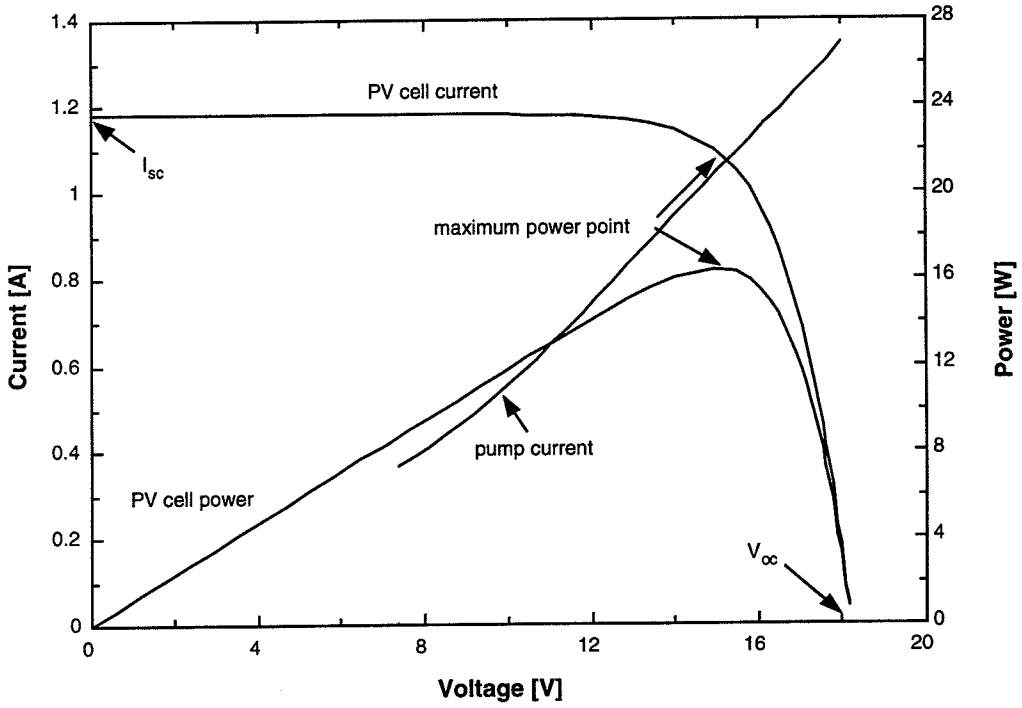

Figure 4.7 Maximum power point for the PV at the operating point.

A TRNSYS type , type 62 (Williams, Al-Ibrahim, Eckstien, 1997), already exists for the model of the PV cell. Type 62 requires information on the cell characteristics as described in section 4.1 and the current input.

Coupling the PV cell, type 62, to the hydraulic system and pump, type 71, requires iteration to find the operating voltage and current as shown in Figure 4.8.

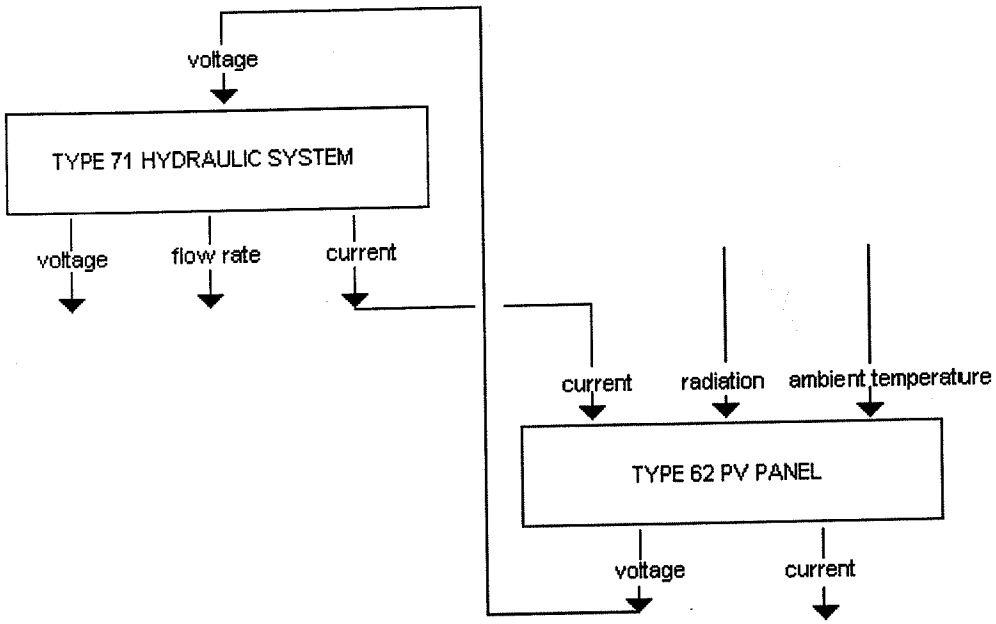

Figure 4.8 Iteration between the hydraulic system and the pump

A yearly simulation with a PV powered pump was performed for Miami and compared to a system with a conventional pump operating at 0.0035 kg/s.m^2 and a conventional system operating at a flow rate of 0.02 kg/s.m^2. The annual solar fraction for the PV driven pump was 69% compared to the annual solar fraction of 73% for the conventional pump low-flow system. The conventional system with a conventional flow rate also had an annual solar fraction of 69 %. The parasitic pump losses for the conventional system were not included in this analysis. Figure 4.9 shows the monthly energy use and solar fraction for a year.

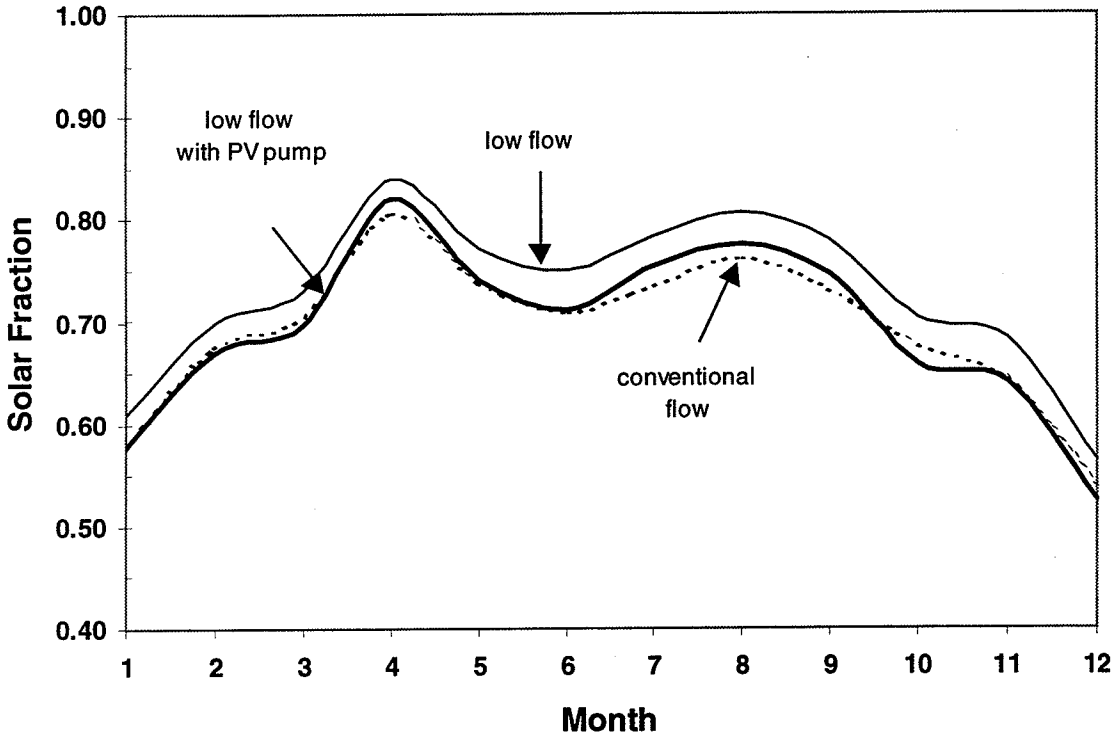

Figure 4.9 Performance comparison of PV driven pump, conventional pump and conventional system

A PV panel was also chosen to operate with the maximum power point for a radiation of 600 W/m^2K coinciding with the pump operating point. Little difference in performance was noted. The annual solar fraction remained 69%.

4.3 Conclusions

Solar domestic hot water systems powered with a PV driven pump offer many advantages with no need for electricity demand. Generally, pumping power requirements are assumed negligible, however if many thousands of SDHW systems were installed the utility would benefit in terms of less heating elements consuming electricity, but the demand reduction anticipated would be reduced due to the thousands of pumps operating at the same time.

The utility's energy demand peaks during midday for summer peaking utilities; this is the time when the SDHW systems require the most energy for pumping.

There is less than 1% difference in annual solar fraction for a low-flow system with a PV driven pump. The use of a PV driven pump is in tune with a solar domestic hot water system. The flow rate is controlled by solar insolation and the need for a control system and strategy eliminated. Control systems are generally the components that are the most complex, require frequent maintenance and prone to problems.

The low-flow PV driven pump SDHW system performed better than the conventional flow SDHW system with a solar fraction increase of 3%. This saving will be larger if pumping power is included in the calculation of the solar fraction of the conventional system.

CHAPTER 5: HEAT EXCHANGER ANALYSIS

Freeze protection is required in many climates. The most common form of freeze protection is the use of a closed loop system with a heat exchanger. The heat exchanger allows the circulation of 'freeze resistant' glycol on the collector side of the heat exchanger. The heat exchanger could also allow higher circulation through the collector side therefore promoting the collector heat removal factor without directly affecting tank stratification. Unfortunately, the use of a heat exchanger incorporates a performance and economic penalty.

Alternatives to heat exchangers include drain-back and drain-out systems. These systems use a controller to activate valves to either drain the water back to the tank in the case of the drain-back system or to drain the water out to waste in the case of the drain-out system (Duffie and Beckman, 1991). Many other novel alternatives have been investigated which are beyond the scope of this research.

5.1 Background

There seems to be a disagreement as to whether optimum flow rates exist for both sides of the heat exchanger. Hollands (1992) argues that there is an optimum if the UA of the heat exchanger is held conceptually fixed. He argues that the difference obtained by Fanney and Klein (1988), who concluded that there were no optimum flow rates for a system, is due to

using a fixed heat exchanger whose overall conductance, UA, is a strongly increasing function of flow rate. Hollands states that a person skilled in heat exchanger design can design a suitable heat exchanger of any specified UA once the flow rates have been specified.

Hollands ascertains that if the collector flow rate is kept at its optimum value for the current tank flow rate, the simulations performed in the past on systems without heat exchangers are directly applicable to systems with heat exchangers.

Fanney and Klein (1988) state that significant improvement of the SDHW system was not observed by reducing the flow rate of the storage side of the heat exchanger. The experiments performed consisted of a 50% by weight ethylene glycol mixture circulated through the collector loop at a flow rate of 0.0151 kg/s.m^2. Flow rates of 0.020 kg/s.m^2 and 0.0025 kg/s.m^2 were circulated through the storage side of the loop. It was found that the system with the lower tank flow rate required almost 7% more auxiliary energy. However, it is difficult to determine whether these tests were sufficient to determine an optimum with just one collector flow rate. The decrease in performance for the lower flow rate is explained by a significant decrease in the heat exchanger UA resulting from the lower flow rate. The heat exchanger penalty was found to more than offset the improved stratification within the storage tank.

5.2 Heat Exchanger Penalty

The effectiveness, ε, is defined as the ratio of the actual heat transfer to the maximum possible heat transfer rate. The actual heat transfer rate, Q_{HX} (W), is then given in terms of the inlet temperature of the hot fluid, T_{hi} (K), the inlet temperature of the cold fluid, T_{ci} (K), and the minimum of the product of capacitance, Cp (J/kg.K) and flow rate, $\dot{m}$ (kg/s), as shown in equation 5.1.

$$Q_{HX} = \varepsilon(\dot{m}Cp)_{min}(T_{hi} - T_{ci}) \tag{5.1}$$

The number of transfer units (NTU) is a dimensionless parameter indicating heat exchanger size and is defined in equation 5.2.

$$NTU = \frac{UA}{(\dot{m}Cp)_{\min}} \tag{5.2}$$

The overall heat transfer coefficient and area product UA (W/K) is given by equation 5.3.

$$\frac{1}{UA} = \frac{1}{h_i A_i} + \frac{ln\left(D_o/D_i\right)}{2\pi kL}\frac{1}{h_o A_o} \tag{5.3}$$

The two outer terms of equation 5.3 represent the product of the heat transfer coefficient, h (W/m^2.K), and the heat transfer area, A (m^2), for the inner and outer surfaces respectively. The inner term represents the conductive heat transfer through a circular tube wall with inner diameter, D_i (m) and outer diameter D_o (m), length, L (m) and conductance, k (W/m.K).

Depending on the heat exchanger flow arrangement and geometry, correlations can be used to find the effectiveness given the NTU or visa-versa.

A convenient method to analyze the impact of a heat exchanger on a solar domestic hot water system is using the modified heat removal factor F_R' as shown in equation 5.4 (Duffie and Beckman, 1991).

$$\frac{F_R'}{F_R} = \left[1 + \left(\frac{A_c F_R U_L}{(\dot{m}C_p)_{collector}}\right)\left(\frac{(\dot{m}C_p)_{collector}}{\varepsilon(\dot{m}C_p)_{\min}} - 1\right)\right] \qquad (5.4)$$

where F_R is the collector heat removal factor described in chapter 3 and A_c is the collector area (m^2).

The modified heat removal factor can be used to determine the useful energy, Q_u (W), shown in equation 5.5.

$$Q_u = A_c F_R' [G_T - U_L(T_i - T_a)] \qquad (5.5)$$

where G_T (W/m^2) is the absorbed radiation and T_i (K) and T_a (K) are the inlet and ambient temperatures respectively.

The heat exchanger penalty, $\frac{F_R'}{F_R}$, gives an indication of the additional collector area requirement for the same useful energy. Figure 5.1 shows $\frac{F_R'}{F_R}$ as a function of $\frac{\varepsilon(\dot{m}Cp)_{\min}}{(\dot{m}Cp)_{collector}}$ and $\frac{\varepsilon(\dot{m}Cp)_{collector}}{F_R U_L A_c}$ (Duffie and Beckman, 1991).

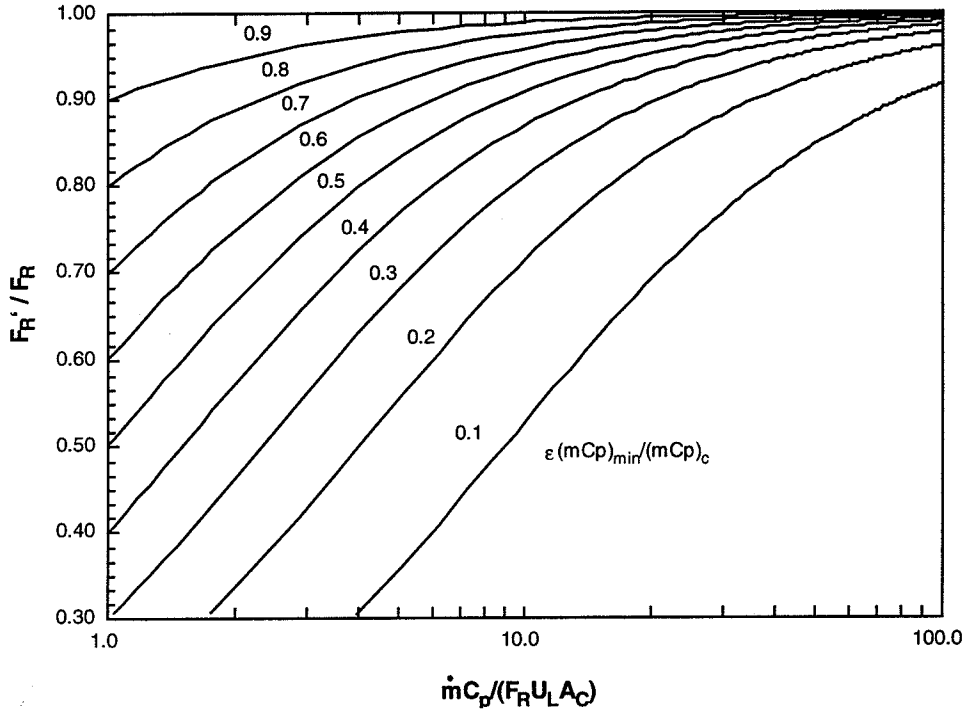

Figure 5.1 Collector heat exchanger correction factor. Adapted from Duffie and Beckman (1991).

However, as mentioned in chapter 2, low-flow systems will tend to have a reduced collector heat removal factor compared to their conventional flow counterparts. Therefore, improved system performance is based on the reduced collector inlet temperature resulting from improved tank stratification and therefore increasing collector efficiency. The collector heat

exchanger correction factor fails to adequately predict the overall system performance for a low-flow system with a stratified tank.

5.3 Optimization of flow rates

Optimal flow rates in solar water heating systems without a heat exchanger have been established (Wuestling, 1985), but the existence of an optimal flow rate for systems using a heat exchanger is still in doubt.

In order to determine the optimal flow rates on either side of the heat exchanger various TRNSYS simulations were performed. All simulations were performed with a collector area of 3.185 m^2, tank volume of 0.4 m^3 and average load of 0.0035 $kg/s.m^2$. In this section, simulations were performed independent of the heat exchanger geometry. A modified NTU was defined as $\frac{UA}{\dot{m}Cp_{collector}}$ regardless of whether $\dot{m}Cp_{collector}$ was the minimum capacitance rate in the collector-tank heat exchanger. Simulations were performed for different ratios of $\dot{m}Cp_{collector}$ to $\dot{m}Cp_{tank}$ ranging from 0.25 to 4.

Figures 5.2 to 5.6 represent the solar fraction as a function of NTU for various ratios of $\dot{m}Cp_{collector}$ to $\dot{m}Cp_{tank}$. Each Figure represents a different constant collector flow rate. The Figures have been organized by different collector flow rates with the NTU values on the abscissa to allow easy comparison of heat exchangers with the same NTU.

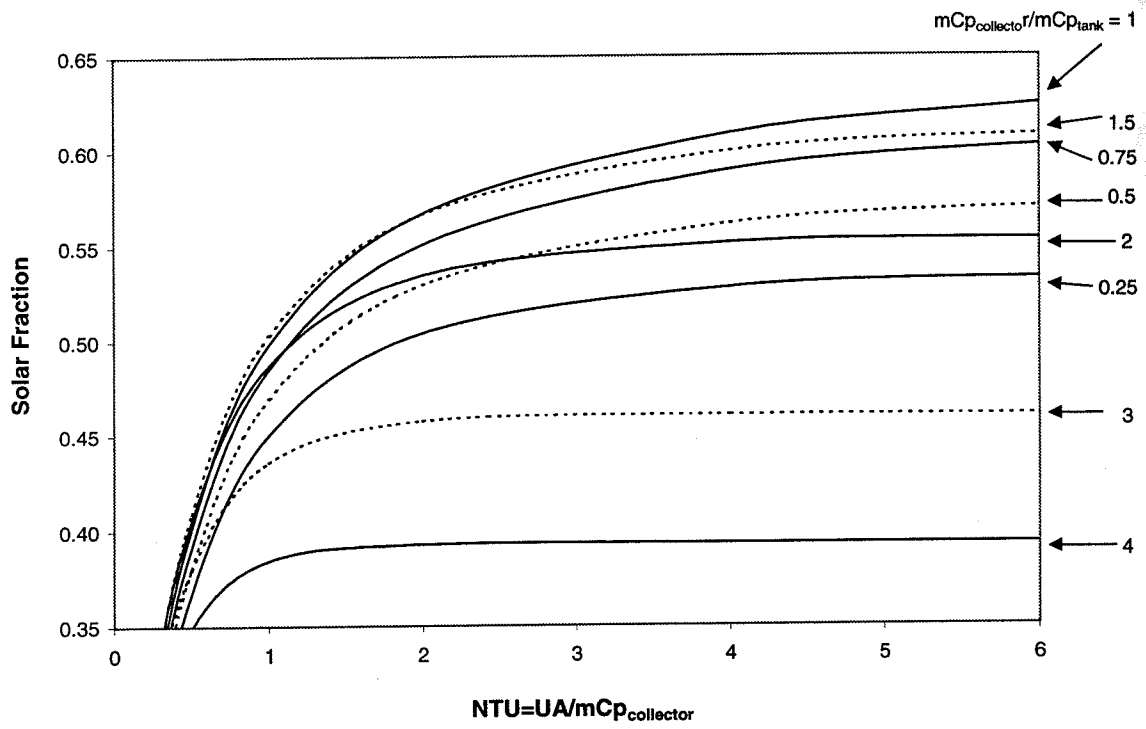

Figure 5.2 NTU vs. solar fraction for a collector flow rate of 0.004 kg/s.m²

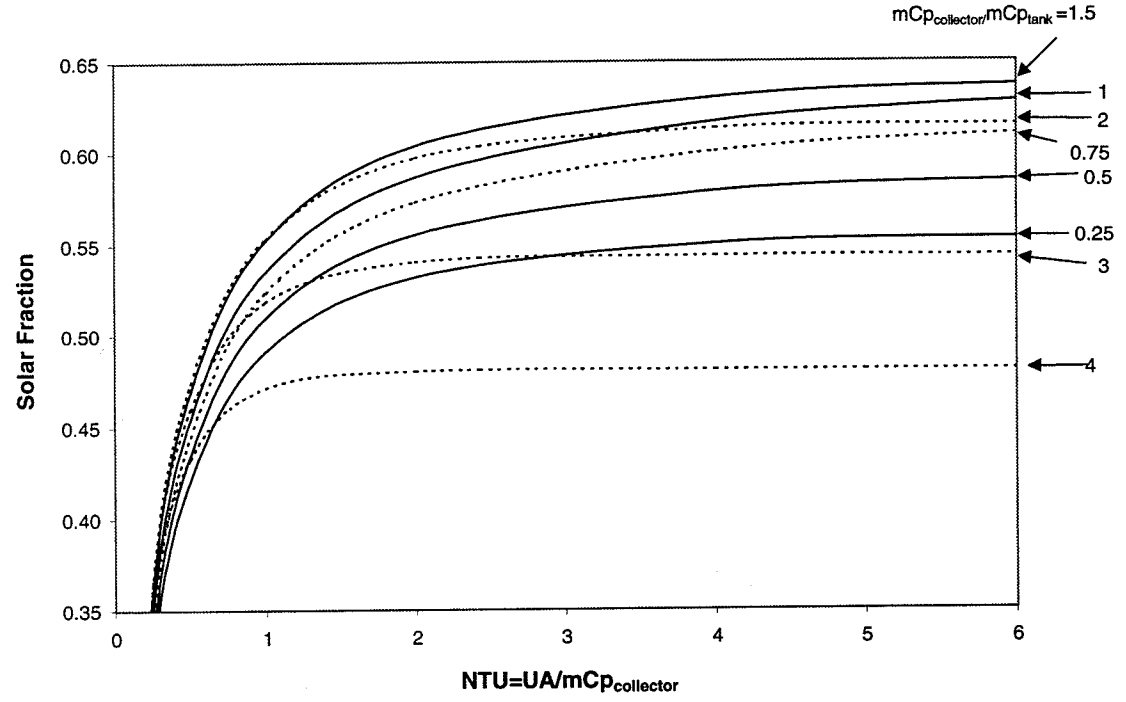

Figure 5.3 NTU vs. solar fraction for a collector flow rate of 0.006 kg/s.m²

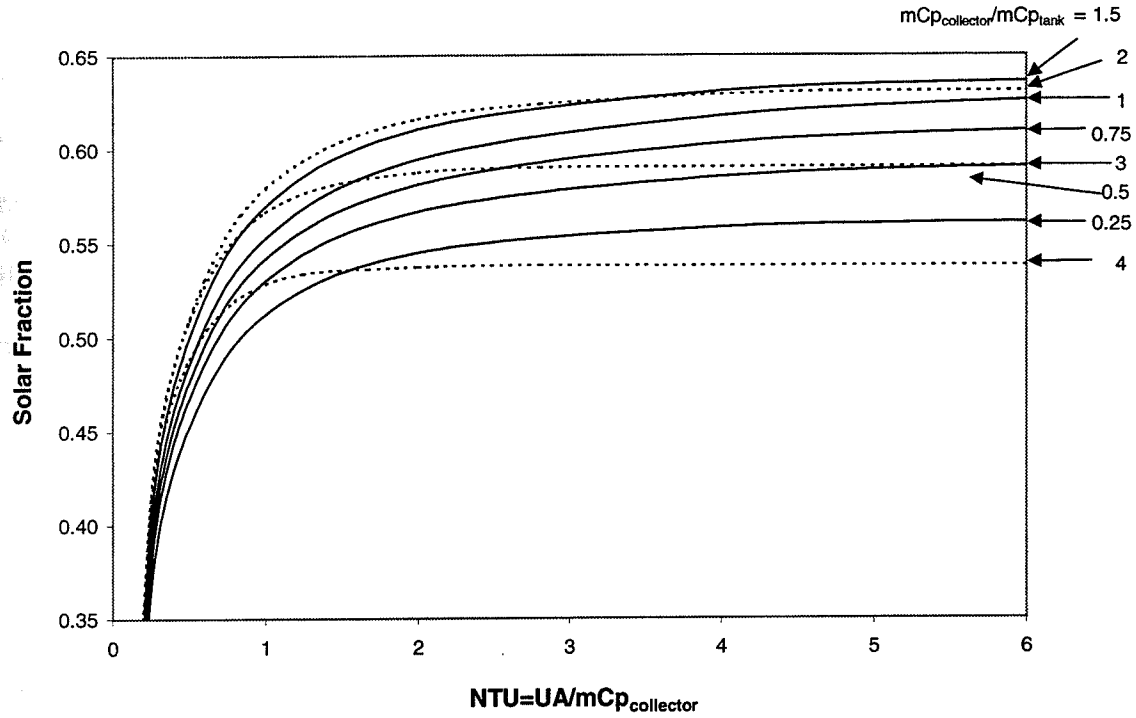

Figure 5.4 NTU vs. solar fraction for a collector flow rate of 0.008 kg/s.m^2

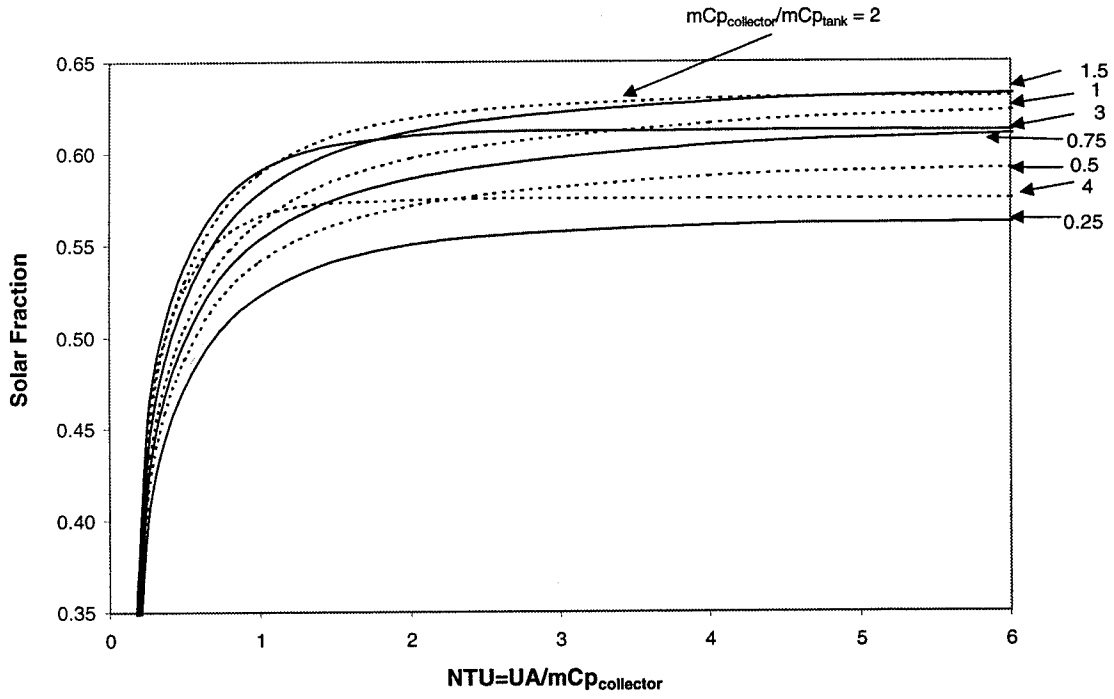

Figure 5.5 NTU vs. solar fraction for a collector flow rate of 0.010 kg/s.m^2

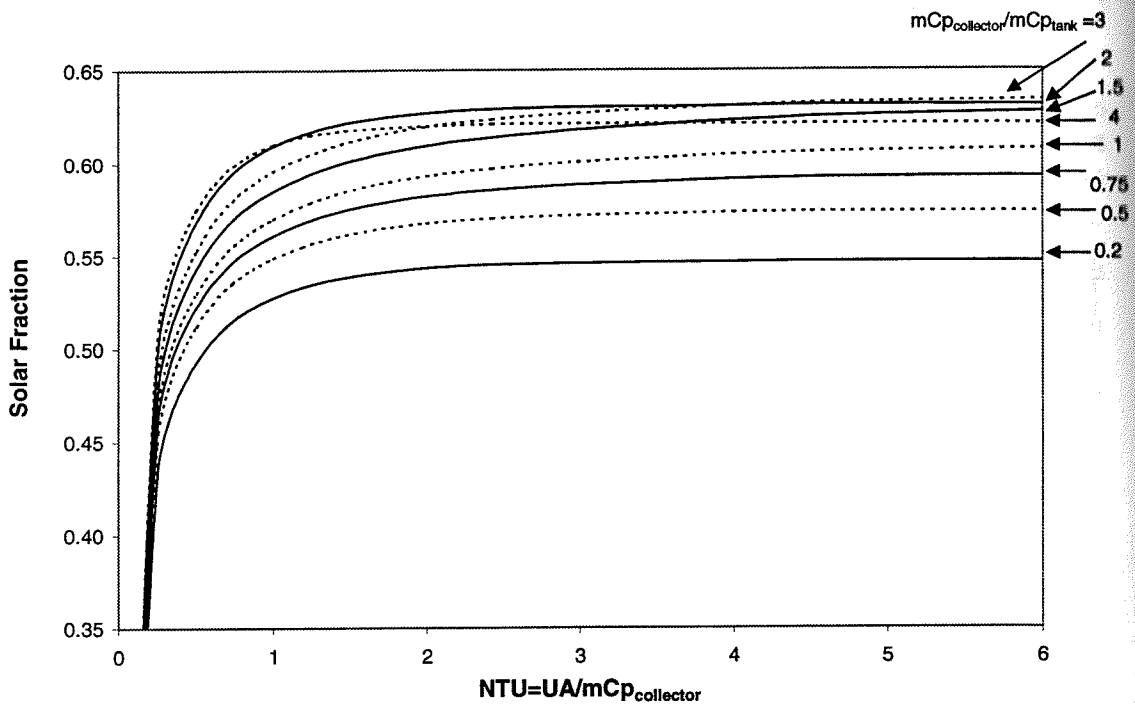

Figure 5.6 NTU vs. solar fraction for a collector flow rate of 0.015 kg/s.m^2

It can be seen that the maximum solar fraction is between 0.63 and 0.64 for all flow rates investigated. The maximum occurs at all flow rates for an NTU of about six. The advantage of a low collector flow rate is that the UA of the heat exchanger need not be as large. For example, the UA for the flow rate of 0.004 kg/sm^2 and $\dot{m}Cp_{collector}$ to $\dot{m}Cp_{tank}$ ratio of 1 has a UA of 273 W/m^2 for an NTU of six, shown in Figure 5.3. For the same NTU and a flow rate of 0.015 kg/sm^2 and $\dot{m}Cp_{collector}$ to $\dot{m}Cp_{tank}$ ratio of 3, shown in Figure 5.6, the UA is 1026 W/m^2. Observing Figure 5.6, it is clear that the same solar fraction can be achieved at an NTU of 3 which signifies a UA of 500 W/m^{2}K, this is still higher than the UA required for lower flows. A smaller UA implies a smaller and more economical heat exchanger.

An interesting outcome of these results is that the optimal ratio of the collector capacitance rate to the tank capacitance rate is not always the same and ranges from 1 to 2 as the collector flow rate increases. For the lower collector flow rates, the optimal tank flow is close to the average daily load draw of 0.0035 kg/s.m^2. Careful observation leads to the conclusion that for the same UA the optimal tank flow rate will be similar at all collector flow rates.

At normal flow rates 0.015 kg/s.m^2 the ratio of the collector capacitance to the tank capacitance has less effect on the solar fraction. For example, ratios of collector capacitance to tank capacitance of 2, 3, 1.5 and 4 result in almost the same solar fraction. However, at low flow rates of 0.004 kg/s.m^2 there is a greater difference in solar fraction at different capacitance rate ratios. It is therefore necessary to carefully choose the flow rates on the tank side when the collector flow rate is low in order to improve system performance.

5.4 Heat Exchanger model

The results presented in section 5.3 are convenient for comparing heat exchangers that have the same NTU for different flow rates. However, it is more intuitive to look at a fixed heat exchanger and examine the effects of varying the flow rate.

An external heat exchanger was chosen to produce the following simulation results. External heat exchangers allow the tank to stratify as opposed to internal heat exchangers which lie inside the tank or wrap-around heat exchangers which are wrapped around the tank and therefore disturb the temperature distribution within the tank. A tube-in-shell heat

exchanger model was used. A propylene or ethylene glycol solution is used inside the tubes, to help prevent fouling, and water is used in the shell. A schematic of a tube-in-shell heat exchanger is shown in Figure 5.7.

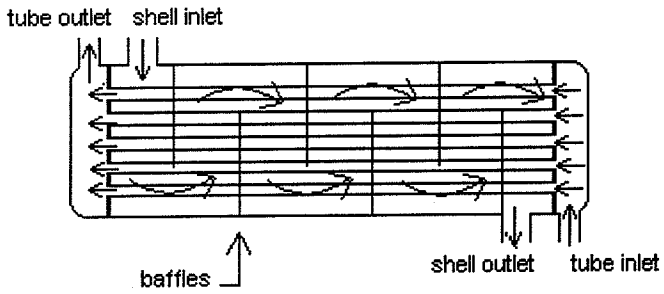

Figure 5.7 Tube-in-Shell Heat Exchanger

In order to model the heat transfer in the tube-in-shell heat exchanger the UA product must be found. Recall from equation 5.3 that the UA product is a function of the heat transfer coefficients of both fluid streams. The heat transfer coefficient is given by the Nusselt number shown in equation 5.6.

$$Nu = \frac{h_{fi} k}{D} \tag{5.6}$$

where h_{fi} (W/m^2.K) is the heat transfer coefficient, D (m) is the hydraulic diameter and k (W/m.K) is the conductivity of the fluid.

The heat transfer coefficient for the glycol stream inside the tubes can be found from the Colburn equation (Incropera and DeWitt, 1990) given in equation 5.7.

$$Nu_D = 0.023 Re_D^{4/5} Pr^{1/3} \tag{5.7}$$

where Re is the Reynolds number and Pr is the Prandtl number.

Zhukauskas (Kakaç et al, 1987) developed a correlation for flow over tube bundles, given in equation 5.8.

$$\overline{Nu}_D = C_1 C_2 Re_{D,max}^m Pr^{0.36} \left(\frac{Pr}{Pr_s} \right)^{1/4} \tag{5.8}$$

where all properties are evaluated at the arithmetic mean of the fluid inlet and outlet temperature, except for Pr_s, which is the Prandtl number evaluated at the surface temperature. C_1 and m are constants listed in table 5.1 and C_2 is the correction factor for less than 20 tubes shown in Figure 5.8. The Reynolds number for the shell side is determined from the velocity through the tube bank. The cross sectional area is required to calculate the velocity from the mass flow rate and is usually taken as the area between the baffles and tubes.

Reynolds Number		C_1	m
10^0-10^2	aligned	0.90	0.40
10^2-10^3	aligned	0.52	0.50
10^3-$2x10^5$	aligned	0.27	0.63
$2x10^5$-$2x10^6$	aligned	0.033	0.80
10^0-$5x10^2$	staggered	1.04	0.40
$5x10^2$-10^3	staggered	0.71	0.50
10^3-$2x10^5$	staggered	$0.35\left(\frac{S_T}{S_L}\right)^{0.2}$	0.60
$2x10^5$-$2x10^6$	staggered	$0.031\left(\frac{S_T}{S_L}\right)^{0.2}$	0.80

Table 5.1 Constants for the Zhukauskas correlation

In table 5.1 S_T is the transverse pitch of the tube bank and S_L is the longitudinal pitch of the tube bank.

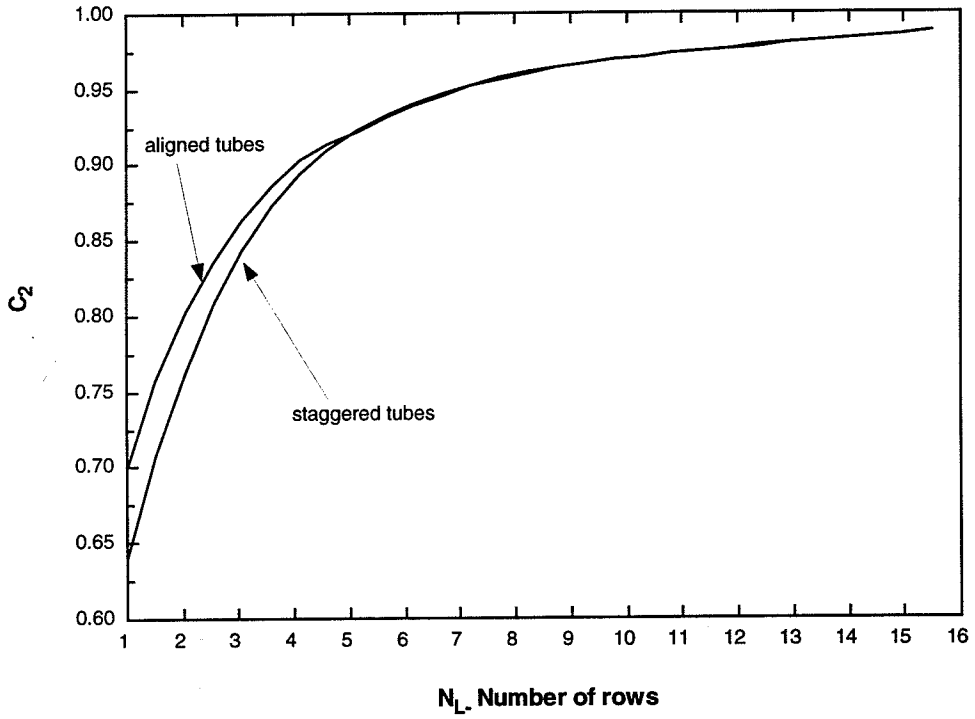

Figure 5.8 Correction factor for less than 20 rows

The standard TRNSYS type for a heat exchanger, TYPE 5, models a heat exchanger based on a constant effectiveness or UA. A new type, TYPE 87, was written with UA as a function of flow rate and temperature for a tube-in-shell heat exchanger using the above correlations. The advantage of having UA as a function of flow rate is that it allows the use of a PV pump that has varying flow rates. However, in order to implement the new type, a modification had to be made to TYPE 5 to allow UA to be entered as a variable input and not as a constant parameter.

5.4.1 Property Data

The fluid in the collector loop is usually a solution of 50% water and 50% glycol. Ethylene glycol or propylene glycol is often used. Ethylene glycol is toxic and often requires a double-wall heat exchanger to comply with domestic hot water regulations whereas a single-wall heat exchanger can be used with propylene glycol.

The viscosities of ethylene glycol and propylene glycol have a large temperature dependence. At low temperatures, it is very viscous and if the flow rate is low the flow regime is laminar and heat transfer is dramatically reduced.

In order to simulate the variation of properties with temperature a new TRNSYS type, TYPE 88, was created which gives viscosity, specific heat, thermal conductivity and density as a function of temperature and composition for propylene glycol, ethylene glycol and water. The new TRNSYS type is documented in appendix A.

A tube-in-shell heat exchanger was designed with a UA of approximately 250 $W/m^2.K$ for a collector flow rate of 0.004 $kg/s.m^2$ and a tank flow rate of 0.004 $kg/s.m^2$ using the results of Figure 5.2. The resulting heat exchanger and dimensions are shown in Figure 5.9.

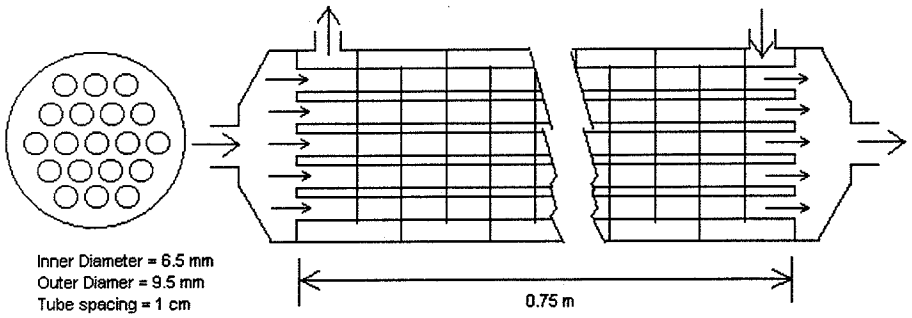

Figure 5.9 Tube-In-Shell Heat Exchanger Dimensions

Figure 5.10 demonstrates the variation of UA with temperature for equal flow rates on both sides of the heat exchanger loop with ethylene glycol and propylene glycol in the collector loop.

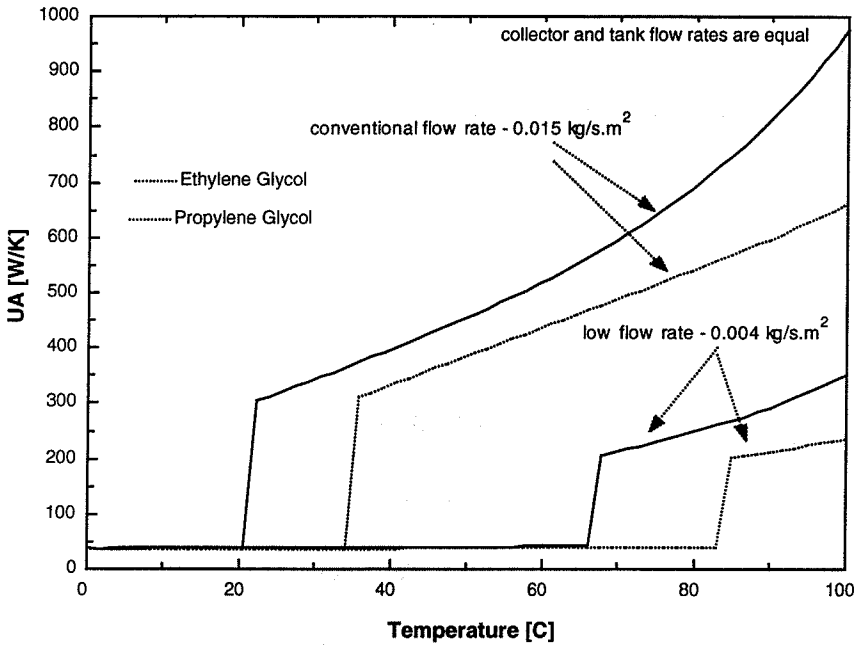

Figure 5.10 Variation of UA with temperature, using a tube-in-shell heat exchanger for collector fluids of ethylene glycol and propylene glycol.

The transition from laminar to turbulent flow, shown in Figure 5.10, for the given heat exchanger, can be seen to occur at about 23°C for conventional flow and 68°C for low flow for ethylene glycol. The transition from laminar to turbulent flow for propylene glycol occurs about 15°C higher than the ethylene glycol. The properties are evaluated at the average of the inlet and outlet temperatures of the heat exchanger. However, with such a sharp change from laminar to turbulent flow, evaluating the properties at the average of the inlet and outlet temperatures of the heat exchanger is probably not correct, except when the flow is far from transition. The temperature of the glycol, on average, should be higher than 23°C when the pump is circulating. Therefore, at low flow rates one will expect laminar flow, for the given heat exchanger, for a greater range of temperatures than the conventional flow system.

Using the specified tube-in-shell heat exchanger, a comparison was made using ethylene glycol with constant properties (independent of temperature) and using TYPE 88 with temperature dependent properties. The results for the annual solar fraction for various tank flow rate and collector flow rate combinations for constant ethylene glycol properties are shown in Figure 5.11, while the results for temperature dependent properties are shown in Figure 5.12. Figure 5.11 reveals that an optimal tank flow rate exists at 0.0035 kg/s.m^2 (equivalent to the average daily load) and an optimal collector flow rate exists at 0.004 kg/s.m^2. However, Figure 5.12 shows this will not be the case. The increased viscosity of glycol impedes the onset of turbulence, which is detrimental to the heat exchanger UA. In this case, the optimal tank flow rate is maintained equivalent to the average daily water draw, but it seems that increasing the collector flow rate will increase the performance. Note that a design would not be far off from the optimal tank flow rate if the designer chose the design based on fixed properties rather than variable properties. The only draw back is that the system performance would be underestimated.

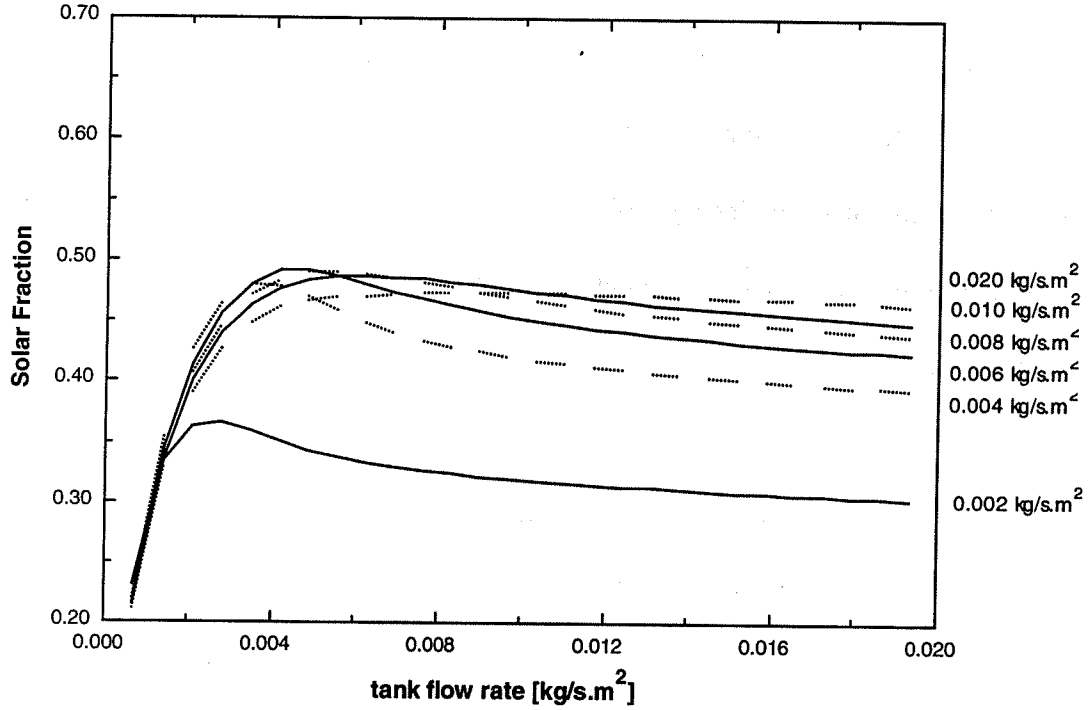

Figure 5.11 Annual solar fraction for Madison maintaining ethylene glycol properties fixed.

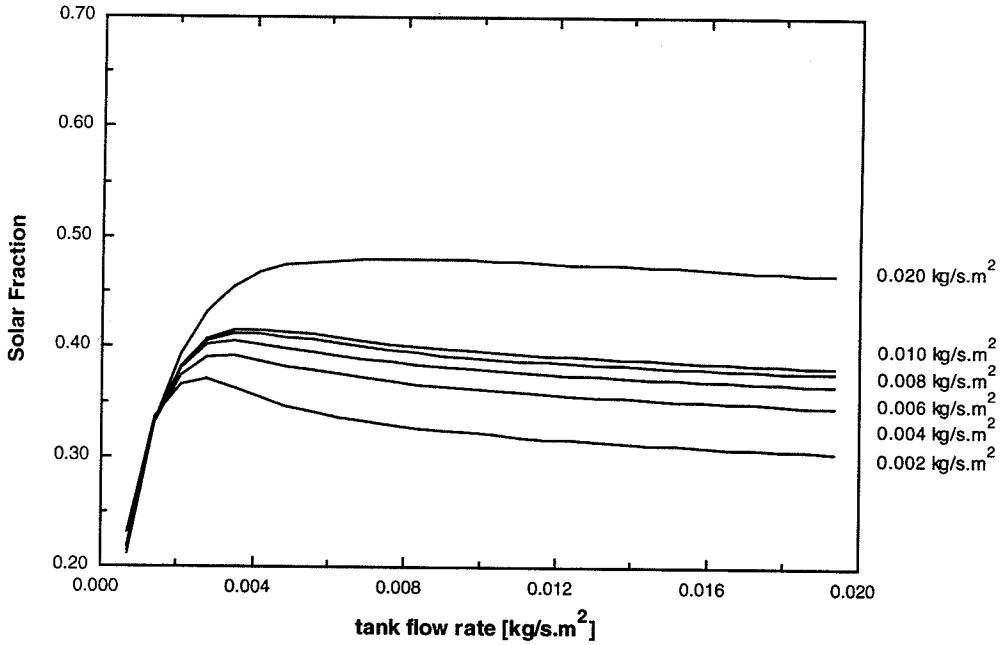

Figure 5.12 Annual solar fraction for Madison with temperature dependent properties for ethylene glycol.

Similarly, the results are shown for propylene glycol in Figure 5.13. The viscosities of both substances are similar, however the thermal conductivity for ethylene glycol is slightly higher than the conductivity for propylene glycol, whereas the specific heat for propylene glycol is higher than ethylene glycol. It seems the increased conductivity for ethylene glycol may give it the advantage as a better antifreeze fluid, although it does require the use of a double-wall heat exchanger.

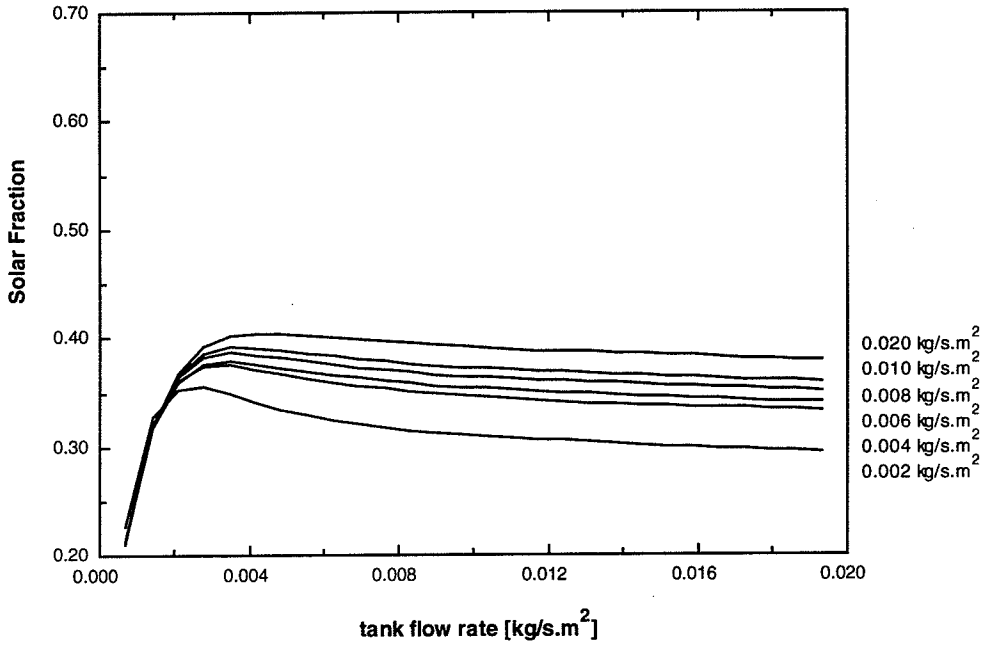

Figure 5.13 Annual solar fraction for Madison with temperature dependent properties for propylene glycol.

To further emphasize the effects of increased viscosity for the antifreeze fluids a simulation with a water-water heat exchanger was performed as shown in Figure 5.14. The results are very similar to those obtained for the ethylene glycol model (Figure 5.11) with constant properties. In Figure 5.14, the water properties are temperature dependent. Again an

optimum tank flow rate is found to be at the average daily load, but the ideal collector flow rate is found quite low, 0.004 kg/s.m^2. Unfortunately, this simulation only points out the penalty of using an antifreeze solution, and has no practical application.

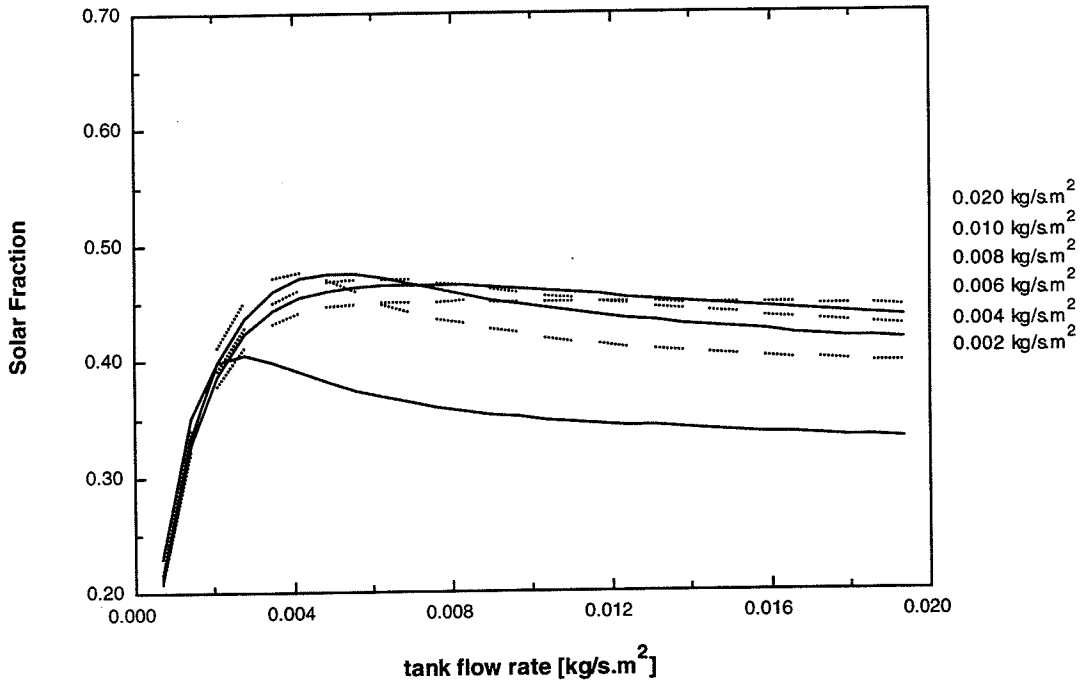

Figure 5.14 Water-Water heat exchanger for Madison

In order to induce turbulent flow, the tube diameters could be reduced, but this leads to very large pressure drops. For example, if the tube diameter were reduced by a third then the pressure increase would be equivalent to 3^5, (362) times the original pressure drop. The increase of 3^5 is derived from equations 5.9-5.11. This high-pressure drop is not acceptable; therefore, the tube diameter will not be reduced in this analysis.

$$P = f\frac{L}{D}\rho\frac{\vec{v}^2}{2} \qquad (5.9)$$

where P is the pressure drop (Pa), f is the friction factor from the Moody chart, L is the tube length (m), D is the tube diameter (m), ρ is the fluid density (kg/m^3) and $\bar{v}$ is the fluid velocity (m/s) given in equation 5.10.

$$\bar{v} = \frac{\dot{m}}{\rho \frac{\pi D^2}{4}} \tag{5.10}$$

where $\dot{m}$ is the mass flow rate (kg/s). Substituting equation 5.10 into 5.9 results in equation 5.11 and it is clear that the pressure drop is proportional to $\frac{1}{D^5}$.

$$P = 8f \frac{L}{D^5} \frac{\dot{m}^2}{\rho \pi^2} \tag{5.11}$$

5.4.2 Tank Stratification

The next stage in heat exchanger analysis is to observe the effects of using propylene glycol with a fully mixed tank. Figure 5.15 demonstrates the impact of a fully mixed tank. Unlike the previous simulations where a stratified tank gave an optimal tank flow rate at the average daily load of 0.0035 kg/s.m^2, there is no optimal tank flow rate. System performance increases with increasing tank flow rate. Also, note that system performance is considerably reduced when compared to the same system with a stratified tank shown in Figure 5.13.

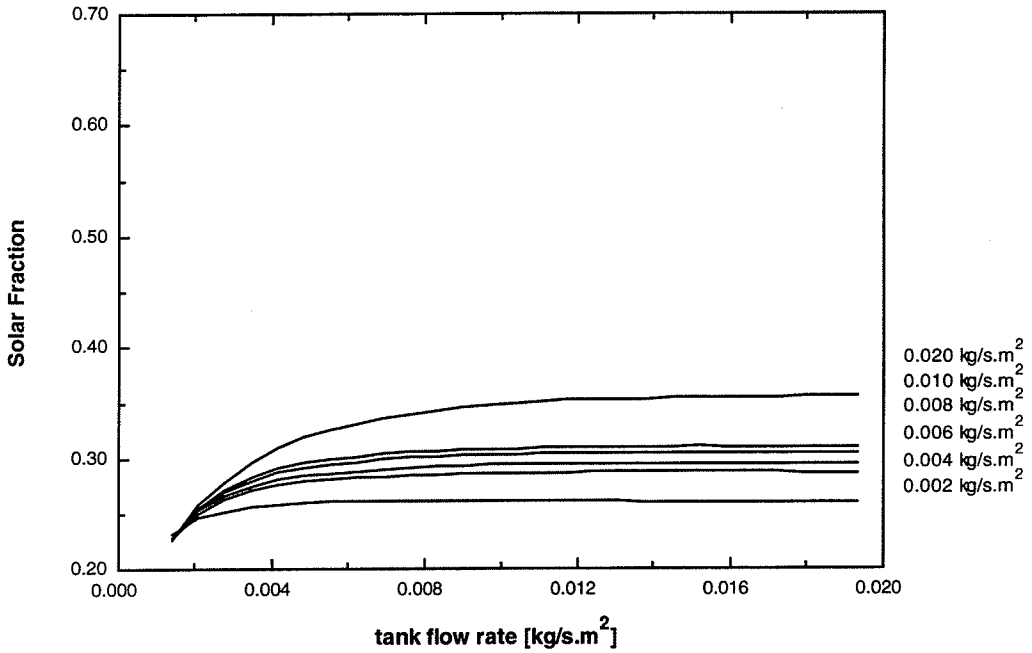

Figure 5.15 Fully mixed tank using propylene glycol for Madison

5.4.3 Effect of Season and Location

The curves given in Figure 5.12 and 5.13 reveal some interesting insights into optimal heat exchanger operation, but in order to generalize these results more information is needed on how performance will be affected by season and location.

Figure 5.16 demonstrates the heat exchanger performance for the month of July in Madison with propylene glycol as the heat transfer fluid. The same trend as shown in Figure 5.13 is observed, however the optimum tank flow rate is more marked.

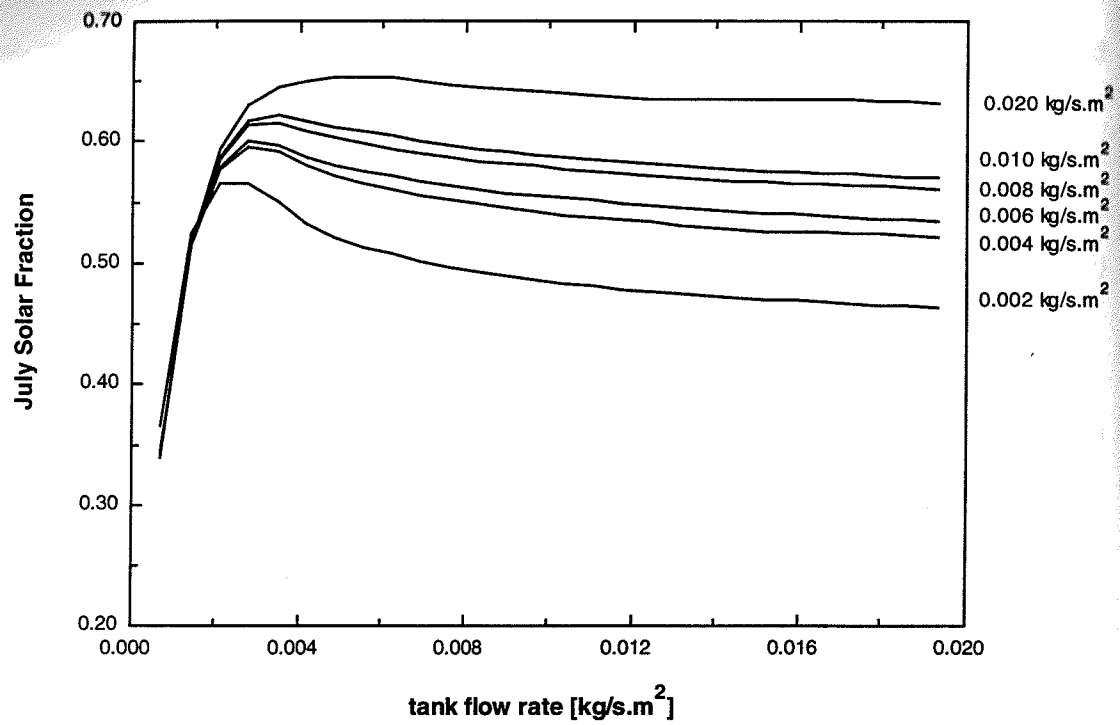

Figure 5.16 Heat exchanger with propylene glycol in Madison for the month of July

Similarly, the same trend is observed for the annual solar fraction for Miami using propylene glycol and ethylene glycol, as shown in Figures 5.17 and 5.18.

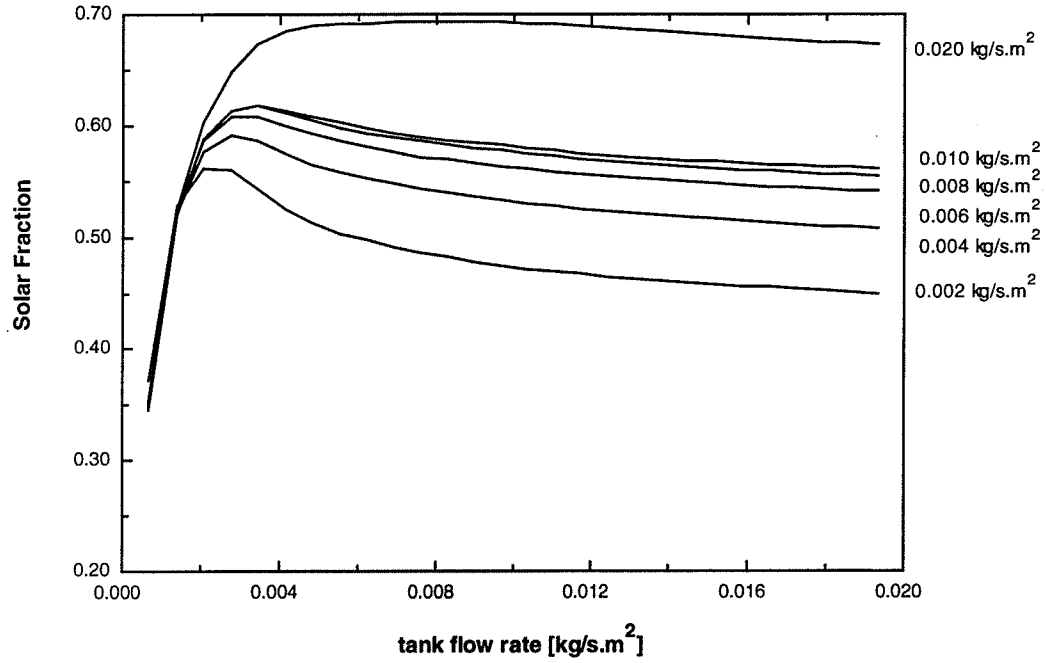

Figure 5.17 Heat exchanger with ethylene glycol in Miami

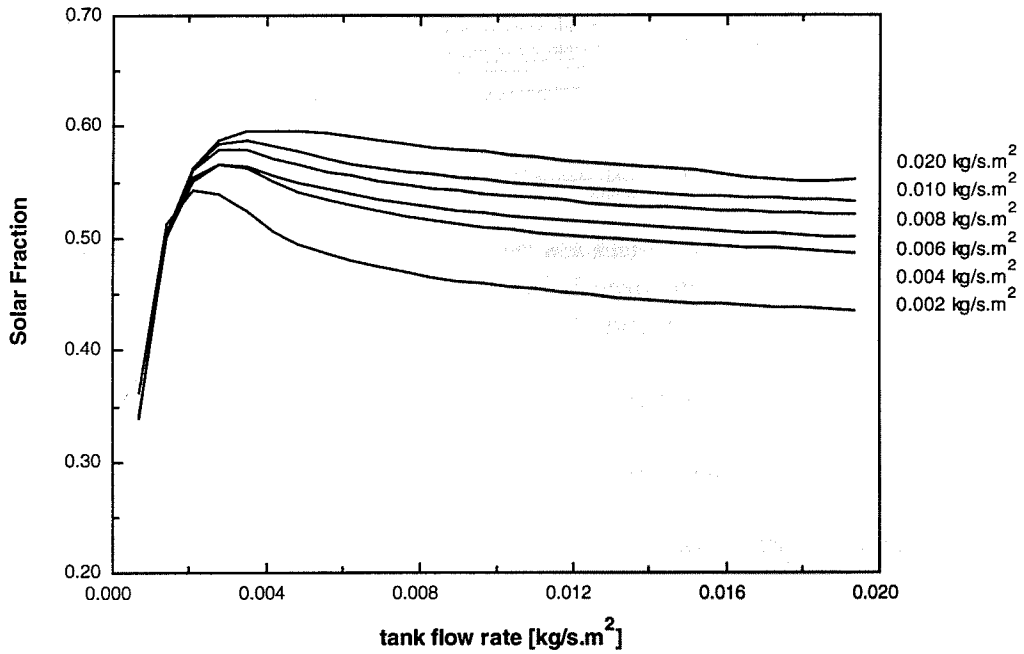

Figure 5.18 Heat exchanger with propylene glycol in Miami

5.4.4 Variation of Heat Exchanger Performance

The heat exchanger used to obtain the results in the previous sections has an extremely good performance. The effect of decreasing and increasing the heat transfer areas is presented in Figures 5.19 and 5.20. Figure 5.21 presents the performance of a propylene–water heat exchanger with an effectiveness of one.

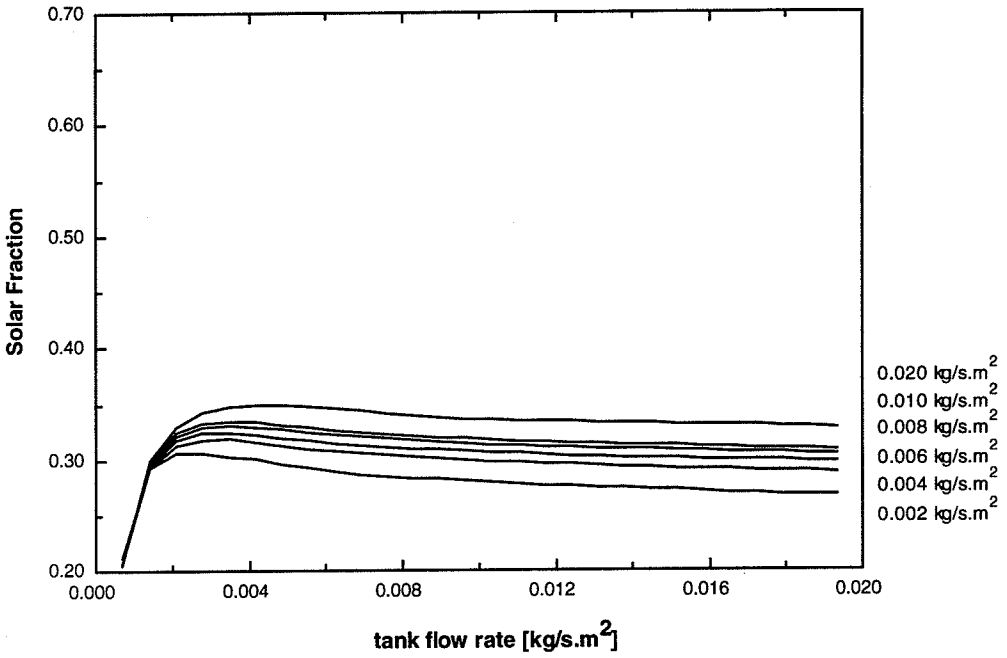

Figure 5.19 Heat exchanger with area halved for Madison

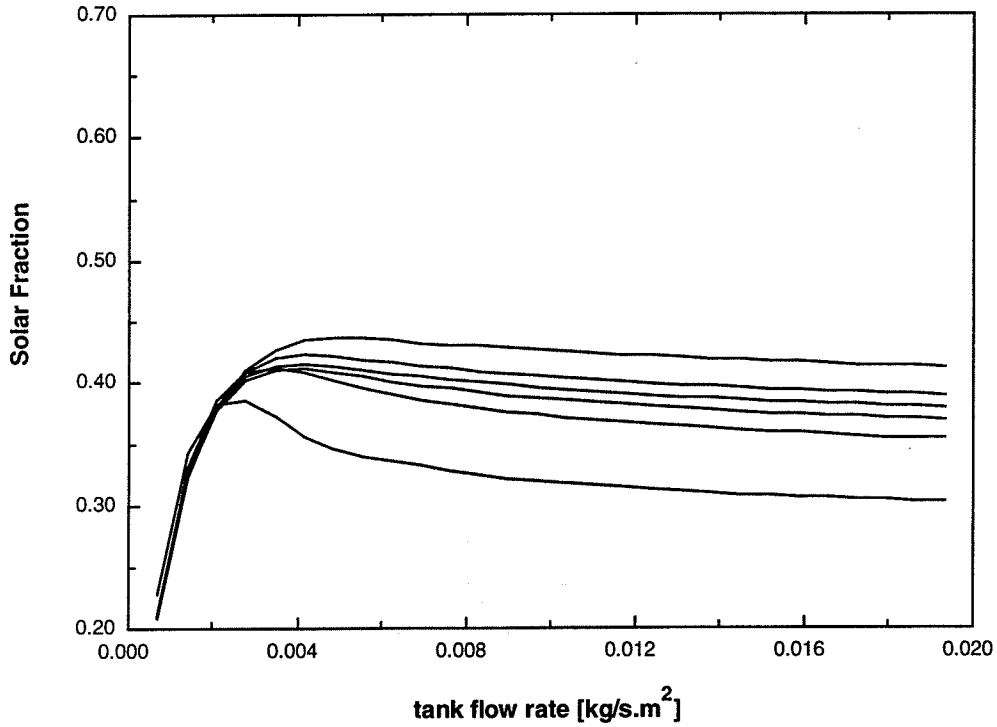

Figure 5.20 Heat exchanger with area doubled for Madison

For a tank flow rate of 0.0035 kg/s.m^2 and a collector flow rate of 0.004 kg/s.m^2 the annual solar fraction is 0.37 for the heat exchanger given in Figure 5.13. Decreasing the heat exchanger length by half and therefore reducing the heat exchange area by half produces an annual solar fraction of 0.32 for the same conditions, shown in Figure 5.19. On the other hand doubling the heat exchanger area, shown in Figure 5.20, increases the solar fraction to about 0.42. Therefore, doubling the heat exchanger area will increase the solar fraction by five percent and decreasing the area will decrease the solar fraction by five percent. A perfect heat exchanger with an effectiveness of one, given in Figure 5.21, yields a solar fraction of almost 0.45.

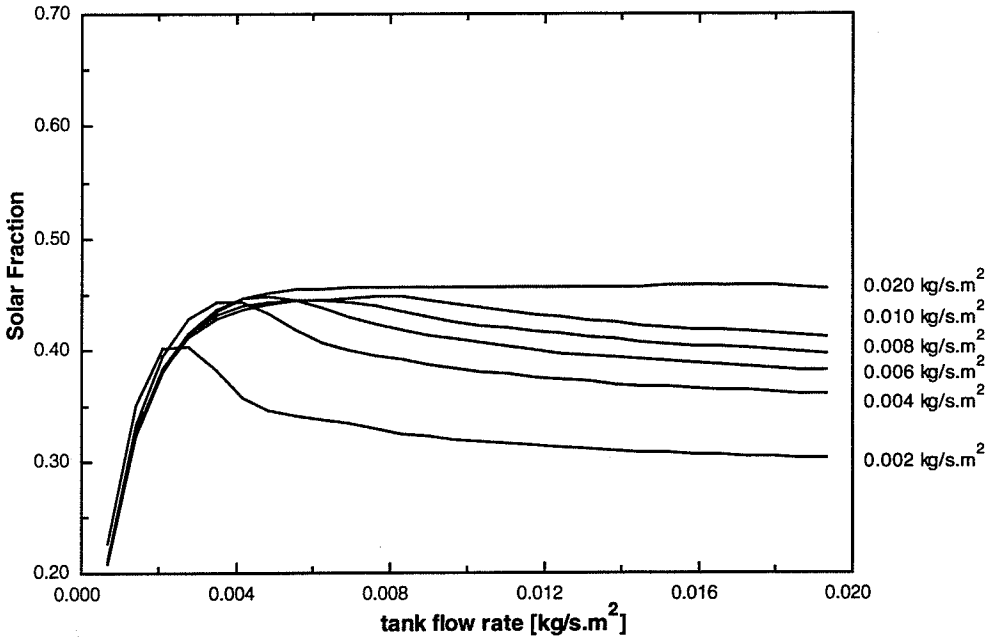

Figure 5.21 Heat Exchanger with an effectiveness of one for Madison

5.4.5 Conclusions for Optimizing Flow Rates

In conclusion, the tube-in-shell heat exchanger is greatly affected by large temperature-dependent property variations. Ethylene glycol performs better than propylene glycol, however as it is toxic it will require a double-wall heat exchanger. Investigation of other antifreeze substances that do not have such temperature dependent properties may yield better system performance. The increase in performance is shown by using a theoretical water-water heat exchanger. Increasing the collector flow rate does increase system performance when glycol antifreeze is used. This increase is due to the onset of turbulent flow, and hence improved heat transfer, which does not occur at low flow rates due to the viscosity of the glycol antifreeze.

System performance is improved with the use of a stratified tank. The optimum tank flow rate is always found to be very close to the load flow rate. Small variations from this flow rate can lead to drastic decreases in system performance.

The general trend for the solar fraction as a function of tank and collector flow rates was found independent of location and season. Small improvements on the order of 5 % can be made by increasing the heat exchanger heat transfer area. The optimization of the heat exchanger size than becomes a question of economics.

It seems that Hollands is correct in stating that optimum flow rates exist for a heat exchanger with a conceptually fixed UA. Even with a heat exchanger with UA as a function of flow rate, an optimum flow rate exists (even if it is just an economic optimum). The results obtained by Fanney and Klein are also correct. For a heat exchanger with a conventional collector flow rate, such as 0.0151 kg/s.m^2 used by Fanney and Klein, the tank flow rate has little influence given the tank flow rate is larger than the average load. Since Fanney and Klein found reduced performance for a lower tank flow rate, it is possible that the tank flow rate used was below the average load and mixing was occurring.

5.5 Natural Convection Heat Exchangers

Recently, there has been much study on the use of natural convection heat exchangers (NCHE) in solar domestic hot water systems. The use of natural convection heat exchangers can reduce system cost and electric demand. The flow rate of the water in the tank side is driven by buoyancy forces that result from the density variations caused by the temperature

of the fluid. The heat exchanger eliminates the need for a pump and control system for the waterside of the loop. The low flow rates induced by the natural convection heat exchanger ensure that the tank remains stratified. NCHEs are capable of producing flow rates of 0.002 kg/s.m^2 in the tank loop (Fraser et al, 1992). Figure 5.22 demonstrates the natural convection heat exchanger loop in a solar domestic hot water system.

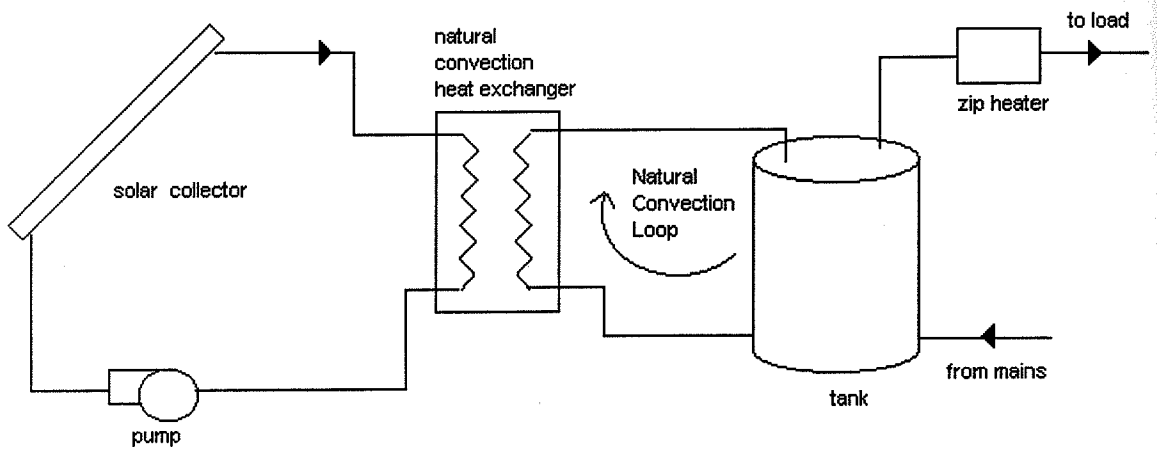

Figure 5.22 Natural convection heat exchanger system (not to scale)

The major difference between a forced flow heat exchanger and a natural convection heat exchanger is that the flow rate depends on the densities (or the temperatures) of the water. These in turn depend on varying system conditions, specifically the tank conditions, the mains temperature, the load draw, and the collector return temperature which is a function of the amount of solar radiation received (Fraser et al, 1992).

Dahl and Davidson (1997) experimentally determined that the heat transfer coefficient area product, UA, is best expressed as a function of Reynolds, Grashoff, and Prandtl numbers on the thermosyphon side of the heat exchanger. They state that existing models for the

thermal and hydraulic performance of thermosyphon heat exchangers, which are functions of the thermosyphon flow rate and collector flow rate only, are not correct.

Dahl and Davidson performed experiments on a natural convection heat exchanger with a constant collector flow rate of 0.03 kg/s. A correlation for the Nusselt number was found, this is shown in equation 5.9.

$$Nu = a\,Pr^{b}\,Re^{c}\,Gr^{d} \qquad (5.12)$$

A linear regression technique was used to determine the parameters a to d. The analysis was performed with a constant collector flow rate in order to determine the effects of natural convection on UA. Unfortunately, no details of optimum collector flow rates are given for this heat exchanger type.

Observing Figures 5.11 to 5.21 it is clear that there exists an optimum tank flow rate. If the tank flow rate is reduced beyond this point, the solar hot water system performance will be dramatically reduced. Increasing the tank flow rate beyond the optimum value will also reduce system performance, with a marked reduction for lower tank flow rates. Therefore, in order to optimize system performance the tank-side flow rate must be appropriately selected. The use of a natural convection heat exchanger may pose difficulties in reaching the optimal tank flow rate if the water draw is very high.

5.6 Conclusions

In determining heat exchanger dimensions and flow rates there exists a thermal optimum in combination with an economical optimum. The optimum heat exchanger flow rates and dimensions are independent of season and location.

The heat exchanger tank-side flow rate should always be approximately equal to the average load flow rate. This optimum is defined in terms of maximum thermal performance, but also in terms of decreased economic costs. Lower flows require smaller hydraulic systems, which are less expensive. For high collector flow rates, the optimum tank flow rate is less marked; therefore increasing the tank flow rate will not largely affect system performance, but will incur increased economical costs.

Large collector flow rates may increase system performance for a given heat exchanger, but will incur larger hydraulic costs in terms of pumping power and piping. Large flow rates also make it more difficult to successfully implement a photovoltaic driven pump due to increased pressure drops.

Use of different antifreeze fluids could also increase system performance. As expected, increasing heat exchanger size will improve the system performance.

Natural convection heat exchangers allow tank stratification. However, if the hot water draw is much greater than the natural circulation, poor system performance could be expected. It has been shown that for forced circulation when the flow rates are lower than the average load the system performance is reduced. The reason that the lower tank flows

destroy system performance is that water is drawn from the tank and replaced by a greater quantity of mains water than solar heated water. Unfortunately, the determination of the tank flow rate must be predicted by the anticipated hot water draw. Over-predicting the hot water draw will be less detrimental to system performance than under-predicting the draw.

There are optimum flow rates on both sides of the heat exchanger as Hollands predicts, even if it is just an economic optimum for the case of conventional flows. The disagreement with the results presented by Fanney and Klein is because they tested the heat exchanger performance for higher collector flow rates. At higher collector flow rates the tank flow rate has less effect on the optimum given that the tank flow rate is greater than the average draw.

CHAPTER 6: OVERALL SYSTEM PERFORMANCE

The performance of serpentine collectors in low-flow systems, the use of PV driven pumps and the optimum flows for heat exchangers have been analyzed. In order to design a high performance system, an assessment of the various system configurations and flow rates was made for four locations in the United States; Albuquerque, New Mexico, Madison, Wisconsin, Miami, Florida, Washington, District of Columbia.

The locations chosen have very different climates. Some climates require freeze protection for more months of the year than others. In the climates where freeze protection is required for very short periods, it may become more feasible not to use the solar hot water system during these months (Bradley, 1997).

The six different systems, which have been compared for each location, are presented below.

The first system is a low-flow system without a heat exchanger. This system uses a serpentine collector with 18 turns and has an area of 3.185 m^2 as described in chapter three. Recall from chapter 3 that the serpentine collector has improved performance over a conventional header-riser collector for low flows. The flow rate used is 0.0035 $kg/s.m^2$, which is approximately matched to the average load draw. The tank is $0.4m^3$ and uses 20 nodes to model stratification.

The second system is similar to the first system, however it incorporates a PV driven pump. The advantage of this system is that complex control systems are eliminated. The pump will only turn on when there is sufficient radiation. In this case, the flow rates will vary throughout the day as the radiation varies.

The third system incorporates a heat exchanger allowing the system to be used in climates where water will freeze. The antifreeze fluid used is ethylene glycol. The heat exchanger used is identical to Figure 5.9. The system is a low-flow system similar to the first system and the collector flow rate is 0.004 kg/s.m^2 through the serpentine collector. The tank flow rate is set to approximately equal the average load with 0.0035 kg/s.m^2. Again, the tank is modeled using 20 nodes.

The fourth system is similar to the third system, however a PV driven pump has been incorporated into the collector side. Similar to the second system, the flow rate will vary throughout the day on the collector side.

The fifth system is a conventional system without a heat exchanger. A header-riser collector is used for a collector flow rate of 0.020 kg/s.m^2. The reason a header-riser collector is normally used for these higher flow rates is to reduce the pressure drop that would otherwise occur in a serpentine collector. The tank is also modeled with 20 nodes.

Last, the sixth system is a conventional system, similar to the fifth system, but with a heat exchanger. The tank flow rate is also maintained equal to the load draw of 0.0035 kg/s.m^2. Simulations were also performed for a tank flow rate of 0.020 kg/s.m^2 and the system was

found to perform slightly lower with a decrease in the solar fraction of less than 1 %. For simplicity, the results for the higher tank flow rate have not been presented.

The collector slopes were chosen to maximize the total annual energy received; Duffie and Beckman (1991) state the maximum occurs when the slope is equal to the latitude. However, for maximum summer availability, the slope should be approximately 10° to 15° less than the latitude. Deviations of fifteen degrees result in performance reductions of up to five percent. In this analysis, the slope is constant at the annual optimum value, which is equal to the latitude of the location.

6.1 Albuquerque, New Mexico

The latitude for Albuquerque, New Mexico is 35.1 degrees and the collector slope was chosen to maximize the annual solar radiation with a value of 35 degrees.

The monthly solar fraction has been calculated for the six different systems and is given in Table 6.1. The TRNSYS simulation decks used are presented in appendix B.

System	*Description*	*Annual solar fraction*
1	Low-flow system without heat exchanger	0.44
2	Low-flow system without heat exchanger and PV driven pump	0.44
3	Low-flow system with heat exchanger	0.64
4	Low-flow system with heat exchanger and PV driven pump	0.62
5	Conventional system without heat exchanger	0.44
6	Conventional system with heat exchanger	0.75

Table 6.1 Solar system performances for Albuquerque, New Mexico.

Because of the clear conditions in Albuquerque, the solar water heating system performs very well with a peak annual solar fraction of 75% using a conventional system with a heat exchanger. The use of a conventional flow heat exchanger is justified since six months of the year typically have freezing temperatures. Freezing temperature data was taken from TRNSYS TMY (Typical Meteorological Year) data. The solar collector was turned off for any month that has temperatures equal or below zero degrees Celsius. The performance of Albuquerque is shown in Figure 6.1. The systems without heat exchangers perform the best during the summer months.

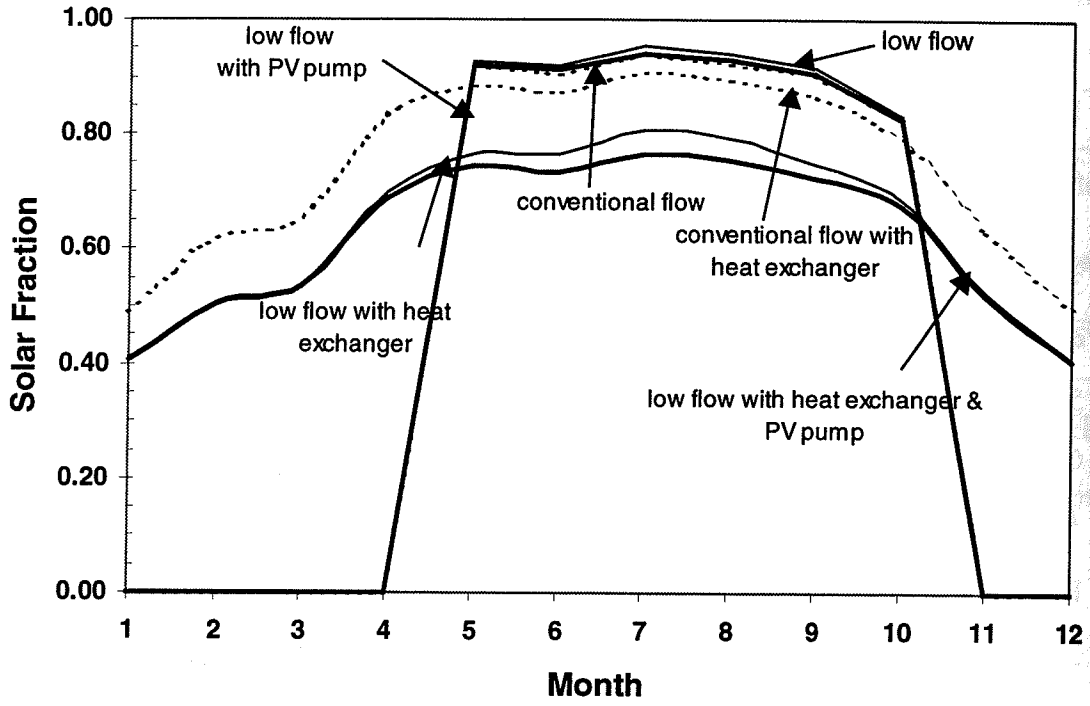

Figure 6.1 Solar hot water system performance in Albuquerque, New Mexico

During the summer months, the low-flow system without a heat exchanger clearly performs better than the conventional flow system. The low-flow system is operating with a flow rate of 0.0035 kg/s.m^2, which is close to the average water draw. As shown in chapter two the optimum flow rate for a direct system is equal to the average water draw as this ensures the tank stays stratified.

For the summer systems, the use of a PV driven pump shows little effect on the performance of the solar hot water system. The PV driven pump has been designed to operate for flow rates ranging from 0.0035 kg/s.m^2 to 0.0045 kg/s.m^2. For lower radiation levels, lower flow rates should be expected whereas for higher radiation levels, higher flow rates will be obtained. PV driven systems have the potential to reduce electricity use during

peak times, when most summer-peaking utilities are experiencing the most electricity demand.

The use of a heat exchanger is needed for Albuquerque where up to six months may have freezing temperatures. The heat exchanger allows the year round use of the solar system thereby increasing the annual solar fraction from 44 % for a low-flow system without a heat exchanger to 75% for a conventional system with a heat exchanger. The conventional system with a heat exchanger performs much better than the low-flow system with a heat exchanger with a solar fraction of 75% compared to 62 %.

Figure 6.2 demonstrates heat exchanger performance for a tank flow rate of 0.0035 kg/s.m^2 subject to various collector flow rates. The specifications for the tube-in-shell heat exchanger are given in Figure 5.9. Two heat exchanger lengths of 0.15 m and 0.75 m have been chosen to demonstrate different heat exchanger effectiveness. The properties for the water and ethylene glycol were taken for 60 °C. Figure 6.2 uses $\varepsilon(\dot{m}Cp)_{min}$ as a measure of performance; recall from chapter 5 that the heat transferred by the heat exchanger is given by equation 6.1

$$Q_{HX} = \varepsilon(\dot{m}Cp)_{min}(T_{hi} - T_{ci}) \qquad (6.1)$$

where Q_{HX} (W) is the actual heat transfer rate, ε is the heat exchanger effectiveness, T_{hi} (K) is the inlet temperature of the hot fluid, T_{ci} (K) is the inlet temperature of the cold fluid, and $(\dot{m}Cp)_{min}$ is the minimum of the product of capacitance, Cp (J/kg.K) and flow rate, $\dot{m}$

(kg/s). T_{hi} and T_{ci} are independent of heat exchanger size and flow rate and therefore the heat transferred for different flow rates and dimensions is directly proportional to $\varepsilon(\dot{m}Cp)_{min}$.

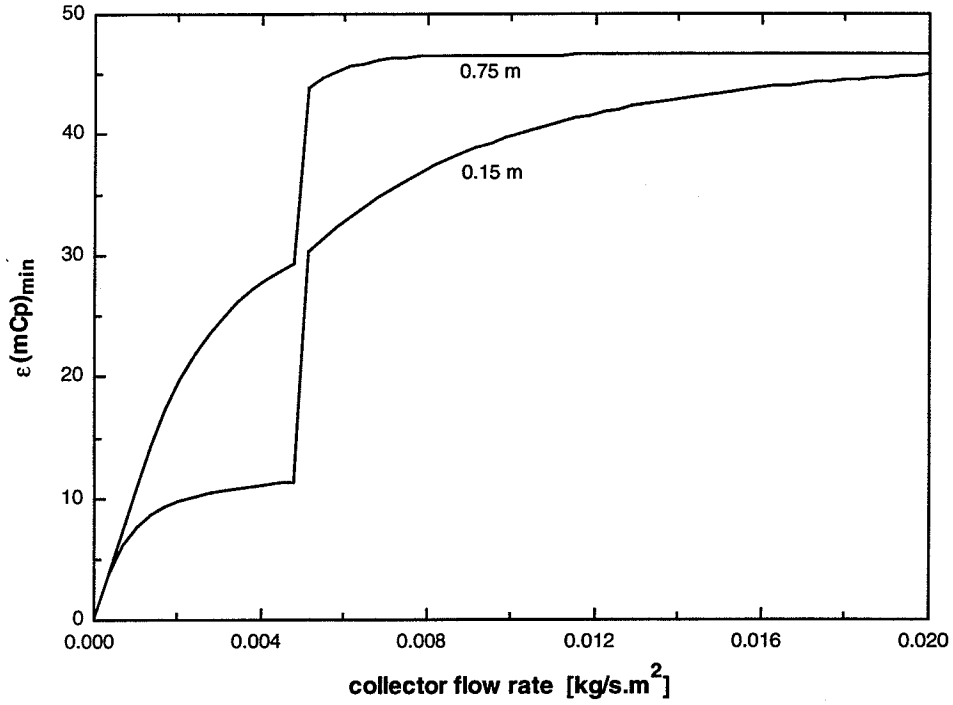

Figure 6.2 Heat Exchanger $\varepsilon(\dot{m}Cp)_{min}$ product as a function of collector flow rate for two heat exchanger lengths.

Figure 6.2 demonstrates the variation of the heat exchanger performance for various flow rates. It is clear that the heat exchanger performs better at conventional flow rates than at low flows. The sudden increase in performance at about 0.005 kg/s.m^2 is due to the transition from laminar to turbulent flow in the tubes of the heat exchanger. In the solar hot water systems tested, the heat exchanger performance is very high. However, if a smaller heat exchanger, for example of 0.15 m in length was used, it can be shown from Figure 6.2 that there would still be a large difference in performance between conventional flow and

low flow. A slightly higher flow on the collector side could potentially improve performance for the lower flow system. Another solution, would be to encourage turbulent flow at lower flow rates by decreasing the tube diameter. The real advantage of lower flows on the collector side is to enable the use of a PV driven pump. A PV driven pump and heat exchanger would have to be designed to encourage turbulent flow through the collector side of the heat exchanger.

6.2 Madison, Wisconsin

The latitude for Madison, Wisconsin is 43.1 degrees and the collector slope used was 40 degrees in order to maximize the annual solar radiation.

The performance of Madison is summarized in Table 6.2 for the various hot water systems.

System	*Description*	*Annual solar fraction*
1	Low-flow system without heat exchanger	0.30
2	Low-flow system without heat exchanger and PV driven pump	0.29
3	Low-flow system with heat exchanger	0.39
4	Low-flow system with heat exchanger and PV driven pump	0.38
5	Conventional system without heat exchanger	0.29
6	Conventional system with heat exchanger	0.46

Table 6.2 Solar system performances for Madison, Wisconsin.

Trends similar to those found in Albuquerque were also found in Madison. Madison experiences long winters with up to seven months of freezing temperatures. It is clear that the use of a heat exchanger is necessary.

For low-flow systems, with or without a heat exchanger, the PV driven pump reduces the annual performance of the system by only one percent. The use of a heat exchanger increases annual performance by nine percent in both the PV driven system and the conventional pump system.

The conventional system without a heat exchanger performs equally to the PV driven low-flow system without a heat exchanger. However, when a heat exchanger is incorporated into the conventional system it performs eight percent better than the low-flow system with a heat exchanger and PV driven pump.

Figure 6.3 demonstrates the yearly performance for the six systems in Madison.

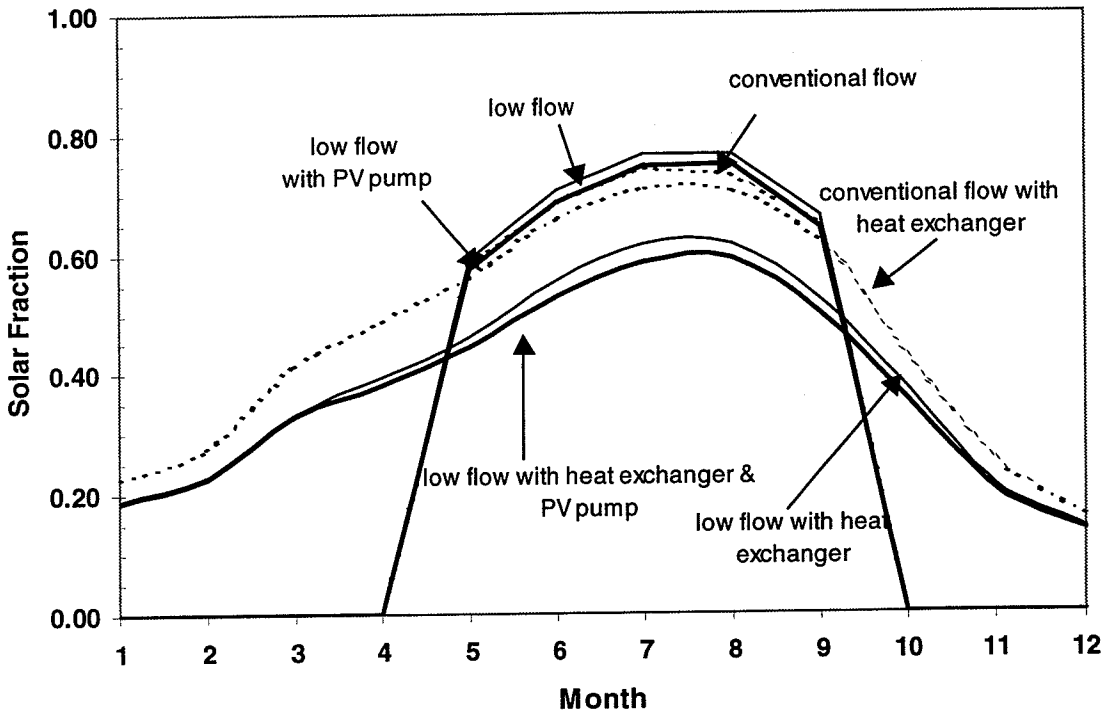

Figure 6.3 Solar hot water system performance in Madison, Wisconsin

Again, similar trends can be seen when comparing the performance of Madison to Albuquerque. The low-flow system with a heat exchanger and a PV driven pump has the same monthly solar fraction than the low-flow system with a heat exchanger for the winter months. The reason for the same performance over the winter months indicates that the collector flow rates for the PV driven pump are closer to those of a conventional circulation system. This is most likely due to the combined effects of reduced solar radiation and lower ambient temperatures influencing the power output of the photovoltaic panel and therefore the flow rate.

6.3 Miami, Florida

Miami, Florida has a latitude 25.8 degrees. The collector slope was set to 25 degrees to ensure that the collector was maximized for a yearly annual fraction.

Miami rarely experiences temperatures at or below the freezing point of water. This means that heat exchangers are not necessary. However, the results for all six systems are presented in Table 6.3 for comparison of the heat exchanger penalties.

System	***Description***	***Annual solar fraction***
1	Low-flow system without heat exchanger	0.73
2	Low-flow system without heat exchanger and PV driven pump	0.69
3	Low-flow system with heat exchanger	0.59
4	Low-flow system with heat exchanger and PV driven pump	0.54
5	Conventional system without heat exchanger	0.69
6	Conventional system with heat exchanger	0.52

Table 6.3 Solar system performances for Miami, Florida.

The highest annual fraction observed for Miami is 73% for a low-flow system without a heat exchanger and with a conventional pump. The low-flow system without a heat exchanger utilizing the PV driven pump performed the same as the conventional system without a heat exchanger with an annual solar fraction of 69%. The penalty imposed by adding a heat exchanger ranged from 14 to 17 % for all systems.

Figure 6.4 shows the yearly performance for the six systems.

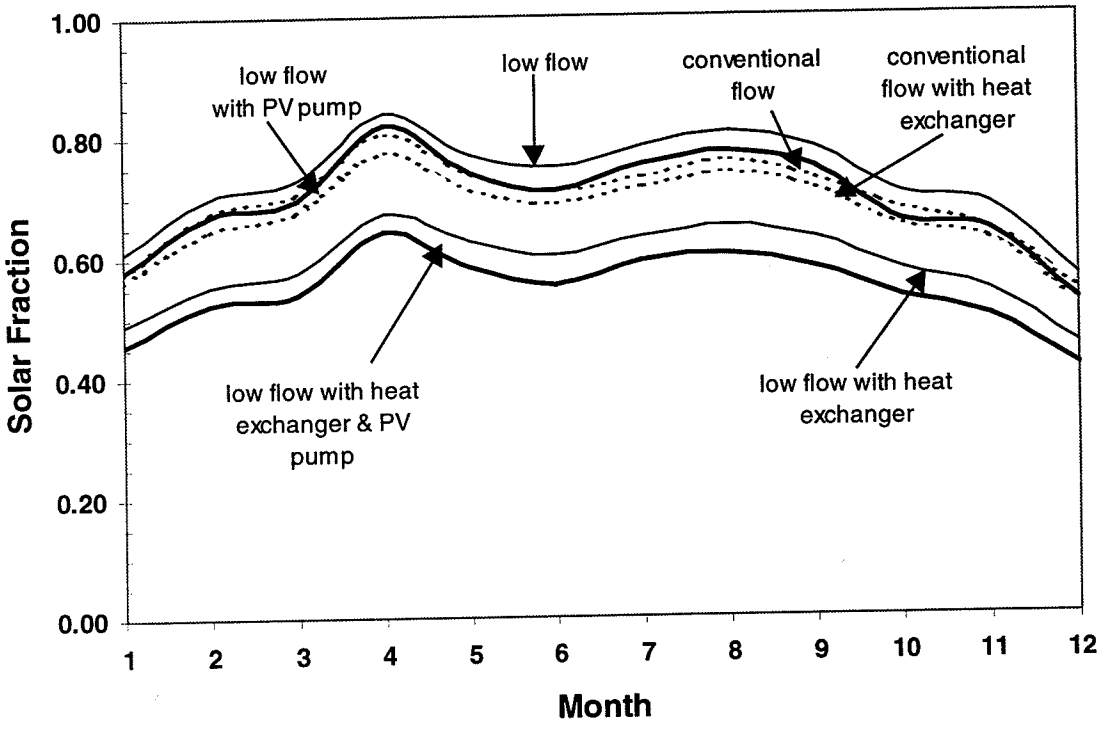

Figure 6.4 Solar hot water system performance in Miami, Florida

For the case of Miami, the PV driven pump systems and the conventional pump systems do not perform the same for the winter months. This contrast to the other locations is

explained by the small variations of ambient temperature and radiation experienced in Miami throughout the year.

The conventional system and the PV driven system have the same annual solar fraction, but they perform differently throughout the year. The PV driven system performs slightly better during the summer months whereas the conventional system performs better during the winter months. Again, these are the effects of the ambient temperature and radiation on the photovoltaic panel.

6.4 Washington, DC

Washington, DC has a latitude of 39 degrees. The collector slope was sloped at 40 degrees to maximize the annual solar fraction.

The climate for Washington is similar to Madison with seven months of freezing temperatures; this is shown by the similar results in annual solar fractions for the six systems in Table 6.2 and Table 6.4.

System	*Description*	*Annual solar fraction*
1	Low-flow system without heat exchanger	0.31
2	Low-flow system without heat exchanger and PV driven pump	0.30
3	Low-flow system with heat exchanger	0.43
4	Low-flow system with heat exchanger and PV driven pump	0.41
5	Conventional system without heat exchanger	0.29
6	Conventional system with heat exchanger	0.50

Table 6.4 Solar system performances for Washington, DC

The system performances are similar to those obtained in other locations. The low-flow system without a heat exchanger yields a solar fraction of 31%, the PV driven low-flow system without a heat exchanger has an annual solar fraction of 30 % and the indirect conventional system has an annual solar fraction of 29%. The addition of a heat exchanger increases the annual solar fraction. The conventional system with a heat exchanger performs the best with an annual solar fraction of 50 %. Solar fractions of 0.43 and 0.41 are obtained for the low-flow system with a heat exchanger and the low-flow system with a heat exchanger and PV driven pump respectively.

Figure 6.5 demonstrates the annual performance for the six systems in Washington.

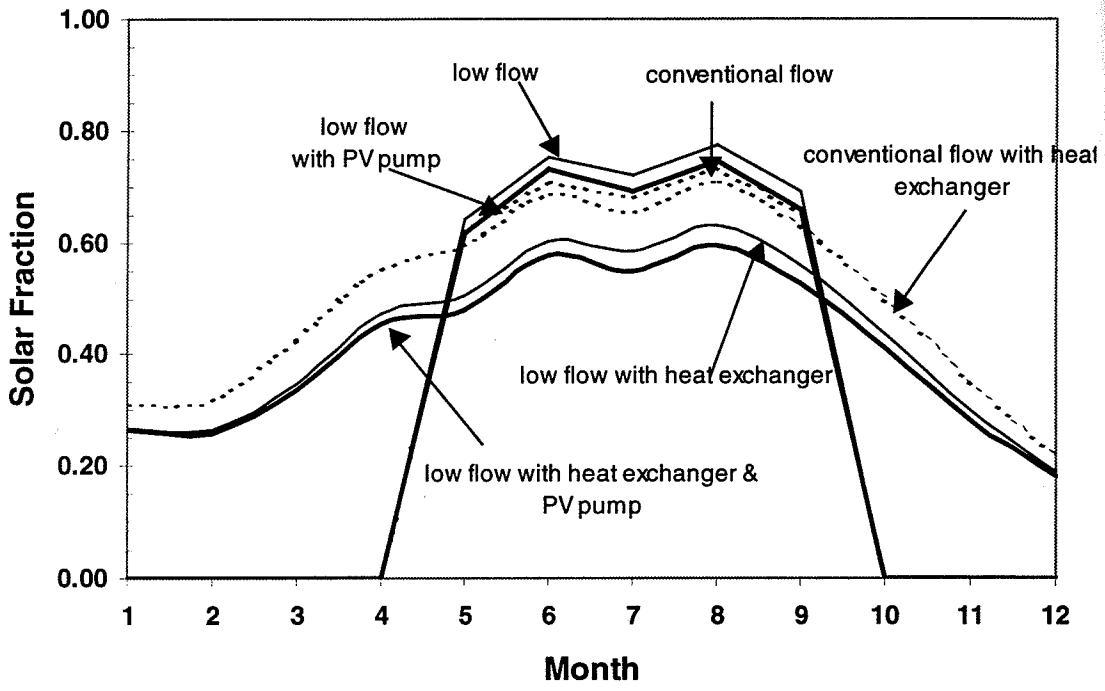

Figure 6.5 Solar hot water system performance in Washington, DC.

TMY data was used to determine the number of hours were freezing temperatures will occur for a typical year. April only has four hours and October has twelve hours so it is very likely that the system without a heat exchanger could be used for more months. This is also true for Albuquerque and Madison.

6.5 Conclusions

The system performance varies from location to location. The greatest factor in determining system performance for climates that require freeze protection is whether the system will use a heat exchanger to enable all-year-round use or simply use a system without a heat exchanger for the summer months. For the four locations investigated, Albuquerque, Madison and Washington experience freezing temperatures where the use of a heat exchanger does improve the annual collection of solar energy. The solar fraction of the summer-only systems may increase slightly if the collector is sloped for maximum summer performance, but this will not be enough to overcome the penalty imposed by running the system for only half the year. Determination of the solar fraction for the summer only systems was quite conservative with the system being turned off when there were only a few hours where freezing occurred. The use of a control system to drain the system at low temperatures could increase the performance by allowing more hours of solar energy collection.

When using a heat exchanger the performance is reduced by low flows in the collector side. In order to increase performance the flow should be turbulent in collector-side. The

advantage of having low flow on the collector side is to allow the use of a PV driven pump that can help reduce peak electricity demands and eliminate the need for a control system. The PV pump and heat exchanger must be designed together to enable turbulent flow on the collector side. This can be accomplished by a combination of heat exchanger geometries and pump flow rates.

The use of a PV driven pump in low-flow systems with heat exchangers reduces the solar fraction by 2 % for Albuquerque and Washington and 1% for Madison when compared to low-flow systems with heat exchangers and conventional pumps. The use of a PV driven pump for direct low-flow system places a penalty of 0% for Albuquerque, 1% for Madison and Washington and 4% for Miami when compared to low-flow systems with conventional pumps. This is a very small penalty when the decreased costs to the utility and the simplified control system are considered.

Low-flow systems perform equally or better than conventional systems in direct solar domestic hot water systems. Albuquerque, Madison and Washington experienced small increases in performance of 0%, 1% and 2% respectively when comparing the low-flow system and the conventional system. Miami, the location where a direct solar system would be the most worthwhile experienced an increase of 4% for the low-flow system compared to the conventional system. The advantage of using low-flow systems lies in the additional reductions of installation, material and hydraulic system costs.

CHAPTER 7: CONCLUSIONS

7.1 Summary

Collector and tank flow rates effect system performance. In direct solar domestic hot water systems, lower flows increase tank stratification, thereby reducing the collector inlet temperature. The reduced inlet temperature will decrease convective losses from the solar collector to the environment and therefore increase the useful energy gain to the collector. It has been shown that regardless of whether the system is direct or indirect, the average daily flow rate circulating to the tank should always be approximately equal the average hot water draw.

The collector heat removal factor is an important parameter governing the amount of useful energy gain to the collector. Since lower flow rates reduce the collector heat removal factor, an alternative to the conventional header-riser flat-plate collector must be found. The use of the serpentine collector allows increased flow rates through the tube, than would otherwise occur in each individual riser of a header-riser type design. The higher flow through the tube, along with a decreased tube diameter invokes turbulent flow. The internal heat transfer coefficient is greatly improved and therefore the serpentine collector performs better than the conventional header-riser collector. Care must be taken in designing the serpentine tube diameters because pressure is inversely proportional to diameter to the fifth

power. This is shown in equations 5.9 to 5.11. Once the flow is turbulent, further reducing the tube diameter will be of little benefit.

Low collector flows allow the use of photovoltaic driven pumps. These PV driven systems have two distinct advantages. First, they eliminate the need for parasitic pumping power, which in turn reduces the demand on utilities, and second, the control system is simplified, as the pump will only turn on when there is sufficient sunshine. The system performance, measured by the solar fraction, is reduced by 0% for Albuquerque, 1% for Madison and Washington and 4% for Miami with the addition of a PV driven pump when compared to a conventional pump low-flow system.

There is the need for freeze protection in many locations. Copper pipes will often break when water freezes and expands within them. The use of a heat exchanger with antifreeze in the collector loop is common practice. However, the addition of a heat exchanger poses the problem of optimizing flow rates on both the collector-side and tank-side of the heat exchanger loop. As mentioned earlier, the tank loop should have a flow rate equivalent to the average hot water draw. For a given heat exchanger design, the performance will increase with increasing collector flow rates. However, if heat exchangers with the same NTU for different flow rates are examined it is found that the system performance is similar for the same NTU. With an appropriate NTU and therefore UA, a heat exchanger can be designed for low flow. A tube-in-shell design was used, but unfortunately, it could only be found that it would perform better for low flow rates if the properties of the glycol antifreeze were assumed independent of temperature. The problem is that the viscosity of

glycol increases with decreasing temperatures meaning that the flow will tend to become laminar and hence heat transfer properties will be reduced. The best system performance is achieved when collector flow rates along with heat exchanger design, induce turbulent flow. The only advantage to decreasing the collector flow rate is to allow the use of a PV driven pump.

Hot water heating makes up eighteen percent of residential energy use. Solar domestic hot water systems can meet up to 75 % of the annual hot water load; this is 13 % of the residential energy use. Utilities will have to supply 13% less energy to the residential energy sector. The decreased demand to the utility will mean that new power plants will not have to be built and the utility can cut down operating costs. The utility and the residential hot water user could find themselves in a win-win situation if the utility aids the hot water user to invest in solar hot water. Various approaches could be taken, such as leasing the system to the customer or giving low interest loans towards the purchase of the system.

Ultimately, the use of solar domestic hot water systems could reduce environmental impacts caused by pollution and water and land degradation.

7.2 Recommendations

The use of natural convection heat exchangers seem to be a promising alternative, provided that the average daily water draw is not more than circulation in the natural convection water loop. It seems for forced flow systems with a heat exchanger that when the tank flow rate is less than the average daily water draw the system performance is drastically reduced.

Tank stratification is destroyed by mains water entering the tank and making up the water displaced by the load. More analysis should be made on this system to determine if it will perform better than a conventional system. Analysis of double-tank storage systems may provide interesting results in terms of increasing tank stratification without directly affecting the natural convection heat exchanger performance.

The increased viscosity of glycol at low temperatures poses a large problem to the optimization of tank flow rates as the flow becomes laminar and heat transfer is reduced. Alternative fluids should be investigated.

Lastly, a detailed economic analysis should be made including the cost of a PV driven pump compared to the cost of the parasitic pumping power of a conventional pump. Investigation into the decreased manufacturing costs associated with a serpentine collector and the cost benefits of a heat exchanger should also be included.

APPENDIX A

TYPE 86 – Serpentine Collector

TYPE 71 – Closed Loop Hydraulic System

TYPE 87 – UA for Tube-In-Shell Heat Exchanger

TYPE 88 – Temperature Dependent Property Data

A.1 TYPE 86 SERPENTINE COLLECTOR

General Description

TYPE 86 models a serpentine collector. Serpentine collectors consist of a flow duct that is bonded to the absorber plate in a serpentine or zigzag fashion. A serpentine collector is shown in Figure A.1.1.

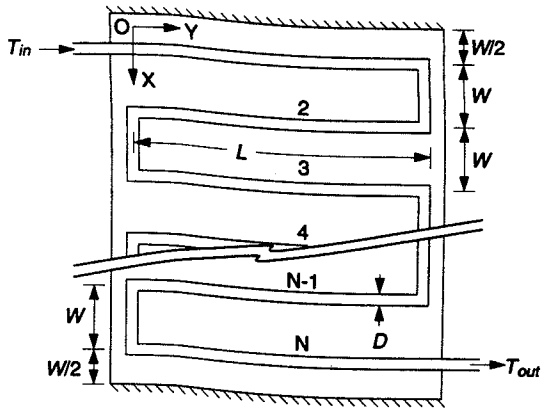

Figure A.1.1 Serpentine Flat Plate Collector

As the number of turns in a serpentine collector increases beyond 10-15 turns the collector numerical solution approximates the analytical solution for a long collector with no turns, N=1. The analytical model for N=1 is essentially the same model as the conventional header-riser flat-plate equation with the exception that the internal heat transfer coefficient is calculated for only one tube.

Mathematical Description

Equation A.1.1 (Duffie and Beckman, 1991) expresses the useful energy gain of a solar collector in the following form.

$$Q_u = A_c F_R [G_T(\tau\alpha) - U_L(T_i - T_a)] \qquad (A.1.1)$$

where F_R is the collector heat removal factor, ($\tau\alpha$) is the transmittance absorptance product, U_L (W/m^2.K) is the overall loss coefficient, A_c (m^2) is the collector area, G_T (W/m^2) is the incident radiation and T_i (K) and T_a (K) are the fluid inlet and ambient temperatures respectively.

The collector heat removal factor, F_R, is the ratio of actual useful energy gain of a collector to the useful gain if the whole collector surface were at the fluid inlet temperature, given in equation A.1.2.

For a header-riser flat-plate collector, the collector heat removal factor can be expressed as shown in equation A.1.2 (Duffie and Beckman, 1991).

$$F_R = \frac{\dot{m}C_p}{A_c U_L}\left[1 - \exp\left(-\frac{A_c U_L F'}{\dot{m}C_p}\right)\right] \qquad (A.1.2)$$

In equation A.1.2, $\dot{m}$ is the mass flow rate, C_p (J/kg.K) is the specific heat of the collector fluid and T_o (K) is the fluid outlet temperature. F_R is analogous to the heat exchanger effectiveness. F' is the collector efficiency factor given by equation A.1.3.

$$F' = \frac{1/U_L}{W\left[\frac{1}{U_L[D + (W - D)F]} + \frac{1}{C_b} + \frac{1}{\pi D_i h_{fi}}\right]} \qquad (A.1.3)$$

In equation A.1.3, W represents tube spacing (m), C_b is the contact resistance (W/m.K), h_{fi} is the internal fluid heat transfer coefficient (W/m^2.K) and F is the standard fin efficiency, given in equation A.1.4.

$$F = \frac{\tanh[m(W-D)/2]}{m(W-D)/2} \qquad (A.1.4)$$

Energy is transferred to the surroundings from the top, sides and bottom of the collector. This energy transfer rate is given in terms of the overall loss coefficient, U_L. An approximate relation for U_L is given by Klein (1975) shown in equation A.1.5.

$$U_L = \frac{1}{\dfrac{N_G}{\dfrac{C}{T_{pm}}\left[\dfrac{(T_{pm}-T_a)}{N_G+f}\right]^{0.33}+\dfrac{1}{h_w}}} + \frac{\sigma(T_{pm}^{\,2}+T_a^{\,2})(T_{pm}+T_a)}{\dfrac{1}{\varepsilon_p+0.05N_G(1-\varepsilon_p)}+\dfrac{2N_G+f-1}{\varepsilon_g}-N_G} + U_{be} \qquad (A.1.5)$$

where

N_G = number of glass covers

$f = (1+0.04h_w+0.0005h_w^{\,2})(1+0.091N_G)$

$C = 365.9(1-0.00883\beta+0.0001298\beta^2)$

β =collector tilt (degrees)

ε_g = emittance of glass

ε_p = emittance of plate

T_a = ambient temperature (K)

T_{pm} = mean plate temperature (K)

$$T_{pm} = T_{f,i} + \frac{Q_u / A_c}{F_R U_L}(1 - F_R)$$

h_w = wind heat transfer coefficient (W/m^2.C)

The internal heat transfer coefficient is dependent on the flow rate through the tubes, the diameter of the tubes, the length of the tubes and the flow regime, that is, whether it is laminar or turbulent.

For laminar flow (Reynolds numbers less than 2100), the Nusselt number is given by equation A.1.6, developed by Heaton et al (Incropera and DeWitt, 1990) for the case of constant heat rate.

$$Nu = 3.7 + \frac{0.0534(\mathrm{Re}\,\mathrm{Pr}\,D_i/L)^{1.15}}{1 + 0.0335(\mathrm{Re}\,\mathrm{Pr}\,D_i/L)^{0.82}} \qquad (A.1.6)$$

Re represents the Reynolds numbers, *Pr*, is the Prandtl number, D_i is the tube diameter (m) and L is the tube length (m).

In the turbulent flow regime where Reynolds numbers are greater than 2100, the Nusselt number is given by Gnielinski's modification of the Petukhov equation (Incropera and DeWitt, 1990) for Reynolds numbers between 3000 and 5 x10^6, shown in equation A.1.7.

$$Nu = \frac{\left(\frac{f}{8}\right)(\mathrm{Re} - 1000)\,\mathrm{Pr}}{\left(1 + 12.7\left(\frac{f}{8}\right)^{1/2}\left(\mathrm{Pr}^{2/3} - 1\right)\right)} \qquad (A.1.7)$$

In the above equation, *f*, represents the friction factor from the Moody chart.

TRNSYS Component description

PARAMETER NO.		DESCRIPTION
1	N	number of turns
2	D_i	inner tube diameter (m)
3	D	outer tube diameter (m)
4	δ	plate thickness (m)
5	L	length of each turn (m)
6	W	tube spacing (m)
7	k	plate conductivity (kJ/hr-m^2)
8	U_{be}	loss coefficient for bottom and edge of collector per unit aperture area (kJ/hr-m^2-K)
9	ε_p	absorber plate emittance
10	α	absorptance of absorber plate
11	N_G	number of glass covers
12	η_R	index of refraction of cover material
13	KL	product of extinctioon coefficient and the thickness of each cover plate

INPUT NUMBER		DESCRIPTION
1	T_{in}	Temperature of fluid entering collector (°C)
2	$\dot{m}_c$	Collector fluid mass flowrate (kg/hr)
3	T_a	Ambient temperature (°C)
4	I_T	Incident radiation (kJ/hr-m^2)
5	Wind	Wind speed (m/s)
6	I	Total horizontal radiation (kJ/hr-m^2)
7	I_d	Horizontal diffuse radiation (kJ/hr-m^2)
8	ρ_g	Ground reflectance
9	θ	Incidence angle (degrees)
10	β	Collector slope (degrees)
11	μ	dynamic viscosity (N-s/m^2)
12	C_{pc}	specific heat of collector fluid (kJ/kg-K)
13	K_f	fluid conductivity (kJ/hr-m^2)
14	ρ	density (kg/m^3)

OUTPUT NUMBER		DESCRIPTION
1	T_{out}	Outlet fluid temperature (°C)
2	$\dot{m}_c$	Outlet fluid mass flowrate (kg/hr)
3	$\dot{Q}_u$	Rate of energy gain (kg/hr)

4	T_{pm}	Mean absorber plate temperature (°C)
5	F_R	Collector heat removal factor
6	$(\tau\alpha)$	Tau alpha product
7	P_loss	Pressure loss (kPa)
8	U_L	Overall heat loss coefficient (kJ/hr-m^2-K)

TYPE 86 - SERPENTINE COLLECTOR

Fortran Code

```
      SUBROUTINE TYPE86(TIME,XIN,OUT,T,DTDT,PAR,INFO,ICNTRL,*)

C**********************************************************************
C     THIS SUBROUTINE MODELS A SERPENTINE COLLECTOR.
C     A SERPENTINE COLLECTOR CAN BE MODELED USING THE CONVENTIONAL
C     HEADER-RISER PARALLEL FLOW COLLECTOR MODEL, IF THE NUMBER OF
C     TURNS ARE GREATER THAN ABOUT FIFTEEN.  THE ONLY DIFFERENCE IS
C     THE CALCULATION OF THE HEAT TRANSFER COEFFICIENT, WHICH IS
C     CALCULATED FOR A LONG TUBE.
C     LAST MODIFIED 25 AUGUST 1997 -- MYRNA DAYAN
C**********************************************************************

      DOUBLE PRECISION XIN,OUT
      INTEGER*4 INFO
      DIMENSION XIN(14),OUT(8),PAR(13),INFO(15)
      CHARACTER*3 YCHECK(14),OCHECK(8)

      INTEGER N,N_G,ITER
      REAL k,delta,D,D_i,T_a,L,W,C_p,T_in,T_pm,T_out
      REAL TauAlpha, L_tube_serpentine,F_1, RefInd
      REAL m_flat,U_L,F,beta,Q_useful,A_c,mu,Pr,kw
      REAL F_R,m_dot, h_fi_serp,pi,wind,U_be,Alpha
      REAL Nusselt_serp, Re_Serp, T_pm_old, change, E_p
      REAL I_D, I_T, I_H, XKL,theta,P_loss, rho, rho_g

      IF (INFO(7).GE.0) GO TO 100

C     FIRST CALL OF SIMULATION
      INFO(6)=8
      INFO(9)=0
      CALL TYPECK(1,INFO,14,13,0)

      DATA YCHECK/'TE1','MF1','TE1','IR1','VE1','IR1','IR1'
     .,'DM1','DG1','DG1','VS1','CP1','KT1','DN1'/

      DATA OCHECK/'TE1','MF1','PW1','TE1','DM1','DM1','PR1','HT1'/
      CALL RCHECK(INFO,YCHECK,OCHECK)

      T_pm=70.0

C  SET PARAMETER VARIABLES
100   N           =PAR(1)
      D_i         =PAR(2)
      D           =PAR(3)
      delta =PAR(4)
      L           =PAR(5)
      W           =PAR(6)
      k           =PAR(7)/3.6
      U_be  =PAR(8)/3.6
      E_p         =PAR(9)
      Alpha =PAR(10)
      N_G         =PAR(11)
      RefInd=PAR(12)
      XKL         =PAR(13)
```

```
c  SET INPUT VARIABLES
      T_in  =XIN(1)
      m_dot =XIN(2)/3600
      T_a         =XIN(3)
      I_T         =XIN(4)/3.6
      wind  =XIN(5)
      I_h         =XIN(6)/3.6
      I_d         =XIN(7)/3.6
      rho_g =XIN(8)
      theta   =XIN(9)
      beta  =XIN(10)
      mu      =XIN(11)
      C_p         =XIN(12)*1000
      kw          =XIN(13)/3.6
      rho     =XIN(14)

      Pr          =mu*C_p/kw

C  TO AVOID FLOATING POINT PROBLEMS
      IF(ABS(m_dot).LE.0.000001) m_dot=0.0
      IF (I_T.GT.0.0.AND.Theta.LT.90) GO TO 200

C  NO RADIATION
      TauAlpha=0.0
      GO TO 300

200   TauAlpha=TauAlf(beta,N_G,XKL,RefInd,Alpha,I_d,I_h,I_T
     .,theta,rho_g)

300   pi=4.0*atan(1.0)
      A_c=N*W*L

      IF (m_dot.LE.0.)GO TO 400

      change=10.0
      T_pm=out(4)

c  HEAT TRANSFER COEFFICIENT
      L_tube_serpentine=N*(L+W)-W
      Call HEATTRANSFER(m_dot,L_tube_serpentine,D_i,mu,Pr, kw,h_fi_serp
     .,Re_serp,Nusselt_serp);

c INITIAL GUESS VALUE FOR PLATE TEMPERATURE
      ITER=0
      DO WHILE (change>0.0001.AND.ITER<10000)
      T_pm_old=T_pm
      Call LOSSCOEFFICIENT(T_a,T_pm,N_G,beta,wind,E_p,U_be
     .,U_L);
      m_flat=sqrt(U_L/(k*delta))
      F=tanh(m_flat*(W-D)/2.0)/(m_flat*(W-D)/2.0)
      F_1=(1.0/U_L)/(W*(1.0/(U_L*(D+(W-D)*F))+1.0/
     .(pi*D*h_fi_serp)))
      F_R =m_dot*C_p/(A_c*U_L)*(1.0-exp(-A_c*U_L*F_1/
     .  (m_dot*C_p)))
      Q_useful=A_c*F_R*(I_T*TauAlpha-U_L*(T_in-T_a))
      T_pm=T_in+(Q_useful/A_c)/(F_R*U_L)*(1.0-F_R)
```

```
      change=abs(T_pm-T_pm_old)
      ITER=ITER+1
      T_out=Q_useful/(m_dot*C_p)+T_in
      END DO
      call PRESSUREDROP(m_dot,D_i,mu,rho,N,L,W,P_loss)
      GO TO 500

c  NO FLOW

400   Q_useful=0.0
      change=10.0
      ITER=0
      U_L=OUT(8)
      DO WHILE (change>0.0001.AND.ITER<10000)
      T_pm_old=T_pm
      Call LOSSCOEFFICIENT(T_a,T_pm,N_G,beta,wind,E_p,U_be
     .,U_L);
      T_out=T_a+I_T*TauAlpha/U_L
      T_pm=T_out

      change =abs(T_pm-T_pm_old)
      ITER=ITER+1
      END DO
      P_loss=0.0


c  PRINT OUTPUTS FOR DEBUGGING
c     print*,F_R,T_pm,T_out,eta,Q_useful

500   OUT(1)=T_out
      OUT(2)=m_dot*3600
      OUT(3)=Q_useful*3.6
      OUT(4)=T_pm
      OUT(5)=F_R
      OUT(6)=TauAlpha
      OUT(7)=P_loss
      OUT(8)=U_L*3.6

      RETURN 1
      END
c*************************************************************************
      Subroutine LOSSCOEFFICIENT(T_a,T_pm,N_G,beta,wind,Epsilon_p,
     .U_be,U_L)

c     CALCULATES THE COLLECTOR LOSS COEFFICIENT BASED ON A FUNCTION BY
KLEIN
      IMPLICIT NONE
      INTEGER N_G
      REAL h_w, beta,c,e,T_pm,T_a,Epsilon_g,Epsilon_p,f
      REAL U_t,U_be,U_L,sigma,Wind, T_pm_temp, stf1, stf2

      T_pm_temp=T_pm

      IF (T_pm.LE.T_a) T_pm_temp=T_a+1.0

c  APPROXIMATION OF WIND HEAT TRANSFER COEFFICIENT
      h_w=5.7+3.8*Wind
```

```
      Epsilon_g=0.88
      sigma=5.67*10.0**(-8)

C     USE KLEIN'S TOP LOSS CORRELATION

      F=(1.0-0.04*H_W+5.0E-04*H_W*H_W)*(1.0+0.091*N_G)
      C=365.9*(1.0-0.00883*beta+0.0001298*beta*beta)
      STF1=C/(T_pm_temp+273.15)*((T_pm_temp-T_a)/(N_G+F))**0.33
      STF1=N_G/STF1+1.0/H_W
      STF1=1.0/STF1
      STF2=1.0/(Epsilon_P+0.05*N_G*(1.0-Epsilon_P))+(2.*N_G+F-1.)/
     .Epsilon_G-N_G
      STF2=SIGMA*((T_PM_TEMP+273.15)**2+(T_A+273.15)**2)*
     .((T_PM_TEMP+273.15)+(T_A+273.15))/STF2
      U_t=(STF1+STF2)+U_BE


      U_L=(U_t+U_be)

      RETURN
      END
C*********************************************************************

      Subroutine HEATTRANSFER(m_dot,L_tube,D_i,mu,Pr,kw,h_fi,Re,Nusselt)

      IMPLICIT NONE
      INTEGER Laminar, Turbulent
      REAL a,b,m_ht,nw,kw,Pr,Re,friction,Nusselt,D_i
      REAL L_tube,pi,h_fi,mu,m_dot


C     CONSTANTS
      a=0.0534
      b=0.0335
      m_ht=1.15
      nw=0.82

      pi=4.0*atan(1.0)

      Re=4.0*m_dot/(pi*D_i*mu)
      If (Re.LE.0.)THEN
      Nusselt=3.7
      ELSE
      If (Re.LT.2100.AND.RE.GT.0.) THEN
C LAMINAR
      friction=64.0/Re
      laminar=1
      turbulent=0
      Nusselt=3.7+a*(Re*Pr*D_i/L_tube)**m_ht/(1.0+b*(Re*Pr*D_i/L_tube)
     .**nw)
      Else
C TURBULENT
      friction=(0.79*log(Re)-1.64)**(-2)
      laminar=0
      turbulent=1
      Nusselt= (friction/8.0)*(Re-1000)*Pr/(1.0+12.7*sqrt(friction/8.0)*
     .(Pr**(2.0/3.0)-1.0))
      EndIf
```

```
      EndIf

      h_fi=Nusselt*kw/D_i
      RETURN
      END
C*****************************************************************
      FUNCTION TauAlf(beta,N_G,XKL,RefInd,Alpha,I_d,I_h,I_T
     .,theta,rho_g)

      IMPLICIT NONE
      INTEGER N_G
      REAL beta,XKL,RefInd,Alpha,Rho_d,radconvert,TALN,theta
      REAL theta_sky,theta_ground,XKATDS,XKATDG,XKATB,XKAT,TALF
      REAL F_sky, F_gnd, ID_sky, ID_gnd, I_d, I_h,I_T,TauAlf, rho_g


      radconvert=0.017453


C COVER TRANSMITTANCE AT NORMAL INCIDENCE
      rho_d=-1.0
      TALN=TALF(N_G,0.0,XKL,RefInd,Alpha,Rho_d)

C  USE THE RELATIONS OF BRANDEMUEHL FOR EFFECTIVE INCIDENCE ANGLES
C  FOR DIFFUSE RADIATION
      theta_sky=59.68-0.1388*beta+0.001497*beta*beta
      theta_ground=90.0-0.5788*beta+0.002693*beta*beta

C  DIFFUSE SKY RADIATION TAUALPHA RATIO
      XKATDS=TALF(N_G,theta_sky,XKL,RefInd,Alpha,Rho_d)/TALN
C  GROUND REFLECTED RADIATION TAUALPHA RATIO
      XKATDG=TALF(N_G,theta_ground,XKL,RefInd,Alpha,Rho_d)/TALN
C  BEAM RADIATION  TAUALPHA RATIO
      XKATB=TALF(N_G,theta,XKL,RefInd,Alpha,Rho_d)/TALN

C VIEW FACTORS
      F_SKY=(1.0+cos(beta*radconvert))/2.0
      F_GND=(1.0-cos(beta*radconvert))/2.0

C  SKY DIFFUSE RADIATION
      ID_SKY=F_SKY*I_D
C  GROUND DIFFUSE RADIATION
      ID_GND=Rho_g*F_GND*I_H

C OVERALL TAUALPHA RATIO
      XKAT=(XKATB*(I_T-ID_SKY-ID_GND)+XKATDS*ID_SKY+XKATDG*ID_GND)/I_T
      TAUALf=TALN*XKAT

      RETURN
      END
C*****************************************************************
      Subroutine PRESSUREDROP(m_dot,D_i,mu,rho,N,L,W,P_loss)
      IMPLICIT NONE
      INTEGER N
      REAL m_dot, D_i, mu, rho, L, pi, f,Re, v_serp
      REAL PipeLossCoefficient, L_eq, L_total, P_loss, W

C     Pressure Drop for the serpentine collector
```

```
C     Find the moody friction factor

      pi=4.0*atan(1.0)

      Re=4.0*m_dot/(pi*D_i*mu)

      If (Re.LT.0.001) Then   !NO FLOW
      f=0.0
        Else
      If (Re.LT.2100)  Then   !LAMINAR
      f=64.0/Re
      Else                              !TURBULENT
        f=(0.79*log(Re)-1.64)**(-2)
      End If
      End If
      v_serp=m_dot/(rho*pi*(D_i/2.0)**2)
      PipeLossCoefficient=0.5
      L_eq=PipeLossCoefficient*D_i/f
      L_total=N*(L+W)-W+(2*N-2)*L_eq
      P_loss=f*L_total/D_i*rho*v_serp**2/2.0*10.0**(-3)
      RETURN
      END
```

A.2 TYPE 71 CLOSED LOOP HYDRAULIC SYSTEM

General Description

Type 71 models a pump and motor coupled to a closed loop system. A given pump has its own unique characteristics which show the interrelation of pump head, capacity, power and efficiency for a specific impeller diameter and casing size. The pump characteristic curves can be fitted to equations. Using these equations the flow rate and current can be found for the hydraulic system. Type 71 requires information about the hydraulic system, the pump curve coefficients and voltage input. The voltage input can be obtained from a photovoltaic cell.

Mathematical Description

A third order linear regression with cross terms is used to give an equation for flow rate in terms of head (m) and voltage (V) as shown in equation A.2.1. A second order linear regression is used to give an equation for current in terms of head and voltage given in equation A.2.2.

$$flowrate = a + b \cdot Head + c \cdot Head^2 + d \cdot Head^3 + e \cdot Voltage + f \cdot Voltage^2 + g \cdot Voltage^3 + h \cdot Head \cdot Voltage + i \cdot Head \cdot Voltage^2 + j \cdot Head^2 \cdot Voltage + k \cdot Head^2 \cdot Voltage^2 \qquad (A.2.1)$$

$$Current = l + m \cdot Voltage + n \cdot Voltage^2 + o \cdot Head + p \cdot Head^2 \qquad (A.2.2)$$

The head loss is given by equation A.2.3 where L_{eq} (m) is the equivalent length including minor loss coefficients for bends, $\vec{v}$ (m/s) is the fluid velocity, D (m) is the tube or pipe diameter, f is the friction factor from the Moody chart and g (m/s^2) is the gravitational

acceleration. The total system head loss is calculated by the addition of the head loss through the serpentine collector and through the system piping.

$$head = \left(f \frac{L_{eq}}{D} \frac{\vec{v}^2}{2g} \right)_{collector} + \left(f \frac{L_{eq}}{D} \frac{\vec{v}^2}{2g} \right)_{system} \qquad (A.2.3)$$

To ensure convergence of equations A.2.1 and A.2.3 the Bisection Solution Method (Murphy et al, 1988) is used. Equation A.2.2 can then be used to find the current output that is used as an input to the photovoltaic cell.

TRNSYS Component Description

PARAMETER NO.		DESCRIPTION
1	D_{pipe}	Inner diameter of piping in loop (m)
2	L_{pipe}	Length of piping in loop (m)
3	N_{bends}	Number of bends of piping in loop
4	N	Number of collector tubes in parallel
5	L	Length of each turn in the collector (m)
6	W	Tube spacing in the collector (m)
7	D_{riser}	Inner tube diameter of collector (m)
8	$V_{threshold}$	Threshold voltage in which pump starts (V)
9-24	a-p	curve fitting parameters for equations A.2.1-A.2.2

INPUT NUMBER		DESCRIPTION
1	V	Input voltage to pump motor (V)
2	μ	Dynamic viscosity of circulating fluid (Pa.s)
3	ρ	Density of circulating fluid (kg/m^3)

OUTPUT NUMBER		DESCRIPTION
1	$\dot{m}_c$	Outlet fluid mass flowrate (kg/hr)
2	I	Currrent (A)
3	V	Voltage (V)
4	P	Pump power (W)

TYPE 71 – CLOSED LOOP HYDRAULIC SYSTEM

Fortran Code

```
      SUBROUTINE TYPE71(TIME,XIN,OUT,T,DTDT,PAR,INFO,ICNTRL,*)

C*********************************************************************
C     THIS SUBROUTINE MODELS A PUMP COUPLED TO A CLOSED LOOP SYSTEM
C     LAST MODIFIED 4 OCTOBER 1997 -- MYRNA DAYAN
C*********************************************************************

      DOUBLE PRECISION XIN,OUT,PASS
      INTEGER*4 INFO
      DIMENSION XIN(3),OUT(4),PAR(24),INFO(15),PASS(20)
      CHARACTER*3 YCHECK(3),OCHECK(4)

      INTEGER iter
      REAL m_dot,voltage,change,head,condition,dummy
      REAL P_pump, current, m_dot_lower,m_dot_higher,eqnMID, eqnLOWER

      IF (INFO(7).GE.0) GO TO 100

C     FIRST CALL OF SIMULATION
      INFO(6)=4
      INFO(9)=0
      CALL TYPECK(1,INFO,3,24,0)
      DATA YCHECK/'NAV','VS1','DN1'/

      DATA OCHECK/'MF1','NAV','NAV','PW2'/
      CALL RCHECK(INFO,YCHECK,OCHECK)

c     SET INPUT PARAMETERS
      PASS(1)=XIN(2)
      PASS(2)=XIN(3)
      PASS(3)=PAR(1)
      PASS(4)=PAR(2)
      PASS(5)=PAR(3)
      PASS(6)=PAR(4)
      PASS(7)=PAR(5)
      PASS(8)=PAR(6)
      PASS(9)=PAR(7)
      PASS(10)=PAR(9)
      PASS(11)=PAR(10)
      PASS(12)=PAR(11)
      PASS(13)=PAR(12)
      PASS(14)=PAR(13)
      PASS(15)=PAR(14)
      PASS(16)=PAR(15)
      PASS(17)=PAR(16)
      PASS(18)=PAR(17)
      PASS(19)=PAR(18)
      PASS(20)=PAR(19)


100   V_threshold=PAR(8)
      l=PAR(20)
```

```
      m=PAR(21)
      n=PAR(22)
      o=PAR(23)
      p=PAR(24)

c     SET INPUT VARIABLES
      voltage=XIN(1)


      IF (voltage.LT.V_threshold) THEN
      m_dot=0.0
      current=0.0
      P_pump=0.0
      GOTO 200
      ENDIF

C   IN ORDER TO FIND THE PUMP OPERATING POINT
C   THE SIMPLE BISECTION METHOD IS USED

      m_dot_lower=0.00001       !LowerBound
      m_dot_higher=1.0     !UpperBound
      change=10
      ITER=0
      CALL HeadandFlow(m_dot_lower,xin,PASS,eqnLOWER,head)
      DO WHILE (change>0.00000001.AND.ITER<10000)
      ITER=ITER+1
      m_dot=(m_dot_higher+m_dot_lower)/2.0
      CALL HeadandFlow(m_dot,XIN,PASS,eqnMID,head)
      condition=eqnMID*eqnLOWER
      IF (condition.GT.0.0) THEN
      m_dot_lower=m_dot
      eqnLOWER=eqnMID
      ELSE
      m_dot_higher=m_dot
      ENDIF
      change=abs(m_dot_higher-m_dot_lower)
      END DO

      Current=0.4640587-9.1174E-02*Voltage+0.01059595*Voltage**2+
     .0.01497438*Head-7.4913E-03*Head**2

      P_pump=current*voltage


c     OUTPUTS
200   OUT(1)=m_dot*3600
      OUT(2)=current
      OUT(3)=voltage
      OUT(4)=P_pump

      RETURN 1
      END
C*************************************************************
      SUBROUTINE MoodyChart(Re,f)
      IMPLICIT NONE
      REAL Re,f

      If (Re.LT.0.0000001) Then  !No flow
```

```
      f=0.0
      Else
      If (Re.LT.2100)  Then !Laminar
        f=64.0/Re
      Else !Turbulent
c     This is a good estimate for smooth pipes
         f=(0.79*log(Re)-1.64)**(-2)
       EndIf
      EndIf
      RETURN
      END

c*****************************************************************
      SUBROUTINE HeadandFlow(m_dot,XIN,PASS,eqn,head)

      IMPLICIT NONE
      DOUBLE PRECISION XIN, PASS
      DIMENSION XIN(3),PASS(20)
      INTEGER N_bends,N
      REAL P_Loss_serp,PipeLossCoefficient,mu,rho,D_pipe,m_dot,voltage
      REAL L_pipe,pi, re_pipe, L_eq_pipe,f_pipe
      REAL L_pipe_total,v_pipe,P_loss_pipe, P_loss_total,PumpingPower
      REAL headloss,headloss_ft,flowrate_system,head,flowrate_pump
      REAL EQN,L,W,D_riser,Re_serp,v_serp,L_eq
      REAL f_serp,L_total_serp, a,b,c,d,e,f,g,h,i,j,k

C     SET PARAMETERS
      mu=PASS(1)
      rho=PASS(2)
      D_pipe=PASS(3)
      L_pipe=PASS(4)
      N_bends=PASS(5)
      N=PASS(6)
      L=PASS(7)
      W=PASS(8)
      D_riser=PASS(9)
      a=PASS(10)
      b=PASS(11)
      c=PASS(12)
      d=PASS(13)
      e=PASS(14)
      f=PASS(15)
      g=PASS(16)
      h=PASS(17)
      i=PASS(18)
      j=PASS(19)
      k=PASS(20)


c  SET INPUT VARIABLES
      voltage=XIN(1)

C     Determine pressure loss of collector
      pi=4.0*atan(1.0)
      PipeLossCoefficient=0.5

      Re_Serp=4.0*(m_dot/2.0)/(pi*D_riser*mu)
      Call MoodyChart (Re_serp,f_serp)
```

```
      v_serp=(m_dot/2.0)/(rho*pi*(D_riser/2.0)**2)
      L_eq=PipeLossCoefficient*D_riser/f_serp
      L_total_serp=N*(L+W)-W+(2.0*N-2.0)*L_eq
      P_loss_serp=f_serp*L_total_serp/D_riser*rho*v_serp**2/
     .2.0*10.0**(-3)

      Re_pipe=4.0*m_dot/(pi*D_pipe*mu)
      Call MoodyChart (Re_pipe,f_pipe)
      L_eq_pipe=PipeLossCoefficient*D_pipe/f_pipe
      L_pipe_total=N_bends*L_eq_pipe+L_pipe
      v_pipe=m_dot/(rho*pi*(D_pipe/2.0)**2)
      P_loss_pipe=f_pipe*L_pipe_total/D_pipe*rho*v_pipe**2/2.0*
     .10.0**(-3)
      P_loss_total=P_loss_serp+P_loss_pipe
      PumpingPower=P_loss_total*m_dot/rho*1000.0 !W
      headloss=P_loss_total/(rho*9.81)*1000.0
      headloss_ft=headloss*3.281
      flowrate_system=m_dot/rho*15850.0
c     Couple pump to system
      head=headloss_ft
c     Hartel Pump Curve fit
c     Using HEH Motor
c     3rd order linear regression for pump variables, R^2=99.64
      Flowrate_pump=a+b*Head+c*Head**2+d*Head**3+e*Voltage+f*Voltage**2+
     .g*Voltage**3+h*Head*Voltage+i*Head*Voltage**2+j*Head**2*Voltage+
     .k*Head**2*Voltage**2

eqn=flowrate_system-flowrate_pump
!this is needed for the bisection method

      RETURN
      END
```

A.3 TYPE 87 UA FOR TUBE-IN-SHELL HEAT EXCHANGER

General Description

TYPE 87 determines UA as a function of flow rate and temperature for a tube-in-shell heat exchanger using the correlations presented below. The advantage of having UA as a function of flow rate is that it allows the use of a PV pump that has varying flow rates. However, in order to implement the new type, a modification had to be made to TYPE 5 to allow UA to be entered as a variable input and not as a constant parameter. Figure A.3.1 represents a simple schematic of a tube-in-shell heat exchanger.

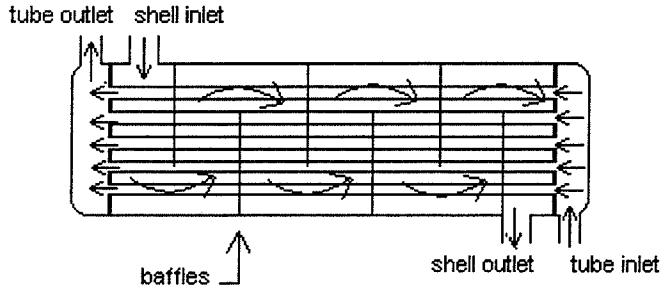

Figure A.3.1 Tube-in-Shell Heat Exchanger

Mathematical Description

The UA product is a function of the heat transfer coefficients of both fluid streams. The heat transfer coefficient is given by the Nusselt number shown in equation A.3.1.

$$Nu = \frac{h_{fi} k}{D} \qquad (A.3.1)$$

where h_{fi} (W/m^2.K) is the heat transfer coefficient, D (m) is the hydraulic diameter and k (W/m.K) is the conductivity of the fluid.

The heat transfer coefficient for the glycol stream inside the tubes can be found from the Colburn equation (Incropera and DeWitt, 1990) given in equation A.3.2.

$$Nu_D = 0.023 Re_D^{4/5} Pr^{1/3} \qquad (A.3.2)$$

where Re is the Reynolds number and Pr is the Prandtl number.

Zhukauskas (Kakaç et al, 1987) developed a correlation for flow over tube bundles, given in equation A.3.3.

$$\overline{Nu}_D = C_1 C_2 Re_{D,max}^m Pr^{0.36} \left(\frac{Pr}{Pr_s} \right)^{1/4} \qquad (A.3.3)$$

where all properties are evaluated at the arithmetic mean of the fluid inlet and outlet temperature, except for Pr_s, which is the Prandtl number evaluated at the surface temperature. C_1 and m are constants listed in table A.3.1 and C_2 is the correction factor for less than 20 tubes shown in Figure A.3.2. The Reynolds number for the shell side is determined from the velocity through the tube bank. A cross sectional area is required to calculate the velocity from the mass flow rate and is usually taken as the area between the baffles and tubes.

Reynolds Number		C_1	m
10^0-10^2	aligned	0.90	0.40
10^2-10^3	aligned	0.52	0.50
10^3-$2x10^5$	aligned	0.27	0.63
$2x10^5$-$2x10^6$	aligned	0.033	0.80
10^0-$5x10^2$	staggered	1.04	0.40
$5x10^2$-10^3	staggered	0.71	0.50
10^3-$2x10^5$	staggered	$0.35\left(\frac{S_T}{S_L}\right)^{0.2}$	0.60
$2x10^5$-$2x10^6$	staggered	$0.031\left(\frac{S_T}{S_L}\right)^{0.2}$	0.80

Table A.1 Constants for the Zhukauskas correlation

In Table A.1 S_T is the transverse pitch of the tube bank and S_L is the longitudinal pitch of the tube bank.

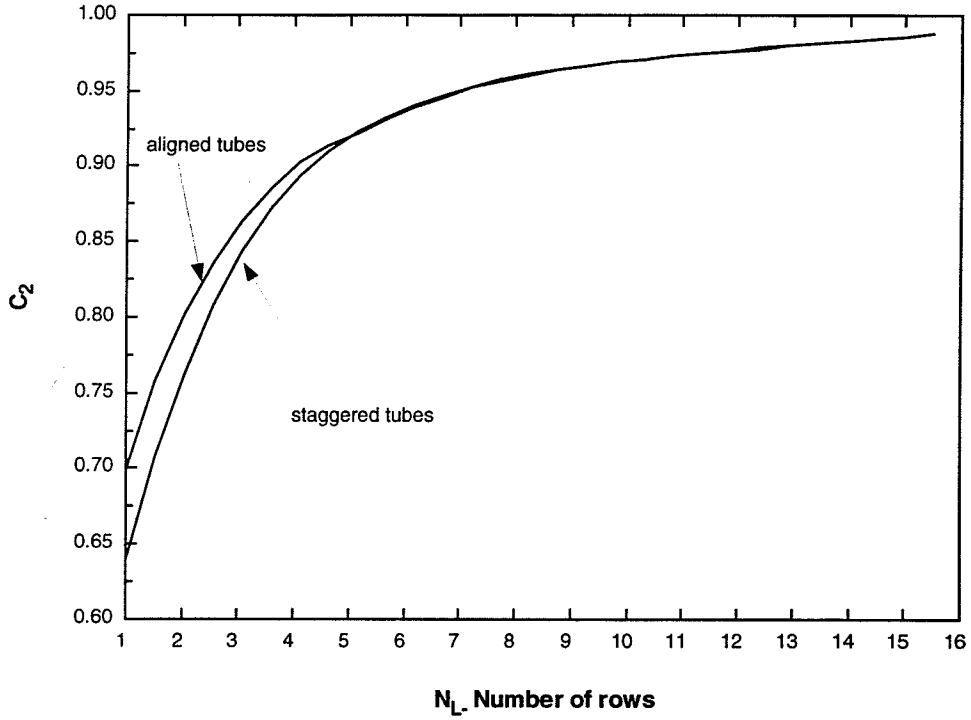

Figure A.3.2 Correction factor for less than 20 rows

TRNSYS Component description

PARAMETER NO.		DESCRIPTION
1	D_i	inner tube diameter (m)
2	D	outer tube diameter (m)
3	S_T	transverse pitch of tube bank
4	S_L	longitudinal pitch of tube bank
5	L_{hx}	heat exchanger length (m)
6	Aligned	1 = aligned tube bank 2 = staggered tube bank
7	N_L	number of tube rows
8	k	conductivity (kJ/hr-m^2)
9	N_{tubes}	number of tubes in total
10	baffle spacing	spacing between baffles (m)

INPUT NUMBER		DESCRIPTION
1	$\dot{m}_c$	Collector fluid mass flowrate (kg/hr)
2	$\dot{m}_t$	Tank fluid mass flowrate (kg/hr)
3	$\mu_{collector}$	dynamic viscosity of collector fluid (N-s/m^2)
4	$Cp_{collector}$	specific heat of collector fluid (kJ/kg-K)
5	$k_{collector}$	collector fluid conductivity (kJ/hr-m^2)
6	μ_{tank}	dynamic viscosity of tank fluid (N-s/m^2)
7	Cp_{tank}	specific heat of tank fluid (kJ/kg-K)
8	k_{tank}	tank fluid conductivity (kJ/hr-m^2)
9	ρ_{tank}	density of tank fluid (kg/m^3)

OUTPUT NUMBER		DESCRIPTION
1	UA	overall heat transfer- area product (kJ/hr.K)

TYPE 87 – UA FOR TUBE-IN-SHELL HEAT EXCHANGER

Fortran Code

```
      SUBROUTINE TYPE87(TIME,XIN,OUT,T,DTDT,PAR,INFO,ICNTRL,*)

C**********************************************************************
C     THIS SUBROUTINE IS USED TO FIND THE UA FOR A SHELL AND TUBE
C     HEAT EXCHANGER USING ZHUKAUSKAS CORRELATION FOR FLOW OVER
C     TUBE BANKS
C     LAST MODIFIED 17 OCTOBER 1997 -- MYRNA DAYAN
C**********************************************************************

      DOUBLE PRECISION XIN,OUT,S_T,S_L
      INTEGER*4 INFO
      DIMENSION XIN(9),OUT(1),PAR(10),INFO(15)
      CHARACTER*3 YCHECK(9),OCHECK(1)

      INTEGER Aligned,N_L, N_tubes
      REAL D_i,D,L_hx, m_dot_collector, m_dot_tank
      REAL mu_collector, Cp_collector, k_collector,Pr_collector
      REAL mu_tank, Cp_tank, k_tank,Pr_tank,Re_collector, Re_tank
      REAL h_fi_collector, A_collector,v_tank, v_tank_max, pi
      REAL Nusselt_collector, Nusselt_tank,h_fi_tank, UA,rho_tank
      REAL C,m, k_copper, baffle_spacing, A_tank

      IF (INFO(7).GE.0) GO TO 100

C     FIRST CALL OF SIMULATION
      INFO(6)=1
      INFO(9)=0
      CALL TYPECK(1,INFO,9,10,0)
      DATA YCHECK/'MF1','MF1','VS1','CP1','KT1','VS1','CP1','KT1','DN1'/

      DATA OCHECK/'NAV'/
      CALL RCHECK(INFO,YCHECK,OCHECK)

C     SET INPUT PARAMETERS
100   D_i=PAR(1)
      D=PAR(2)
      S_t=PAR(3)
      S_L=PAR(4)
      L_hx=PAR(5)
      Aligned=PAR(6)
      N_L=PAR(7)
      k_copper=PAR(8)
      N_tubes=PAR(9)
      baffle_spacing=PAR(10)

C     SET INPUT VARIABLES
      m_dot_collector=XIN(1)/3600
      m_dot_tank=XIN(2)/3600
      mu_collector=XIN(3)
      Cp_collector=XIN(4)*1000
      k_collector=XIN(5)/3.6
      mu_tank=XIN(6)
```

```
      Cp_tank=XIN(7)*1000
      k_tank=XIN(8)/3.6
      rho_tank=XIN(9)

      pi=4.0*atan(1.0)


      IF(m_dot_collector.LE.0.000001.OR.m_dot_tank.LE.0.000001)THEN
      UA=30.0         !dummy value
      GOTO 300
      ENDIF



      Pr_collector=mu_collector*Cp_collector/k_collector
      Re_collector=4.0*m_dot_collector/(pi*D_i*mu_collector)
      call LaminarTurbulent(Re_collector,Pr_collector,Nusselt_collector)
      h_fi_collector=Nusselt_collector*k_collector/(D_i)
      A_collector=pi*D_i*L_hx*N_tubes


      Pr_tank=mu_tank*Cp_tank/k_tank
      v_tank=m_dot_tank/(rho_tank*baffle_spacing*S_t)
      call MaximumTankVelocity(S_t,S_L,D,V_tank,Aligned,V_tank_max)
      Re_tank=rho_tank*V_tank_max*D/mu_tank

C     Zukaukas' correltation for tube bundles in cross flow
      Call CandM(Aligned,N_L,Re_tank,S_T,S_L,C,m)
      Nusselt_tank=C*Re_tank**m*Pr_tank**0.36*1.0**0.25
      h_fi_tank=Nusselt_tank*k_tank/D
      A_tank=pi*D*L_hx*N_tubes


      UA=1.0/(1.0/(h_fi_tank*A_tank)
     .   +((log(D/D_i))/(N_tubes*(2.0*pi*L_hx*k_copper)))
     .       +1.0/(h_fi_collector*A_collector))

300   OUT(1)=UA*3.6

      RETURN 1
      END


C     ************************************************************
      Subroutine CandM(A,N_L,Re,S_T,S_L,C,m)
      IMPLICIT NONE
      INTEGER     A,N_L
      REAL  Re,C,m,C_2
      DOUBLE PRECISION S_T,S_L

      If (A.eq.1) Then !Aligned Tube bank
            If (Re<100) Then
            C=0.9;m=0.40
            else
                  if (Re.lt.1000) Then
                  C=0.52
                  m=0.5
                  else
```

```
                        if (Re.lt.2*10**5) Then
                        C=0.27
                        m=0.63
                        else
                              C=0.033
                              m=0.8
                        endif
                  endif
            endif
      If (N_L.lt.20) Then
      C_2=0.5790687+0.1446209*N_L-2.1087E-02*N_L**2+0.00137222*N_L**3
     .-3.2443E-05*N_L**4
      C=C*C_2
      endif
      Endif

      If (A.eq.2) Then !Staggered Tube bank
      If (Re.lt.500) Then
      C=1.04
      m=0.4
      else
            if (Re.lt.1000) Then
            C=0.71
            m=0.5
            else
                  if (Re.lt.2*10**5) Then
                  C=0.35d00 *(S_T/S_L)**(0.2d00)
                  m=0.6
                  else
                  C=0.031*(S_T/S_L)**0.2
                  m=0.8
                  endif
            endif
      endif
      If (N_L.lt.20) Then
      C_2=0.4844661+0.1829911*N_L-2.6572E-02*N_L**2+0.00170415*N_L**3
     .-3.9686E-05*N_L**4
      C=C*C_2
      EndIf
      Endif

      Return
      End
C     ************************************************************
      Subroutine LaminarTurbulent(Re,Pr,Nusselt)
      IMPLICIT NONE

      REAL Re,Pr,Nusselt

      If (Re.LT.2100) Then !Laminar
      Nusselt=4.36
      Else                       !Turbulent
      Nusselt=0.023*Re**(0.8)*Pr**(1.0/3.0) !Colburn Equation
      Endif

      Return
      End
C     ************************************************************
```

```
      Subroutine MaximumTankVelocity(S_t,S_L,D,V_tank,Aligned,
     .V_tank_max)
      IMPLICIT NONE

      DOUBLE PRECISION S_t, S_L
      REAL  D, S_D, V_tank, V_tank_max
      INTEGER Aligned

      S_D=sqrt(S_L**2+(S_t/2.0)**2)
      If ((Aligned.eq.2).and.(S_D.lt.((S_T+D)/2.0))) then !staggered
            v_tank_max=S_t/(2.0*(S_D-D)*V_tank)
      Else
            v_tank_max=S_T*V_tank/(S_t-D)
      EndIf

      Return
      End
C     ************************************************************
```

A.4 TYPE 88 TEMPERATURE-DEPENDENT PROPERTY DATA

General Description

Type 88 models temperature-dependent property data for three fluids: water, ethylene glycol and propylene glycol. The properties include viscosity, specific heat, conductivity and density.

Mathematical Description

The property data is based on curve fits from EES (Klein and Alvarado, 1997) for the propylene glycol and ethylene glycol. The property data for water is taken from curve fits of data given in Incropera and DeWitt (1990).

TRNSYS Component description

PARAMETER NO.		DESCRIPTION
1	substance	1 = water 2 = ethylene glycol 3 = propylene glycol
2	composition	percent of glycol by volume

INPUT NUMBER		DESCRIPTION
1	T	temperature (C)

OUTPUT NUMBER		DESCRIPTION
1	μ	dynamic viscosity of fluid (N-s/m^2)
2	Cp	specific heat of fluid (kJ/kg-K)
3	k	fluid conductivity (kJ/hr-m^2)
4	ρ	density of fluid (kg/m^3)

TYPE 88 – TEMPERATURE DEPENDENT PROPERTY DATA

Fortran Code

```
      SUBROUTINE TYPE88(TIME,XIN,OUT,T,DTDT,PAR,INFO,ICNTRL,*)

C**********************************************************************
C     THIS SUBROUTINE IS USED TO FIND TEMPERATURE DEPENDENT PROPERTY DATA
C     The data is based on curve fits using data from Incroprera and
Dewitt
C     LAST MODIFIED 19 OCTOBER 1997 -- MYRNA DAYAN
C**********************************************************************

      DOUBLE PRECISION XIN,OUT
      INTEGER*4 INFO
      DIMENSION XIN(1),OUT(4),PAR(2),INFO(15)
      CHARACTER*3 YCHECK(1),OCHECK(4)

      INTEGER  substance
      REAL  T, mu,k,Cp,rho, B,C,D, percent


      IF (INFO(7).GE.0) GO TO 100

C     FIRST CALL OF SIMULATION
      INFO(6)=4
      INFO(9)=0
      CALL TYPECK(1,INFO,1,2,0)
      DATA YCHECK/'DM1'/
      DATA OCHECK/'VS1','CP1','KT1','DN1'/
      CALL RCHECK(INFO,YCHECK,OCHECK)

c     SET INPUT PARAMETERS
100   substance=PAR(1)
      percent=PAR(2)

c     SET INPUT VARIABLES
      T=XIN(1)+273.15

      If (substance.eq.1)      then    !WATER
c     Linear regression for viscosity
      mu=0.1016859-8.6224E-04*T+2.4574E-06
     .*T**2-2.3453E-09*T**3

c     Linear regression for specific heat
      Cp=45.3589-4.9161E-01*T+0.00220051*T**2
     .-4.3807E-06*T**3+3.2760E-09*T**4

c     Linear regression for conductivity
      k=-4.9429E-01+0.00592939*T-7.4528E-06*T**2

c     Linear regression for density
      rho=758.1536+1.855018*T-3.5391E-03*T**2

      EndIf
```

```
      If (substance.eq.2) then !ETHYLENE GLYCOL
c     Linear regression for viscosity

      B = 970.43146598 - 10.001392253*T + 0.034056662648*T**2
     .- 3.8613683343e-5*T**3
      C = -27.036068044 + 0.27995557712*T - 0.00096062280174*T**2
     .+ 1.0941819338e-6*T**3
      D = 0.19624504556 - 0.0020225892738*T + 6.9220560583e-6*T**2
     .- 7.8710335530e-9*T**3
      mu= exp(B + C*percent + D*percent**2)

c     Linear regression for specific heat
      B = 3.9189 - 0.035267*percent
      C = 0.0014555 + 4.8423e-5*percent
      Cp = B + C*T

c     Linear regression for conductivity
      B = -0.84402 + 0.016948*percent - 6.99691e-5*percent**2
      C = 0.0079877 - 0.00012444*percent + 5.00412e-7*percent**2
      D = -1.06474e-5 + 1.708955e-7*percent - 7.065844e-10*percent**2
      k= B + C*T + D*T**2

c     Linear regression for density
      B = 884.53 + 2.1741*percent
      C = 1.1613 - 0.0033403*percent
      D = -0.0024393 + 2.994e-8*percent
      rho = B + C*T + D*T**2

      EndIf

      If (substance.eq.3) then ! PROPYLENE GLYCOL
c     Linear regression for viscosity

      B = 71.639163222 - 0.66981698459*T + 0.0019150513174*T**2
     . - 1.8587687783e-6*T**3
      C = 0.27019804611 - 0.0012299975866*T + 1.5045427918e-6*T**2
      mu= exp(B+C*percent)

c     Linear regression for specific heat
      B =3.8649883866-0.023691954902*percent-0.00011278222908*percent**2
      C = 0.001023655712 + 5.6633876714e-5*percent
      Cp = B + C*T

c     Linear regression for conductivity
      B = -0.78595253278 + 0.015561899561*percent
     . - 4.8933521576e-5*percent**2
      C = 0.0076866167254 - 0.0001155974176*percent
     .+ 3.6603360830e-7*percent**2
      D = -9.9976810237e-6 + 1.4560615474e-7*percent
     .- 4.5879383578e-10*percent**2
      k = B + C*T + D*T**2

c     Linear regression for density
      B = 875.54696219 + 2.151387542*percent
      C=1.1191046068-0.0007599907262*percent-4.9236799989e-5*percent**2
      D=-0.002377960199-9.1377252136e-6*percent
     .+1.0872237562e-7*percent**2
```

```
rho = B + C*T + D*T**2

EndIf

OUT(1)=mu   !N-s/m2
OUT(2)=Cp   !KJ/kg.K
OUT(3)=k*3.6 !kJ/hr-m-K
OUT(4)=rho  !kg/m3


RETURN 1
END
```

APPENDIX B

Conventional header-riser collector SDHW system

Conventional header-riser collector SDHW system with a heat exchanger

Serpentine collector SDHW system

Serpentine collector SDHW system with a PV driven pump

Serpentine collector SDHW system with a heat exchanger

Serpentine collector SDHW system with a PV driven pump and heat exchanger

TRNSYS DECK FOR A CONVENTIONAL HEADER-RISER COLLECTOR SDHW SYSTEM

```
ASSIGN C:\TRNWIN\WEATHER\ALBUQE.NM 10
ASSIGN M:\THESIS\wTMY\flat.LST 6
ASSIGN M:\THESIS\wTMY\flat.OUT 12
ASSIGN M:\THESIS\DRAW8760\Neuhou4.TXT 14

**********************************************
*      SOLAR DOMESTIC HOT WATER SYSTEM
*      INCORPORATING A CONVENTIONAL HEADER-RISER COLLECTOR
*      22 AUGUST 1997
*      MYRNA DAYAN
**********************************************

CONSTANTS 26
AREA=3.185
STARTDAY=1
STARTTIME=1
ENDTIME=8760
STEPTIME=0.1
PRINTTIME=1
CP_WATER=4.184
RHO_WATER=984
K_WATER=2.34
mu_WATER=0.000489
LATITUDE=35.1
REFL_GROUND=0.2
SLOPE=35
AZIMUTH=0
T_SET=55
T_ENV=20
T_MAINS=15
UA_TANK=1.44
V_TANK=0.4
HEIGHT_TANK=1.5
UA_HEATER=0
D_riser=0.004928
L=1.524
W=0.11
N_SERP=19
flowperarea=0.020

EQUATIONS 1
FLOWRATE= flowperarea*AREA*3600

EQUATIONS 1
n_PICTURES=(ENDTIME-STARTTIME)/24/4

SIMULATION STARTTIME ENDTIME STEPTIME
WIDTH 72
LIMITS 250 50

UNIT 1 TYPE 9 DATA READER
PARAMETERS 2
* MODE,  LOGICAL UNIT NUMBER
-1 10
```

```
*OUTPUTS
*month, hour, I_dn, I, T_db, w, W_vel, W_dir, t_d1, T-d2
*month_next, hour_next, I_dn_next, I_next, T_db_next,
*w_next, W_vel_next, W_dir_next,

UNIT 2 TYPE 16 SOLAR RADIATION PROCESSOR
PARAMETERS 9
* erbs correlation, tracking mode, tilted surface radiation mode,
* startday,latitude, solar constant, SHFT, SMOOTH, IE
3 1 1 STARTDAY LATITUDE 4871 0. 2 -1
INPUTS 6
* I, Tdl, Td2, rho_g, beta, gamma
1,4 1,19 1,20 0,0 0,0 0,0
0 0 0 REFL_GROUND SLOPE AZIMUTH
*OUTPUTS
*I_o,Theta_z, Gamma_s, I, I_d, I_T1, I_b1, I_d1, Theta_1, Beta_1
*I_Ti, I_bTi, Theta_i

UNIT 4 TYPE 3 PUMP IN COLLECTOR LOOP
PARAMETERS 4
*m_dot_max, Cp, P_max, f_par
FLOWRATE CP_WATER 1000. 0
INPUTS 3
*T_inlet, m_dot_inlet, control function
10,5 10,2 15,1
20. FLOWRATE 0
*OUTPUTS
*T_o,m_dot,Power consumption,Power supplied


UNIT 6 TYPE 1 FLAT PLATE COLLECTOR
PARAMETERS 11
*N, D_i, D, delta, L,W,k,U_be, E_p, alpha, N_G, eta_R
*Kl
3 1 AREA CP_WATER 0.9441  3.6 0.98 0.98 1 1.526  0.0524
INPUTS 10
*T_inlet, m_dot_collector, T_ambient, I_T,wind,I_h,I_d,rho_g,theta,beta
4,1 4,2 1,5 2,6 1,7 2,4 2,5 0,0 2,9 2,10
20 flowrate 20 3600 1 3600 3600 REFL_GROUND 40 40
*OUTPUTS
*I_o,Theta_z, Gamma_s, I, I_d, I_T1, I_b1, I_d1, Theta_1, Beta_1
*I_Ti, I_bTi, Theta_i

EQUATIONS 3
*THESE EQUATIONS ACT AS A TEMPERING VALVE
TDIFF=MAX(0.000001,([10,6]-T_MAINS))
TNKDRW=MIN(1,((T_SET-T_MAINS)/TDIFF))
M_LOAD=[19,2]*TNKDRW

UNIT 10 TYPE 60 STRATIFIED FLUID STORAGE TANK
PARAMETERS 32
*inlet position, tank volume, tank height, perimeter
*height inlet 1, height outlet 1, height inlet 2, height outlet 2
*Cp, rho, U_tank, k,  DELk, T_boil,Aux Mode, H_aux1,Hstat1
*Tset1,delTdb1, Q_aux1, H_aux2,Hstat2,Tset2,delTdb2, Q_aux2,UA_flue
*T_flue,Crit_fraction,Gas aux, hxMode,Hmode,umode
1 V_TANK HEIGHT_TANK -1 1.5 0.0 0.1 1.5 CP_WATER RHO_WATER  UA_TANK
k_WATER 0
```

```
100 2 1.2 1.2 T_SET 0 16000 0.7 0.7 T_SET 0 16000 0 20 10 0 0 0 0
INPUTS 9
*m_dot_1_in, m_dot_1_out, m_dot_2_in, m_dot_2_out
*T_1_in,T_2_in, T_env gamma_1, gamma_2
6,2 6,2 0,0 M_LOAD 6,1 0,0 0,0 0,0 0,0
FLOWRATE FLOWRATE -2 12.1 15 T_MAINS T_ENV 0 0
*OUTPUTS
*m_1_in, m_1_out, m_2_in, m_2_out, T_1_out,T_2_out,Q_env, Q_1_in,Q_1_out
*Q_2_in, Q_2_out, Q_aux, Q_aux_1, Q_aux_2, Q_flue, DEL_E, T_ave
*DEL_P_1_in, DEL_P_1_out, DEL_P_2_in, DEL_P_2_out
DERIVATIVES 20
20 20 20 20 20 20 20 20 20 20
20 20 20 20 20 20 20 20 20 20

UNIT 16 TYPE 6 ON/OFF AUXILIARY HEATER
PARAMETERS 5
*Q_max, T_set, Cp, UA , eta
16000 T_SET CP_WATER UA_HEATER 1
INPUTS 4
*T_inlet, m_dot_inlet, gamma, T_env
10,6 10,4 0,0 0,0
45 FLOWRATE 1 T_ENV
*OUTPUTS
*T_o,m_o,Q_aux,Q_loss,Q_fluid

UNIT 15 TYPE 2 ON/OFF DIFFERENTIAL CONTROLLER PUMP
PARAMETERS 4
*NSTK,deltaT_h,deltaT_l,T_MAX
7 0 0 300
INPUTS 4
*T_H,T_L,T_IN,GAMMA_i
6,1 10,5 6,1 15,1
20 20 90 0
*OUTPUTS
*GAMMA_o

UNIT 19 TYPE 9 DATA READER for water draw
PARAMETERS 11
*MODE, N, deltat_d, i, mi, ai, Logical unit #, FRMT
-2 2 1 -1 1 0 2 3.785 0 14 -1
*OUTPUT
*Hour, water draw

*UNIT 12 TYPE 25 PRINTER 1
*PARAMETERS 5
*TIME INTERVAL WHICH PRINTING WILL OCCUR, TIME AT WHICH PRINTING STARTS
*TIME AT WHICH PRINTING FINISHES, LOGICAL UNIT, UNITS
*STEPTIME STARTTIME ENDTIME 11 2
*INPUTS 9
*1,5 6,1 4,1 10,17 10,5 16,1 6,3  6,5 6,8
*TAMB TCOLL TPO TTANK TTANKCOL TTANKO QU FR UL

EQUATIONS 3
DHW=[10,4]*CP_WATER*(T_SET-15)+[16,4]
AUX=[16,3]
Q_ENV=[16,4]
```

```
UNIT 11 TYPE 24 INTEGRATOR
PARAMETERS 1
*TIME INTERVAL OVER WHICH INTEGRATED
-1
INPUTS 4
* SOLAR RADIATION, USEFUL ENERGY TO TANK, Q_AUX FROM TANK SOLAR FRACTION
2,6 DHW AUX Q_ENV
0.0 0.0 0.0 0.0
*OUTPUTS
*INTEGRAL OF ABOVE QUANTITIES

EQUATIONS 6
Q_SOLAR=[11,1]/1000000*AREA
Q_LOAD= [11,2]/1000000
Q_AUX=  [11,3]/1000000
Q_LOSS= [11,4]/1000000
DEN=EQL(Q_LOAD,0)+Q_LOAD
SF=1-Q_AUX/DEN

UNIT 13 TYPE 25 PRINTER 2
PARAMETERS 5
*TIME INTERVAL WHICH PRINTING WILL OCCUR, TIME AT WHICH PRINTING STARTS
*TIME AT WHICH PRINTING FINISHES, LOGICAL UNIT, UNITS
-1 STARTTIME ENDTIME 12 1
INPUTS 4
Q_SOLAR Q_LOAD  Q_AUX SF
Q_SOLAR Q_LOAD  Q_AUX SF
GJ GJ GJ 0


UNIT 14 TYPE 65 ONLINE PLOTTER
PARAMETERS 14
*N_top, N_bot, Y_min,1, Y_max,1, Y_min,2, Y_max,2, I_ref, I_upd
*units,N_pic,Grid,stop,symbols, on/off
8 3 0 180 0 5000 1 1 3 n_PICTURES 7 0 2 0
INPUTS 11
*VARIABLES TO BE PLOTTED
1,5 4,1 6,1 16,1 10,17 10,5 4,2 19,2 6,3 1,4 16,3
TA TPO TCOLL TTANKO TTANK TTANKCOL FLOW WATERDRAW QU I Q_aux
LABELS 4
C KG/HR
TEMPERATURE
ENERGY


END
```

TRNSYS DECK FOR A CONVENTIONAL HEADER-RISER COLLECTOR SDHW SYSTEM WITH A HEAT EXCHANGER

```
ASSIGN C:\TRNWIN\WEATHER\ALBUQE.NM 10
ASSIGN M:\THESIS\wTMY\FLAThtx.LST 6
ASSIGN M:\THESIS\wTMY\FLAThtx.OUT 12
ASSIGN M:\THESIS\DRAW8760\Neuhou4.TXT 14

*************************************************************
*      LOW FLOW SOLAR DOMESTIC HOT WATER SYSTEM
*      INCORPORATING A CONVENTIONAL HEADER-RISER COLLECTOR
*      AND A HEAT EXCHANGER.  THE HEAT EXCHANGER UA IS
*      DETERMINED IN TERMS OF FLOW RATE AND FLUID TEMPERATURES
*      11 NOVEMBER 1997
*      MYRNA DAYAN
*************************************************************

CONSTANTS 34
PI=3.14159
AREA=3.185
STARTDAY=1
STARTTIME=1
ENDTIME=8760
STEPTIME=0.1
PRINTTIME=1
CP_WATER=4.184
RHO_WATER=984
K_WATER=2.34
mu_WATER=0.000489
PR_WATER=3.148
CP_GLYCOL=3.580
RHO_GLYCOL=1058
k_GLYCOL=1.44
mu_GLYCOL=0.0011
PR_glycol=9.845
LATITUDE=35.1
REFL_GROUND=0.2
SLOPE=35
AZIMUTH=0
T_SET=55
T_ENV=20
T_MAINS=15
UA_TANK=1.44
V_TANK=0.4
HEIGHT_TANK=1.5
UA_HEATER=0
D_riser=0.004928
L=1.524
W=0.11
N_SERP=19
m_coll=0.02
m_tank=0.0035
*MATCHED TO THE WATER DRAW

EQUATIONS 2
flow_TANK=m_tank*Area*3600
```

```
flow_COLL=m_coll*Area*3600

EQUATIONS 1
n_PICTURES=(ENDTIME-STARTTIME)/24/4

SIMULATION STARTTIME ENDTIME STEPTIME
WIDTH 72
LIMITS 50 10

UNIT 1 TYPE 9 DATA READER
PARAMETERS 2
* MODE,  LOGICAL UNIT NUMBER
-1 10
*OUTPUTS
*month, hour, I_dn, I, T_db, w, W_vel, W_dir, t_d1, T-d2
*month_next, hour_next, I_dn_next, I_next, T_db_next,
*w_next, W_vel_next, W_dir_next,

UNIT 2 TYPE 16 SOLAR RADIATION PROCESSOR
PARAMETERS 9
* erbs correlation, tracking mode, tilted surface radiation mode,
* startday,latitude, solar constant, SHFT, SMOOTH, IE
3 1 1 STARTDAY LATITUDE 4871 0. 2 -1
INPUTS 6
* I, Tdl, Td2, rho_g, beta, gamma
1,4 1,19 1,20 0,0 0,0 0,0
0 0 0 REFL_GROUND SLOPE AZIMUTH
*OUTPUTS
*I_o,Theta_z, Gamma_s, I, I_d, I_T1, I_b1, I_d1, Theta_1, Beta_1
*I_Ti, I_bTi, Theta_i

UNIT 4 TYPE 3 PUMP IN COLLECTOR LOOP
PARAMETERS 4
*m_dot_max, Cp, P_max, f_par
flow_coll CP_GLYCOL 1000. 0
INPUTS 3
*T_inlet, m_dot_inlet, control function
8,1 8,2 15,1
20. flow_coll 0
*OUTPUTS
*T_o,m_dot,Power consumption,Power supplied

UNIT 6 TYPE 1 FLAT PLATE COLLECTOR
PARAMETERS 11
*N, D_i, D, delta, L,W,k,U_be, E_p, alpha, N_G, eta_R
*Kl
3 1 AREA CP_GLYCOL 0.9441  3.6 0.98 0.98 1 1.526  0.0524
INPUTS 10
*T_inlet, m_dot_collector, T_ambient, I_T,wind,I_h,I_d,rho_g,theta,beta
4,1 4,2 1,5 2,6 1,7 2,4 2,5 0,0 2,9 2,10
20 flow_COLL 20 3600 1 3600 3600 REFL_GROUND 40 40
*OUTPUTS
*I_o,Theta_z, Gamma_s, I, I_d, I_T1, I_b1, I_d1, Theta_1, Beta_1
*I_Ti, I_bTi, Theta_i

EQUATIONS 2
T_glycol_hx=([6,1]+[8,1])/2
T_water_hx=([9,1]+[8,3])/2
```

```
UNIT 3 TYPE 88 THERMODYNAMIC PROPERTIES FOR GLYCOL
PARAMETERS 2
*substance percent
2 55
INPUTS 1
*temperature
T_glycol_hx
60
*OUTPUTS
*mu, cp, k, rho

UNIT 5 TYPE 88 THERMODYNAMIC PROPERTIES FOR WATER
PARAMETERS 2
*substance percent (not used)
1 100
INPUTS 1
*temperature
T_water_hx
60
*OUTPUTS
*mu, cp, k, rho


UNIT 7 TYPE 87 UA FOR SHELL AND TUBE HEAT EXCHANGER
PARAMETERS 10
*D_i,D,S_t,S_L,L_hx,A,N_L,k_copper, N_tubes, baffle_spacing
0.0065 0.0095 0.01 0.01 0.75 2 5 401 19 0.05
INPUTS 9
*m_dot_collector,m_dot_tank,mu_collector,Cp_collector,k_collector
*mu_tank,Cp_tank,k_tank,rho_tank
6,2 9,2 3,1 0,0 0,0 5,1 0,0 0,0 0,0
*3,1 3,2 3,3 5,1 5,2 5,3 5,4
flow_coll flow_tank mu_glycol Cp_glycol k_glycol
mu_water Cp_water k_water rho_water
*OUTPUTS
*UA

UNIT 8 TYPE 5 HEAT EXCHANGER
PARAMETERS 4
*mode, dummy, Cp_hot,Cp_cold
2 1 CP_glycol CP_water
INPUTS 5
*T_hi,m_dot_hot, T_cold_inlet, m_dot_cold UA
6,1 6,2 9,1 9,2 7,1
20. flow_coll 20. FLOW_TANK 200
*OUTPUTS
*T_ho, m_dot_h, T_co, m_dot_c, Q_dot_T, Epsilon

UNIT 9 TYPE 3 PUMP - TANK SIDE
PARAMETERS 4
*m_dot_max, Cp, P_max, f_par
FLOW_TANK CP_WATER 1000. 0.
INPUTS 3
*T_inlet, m_dot_inlet, control function
10,5 10,2 15,1
20. FLOW_TANK 1.
*OUTPUTS
```

```
*T_o,m_dot,Power consumption,Power supplied

EQUATIONS 3
*THESE EQUATIONS ACT AS A TEMPERING VALVE
TDIFF=MAX(0.000001,([10,6]-T_MAINS))
TNKDRW=MIN(1,((T_SET-T_MAINS)/TDIFF))
M_LOAD=[19,2]*TNKDRW


UNIT 10 TYPE 60 STRATIFIED FLUID STORAGE TANK
PARAMETERS 32
*inlet position, tank volume, tank height, perimeter
*height inlet 1, height outlet 1, height inlet 2, height outlet 2
*Cp, rho, U_tank, k,  DELk, T_boil,Aux Mode, H_aux1,Hstat1
*Tset1,delTdb1, Q_aux1, H_aux2,Hstat2,Tset2,delTdb2, Q_aux2,UA_flue
*T_flue,Crit_fraction,Gas aux, hxMode,Hmode,umode
1 V_TANK HEIGHT_TANK -1 1.5 0.0 0.1 1.5 CP_WATER RHO_WATER  UA_TANK
k_WATER 0
100 2 1.2 1.2 T_SET 0 16000 0.7 0.7 T_SET 0 16000 0 20 10 0 0 0 0
INPUTS 9
*m_dot_1_in, m_dot_1_out, m_dot_2_in, m_dot_2_out
*T_1_in,T_2_in, T_env, gamma_1, gamma_2
8,4 8,4 0,0 M_LOAD 8,3 0,0 0,0 0,0 0,0
45 45 -2 12.1 15 T_MAINS T_ENV 0 0
*OUTPUTS
*m_1_in, m_1_out, m_2_in, m_2_out, T_1_out,T_2_out,Q_env , Q_1_in,Q_1_out
*Q_2_in, Q_2_out, Q_aux, Q_aux_1, Q_aux_2, Q_flue, DEL_E, T_ave
*DEL_P_1_in, DEL_P_1_out, DEL_P_2_in, DEL_P_2_out
DERIVATIVES 20
20 20 20 20 20 20 20 20 20 20
20 20 20 20 20 20 20 20 20 20

UNIT 16 TYPE 6 ON/OFF AUXILIARY HEATER
PARAMETERS 5
*Q_max, T_set, Cp, UA , eta
16000 T_SET CP_WATER UA_HEATER 1
INPUTS 4
*T_inlet, m_dot_inlet, gamma, T_env
10,6 10,4 0,0 0,0
45 45 1 T_ENV
*OUTPUTS
*T_o,m_o,Q_aux,Q_loss,Q_fluid

UNIT 15 TYPE 2 ON/OFF DIFFERENTIAL CONTROLLER PUMP
PARAMETERS 4
*NSTK,deltaT_h,deltaT_l,T_MAX
7 0 0 300
INPUTS 4
*T_H,T_L,T_IN,GAMMA_i
6,1 10,5 6,1 15,1
20 20 90 0
*OUTPUTS
*GAMMA_o

UNIT 19 TYPE 9 DATA READER for water draw
PARAMETERS 11
*MODE, N, deltat_d, i, mi, ai, Logical unit #, FRMT
-2 2 1 -1 1 0 2 3.785 0 14 -1
```

```
*OUTPUT
*Hour, water draw

*UNIT 12 TYPE 25 PRINTER 1
*PARAMETERS 5
*TIME INTERVAL WHICH PRINTING WILL OCCUR, TIME AT WHICH PRINTING STARTS
*TIME AT WHICH PRINTING FINISHES, LOGICAL UNIT, UNITS
*STEPTIME STARTTIME ENDTIME 11 2
*INPUTS 10
*3,1 3,2 3,3 3,4 5,1 5,2 5,3 5,4 7,1 8,6
*mu_glycol cp_glycol k_glycol rho_glycol
*mu_water cp_water k_water rho_water  UA epsilon

EQUATIONS 3
DHW=[10,4]*CP_WATER*(T_SET-15)+[16,4]
AUX=[16,3]
Q_ENV=[16,4]

UNIT 11 TYPE 24 INTEGRATOR
PARAMETERS 1
*TIME INTERVAL OVER WHICH INTEGRATED
-1
INPUTS 4
* SOLAR RADIATION, USEFUL ENERGY TO TANK, Q_AUX FROM TANK SOLAR FRACTION
2,6 DHW AUX Q_ENV
0.0 0.0 0.0 0.0
*OUTPUTS
*INTEGRAL OF ABOVE QUANTITIES

EQUATIONS 7
Q_SOLAR=[11,1]/1000000*AREA
Q_LOAD= [11,2]/1000000
Q_AUX=  [11,3]/1000000
Q_LOSS= [11,4]/1000000
DEN=EQL(Q_LOAD,0)+Q_LOAD
SF=1-Q_AUX/DEN
epsilon=[8,6]*100

UNIT 13 TYPE 25 PRINTER 2
PARAMETERS 5
*TIME INTERVAL WHICH PRINTING WILL OCCUR, TIME AT WHICH PRINTING STARTS
*TIME AT WHICH PRINTING FINISHES, LOGICAL UNIT, UNITS
-1 STARTTIME ENDTIME 12 1
INPUTS 4
Q_SOLAR Q_LOAD Q_AUX  SF
Q_SOLAR Q_LOAD Q_AUX  SF
GJ GJ GJ  0

UNIT 14 TYPE 65 ONLINE PLOTTER
PARAMETERS 14
*N_top, N_bot, Y_min,1, Y_max,1, Y_min,2, Y_max,2, I_ref, I_upd
*units,N_pic,Grid,stop,symbols, on/off
7 4 0 200 0 5000 1 1 3 n_PICTURES 7 0 2 0
INPUTS 11
*VARIABLES TO BE PLOTTED
1,5  6,1 16,1 10,17 epsilon 19,2 3,2 6,3 1,4 16,3 7,1
TA  TCOLL TTANKO TTANK effectiveness WATERDRAW flow QU I Q_aux UA
LABELS 4
```

```
C KG/HR
TEMPERATURE
ENERGY

END
```

TRNSYS DECK FOR A SERPENTINE COLLECTOR SDHW SYSTEM

```
ASSIGN C:\TRNWIN\WEATHER\miamif.fl 10
ASSIGN C:\THESIS\wTMY\serpen.LST 6
ASSIGN C:\THESIS\wTMY\serpen.OUT 12
ASSIGN C:\THESIS\DRAW8760\Neuhou4.TXT 14

**********************************************
*      LOW FLOW SOLAR DOMESTIC HOT WATER SYSTEM
*      INCORPORATING A SERPENTINE COLLECTOR
*      22 AUGUST 1997
*      MYRNA DAYAN
**********************************************

CONSTANTS 26
AREA=3.185
STARTDAY=1
STARTTIME=1
ENDTIME=8760
STEPTIME=0.1
PRINTTIME=1
CP_WATER=4.184
RHO_WATER=984
K_WATER=2.34
mu_WATER=0.000489
LATITUDE=25.8
REFL_GROUND=0.2
SLOPE=25
AZIMUTH=0
T_SET=55
T_ENV=20
T_MAINS=15
UA_TANK=1.44
V_TANK=0.4
HEIGHT_TANK=1.5
UA_HEATER=0
D_riser=0.004928
L=1.524
W=0.11
N_SERP=19
flowperarea=0.020
EQUATIONS 1
FLOWRATE= flowperarea*AREA*3600
EQUATIONS 1
n_PICTURES=(ENDTIME-STARTTIME)/24/4

SIMULATION STARTTIME ENDTIME STEPTIME
WIDTH 72
LIMITS 500 100

UNIT 1 TYPE 9 DATA READER
PARAMETERS 2
* MODE,  LOGICAL UNIT NUMBER
-1 10
*OUTPUTS
*month, hour, I_dn, I, T_db, w, W_vel, W_dir, t_d1, T-d2
*month_next, hour_next, I_dn_next, I_next, T_db_next,
```

```
*w_next, W_vel_next, W_dir_next,

UNIT 2 TYPE 16 SOLAR RADIATION PROCESSOR
PARAMETERS 9
* erbs correlation, tracking mode, tilted surface radiation mode,
* startday,latitude, solar constant, SHFT, SMOOTH, IE
3 1 1 STARTDAY LATITUDE 4871 0. 2 -1
INPUTS 6
* I, Td1, Td2, rho_g, beta, gamma
1,4 1,19 1,20 0,0 0,0 0,0
0 0 0 REFL_GROUND SLOPE AZIMUTH
*OUTPUTS
*I_o,Theta_z, Gamma_s, I, I_d, I_T1, I_b1, I_d1, Theta_1, Beta_1
*I_Ti, I_bTi, Theta_i

UNIT 4 TYPE 3 PUMP IN COLLECTOR LOOP
PARAMETERS 4
*m_dot_max, Cp, P_max, f_par
FLOWRATE CP_WATER 1000. 0
INPUTS 3
*T_inlet, m_dot_inlet, control function
10,5 10,2 15,1
20. FLOWRATE 0
*OUTPUTS
*T_o,m_dot,Power consumption,Power supplied

EQUATIONS 1
T_WATER_AV=([4,1]+[6,1])/2

UNIT 3 TYPE 88 THERMODYNAMIC PROPERTIES FOR GLYCOL
PARAMETERS 2
*substance percent
1 55
INPUTS 1
*temperature
T_WATER_AV
60
*OUTPUTS
*mu, cp, k, rho


UNIT 6 TYPE 86 SERPENTINE COLLECTOR
PARAMETERS 13
*N, D_i, D, delta, L,W,k,U_be, E_p, alpha, N_G, eta_R
*Kl
N_SERP D_riser 0.00635 0.0002 L 0.11 1386 3.6 0.98
0.98 1 1.526  0.0524
INPUTS 14
*T_inlet, m_dot_collector, T_ambient, I_T,wind,I_h,I_d,rho_g,theta,beta
4,1 4,2 1,5 2,6 1,7 2,4 2,5 0,0 2,9 2,10 3,1 3,2 3,3 3,4
20 flowrate 20 3600 1 3600 3600 REFL_GROUND 40 40
mu_WATER Cp_WATER k_WATER rho_WATER
*OUTPUTS
*I_o,Theta_z, Gamma_s, I, I_d, I_T1, I_b1, I_d1, Theta_1, Beta_1
*I_Ti, I_bTi, Theta_i

EQUATIONS 3
*THESE EQUATIONS ACT AS A TEMPERING VALVE
```

```
TDIFF=MAX(0.000001,([10,6]-T_MAINS))
TNKDRW=MIN(1,((T_SET-T_MAINS)/TDIFF))
M_LOAD=[19,2]*TNKDRW

UNIT 10 TYPE 60 STRATIFIED FLUID STORAGE TANK
PARAMETERS 32
*inlet position, tank volume, tank height, perimeter
*height inlet 1, height outlet 1, height inlet 2, height outlet 2
*Cp, rho, U_tank, k,  DELk, T_boil,Aux Mode, H_aux1,Hstat1
*Tset1,delTdb1, Q_aux1, H_aux2,Hstat2,Tset2,delTdb2, Q_aux2,UA_flue
*T_flue,Crit_fraction,Gas aux, hxMode,Hmode,umode
1 V_TANK HEIGHT_TANK -1 1.5 0.0 0.1 1.5 CP_WATER RHO_WATER  UA_TANK
k_WATER 0
100 2 1.2 1.2 T_SET 0 16000 0.7 0.7 T_SET 0 16000 0 20 10 0 0 0 0
INPUTS 9
*m_dot_1_in, m_dot_1_out, m_dot_2_in, m_dot_2_out
*T_1_in,T_2_in, T_env gamma_1, gamma_2
6,2 6,2 0,0 M_LOAD 6,1 0,0 0,0 0,0 0,0
FLOWRATE FLOWRATE -2 12.1 15 T_MAINS T_ENV 0 0
*OUTPUTS
*m_1_in, m_1_out, m_2_in, m_2_out, T_1_out,T_2_out,Q_env, Q_1_in,Q_1_out
*Q_2_in, Q_2_out, Q_aux, Q_aux_1, Q_aux_2, Q_flue, DEL_E, T_ave
*DEL_P_1_in, DEL_P_1_out, DEL_P_2_in, DEL_P_2_out
DERIVATIVES 20
20 20 20 20 20 20 20 20 20 20
20 20 20 20 20 20 20 20 20 20

UNIT 16 TYPE 6 ON/OFF AUXILIARY HEATER
PARAMETERS 5
*Q_max, T_set, Cp, UA , eta
16000 T_SET CP_WATER UA_HEATER 1
INPUTS 4
*T_inlet, m_dot_inlet, gamma, T_env
10,6 10,4 0,0 0,0
45 FLOWRATE 1 T_ENV
*OUTPUTS
*T_o,m_o,Q_aux,Q_loss,Q_fluid

UNIT 15 TYPE 2 ON/OFF DIFFERENTIAL CONTROLLER PUMP
PARAMETERS 4
*NSTK,deltaT_h,deltaT_l,T_MAX
7 0 0 300
INPUTS 4
*T_H,T_L,T_IN,GAMMA_i
6,1 10,5 6,1 15,1
20 20 90 0
*OUTPUTS
*GAMMA_o

UNIT 19 TYPE 9 DATA READER for water draw
PARAMETERS 11
*MODE, N, deltat_d, i, mi, ai, Logical unit #, FRMT
-2 2 1 -1 1 0 2 3.785 0 14 -1
*OUTPUT
*Hour, water draw

*UNIT 12 TYPE 25 PRINTER 1
*PARAMETERS 5
```

```
*TIME INTERVAL WHICH PRINTING WILL OCCUR, TIME AT WHICH PRINTING STARTS
*TIME AT WHICH PRINTING FINISHES, LOGICAL UNIT, UNITS
*STEPTIME STARTTIME ENDTIME 11 2
*INPUTS 9
*1,5 6,1 4,1 10,17 10,5 16,1 6,3  6,5 6,8
*TAMB TCOLL TPO TTANK TTANKCOL TTANKO QU FR UL

EQUATIONS 3
DHW=[10,4]*CP_WATER*(T_SET-15)+[16,4]
AUX=[16,3]
Q_ENV=[16,4]


UNIT 11 TYPE 24 INTEGRATOR
PARAMETERS 1
*TIME INTERVAL OVER WHICH INTEGRATED
-1
INPUTS 4
* SOLAR RADIATION, USEFUL ENERGY TO TANK, Q_AUX FROM TANK SOLAR FRACTION
2,6 DHW AUX Q_ENV
0.0 0.0 0.0 0.0
*OUTPUTS
*INTEGRAL OF ABOVE QUANTITIES

EQUATIONS 6
Q_SOLAR=[11,1]/1000000*AREA
Q_LOAD= [11,2]/1000000
Q_AUX=  [11,3]/1000000
Q_LOSS= [11,4]/1000000
DEN=EQL(Q_LOAD,0)+Q_LOAD
SF=1-Q_AUX/DEN

UNIT 13 TYPE 25 PRINTER 2
PARAMETERS 5
*TIME INTERVAL WHICH PRINTING WILL OCCUR, TIME AT WHICH PRINTING STARTS
*TIME AT WHICH PRINTING FINISHES, LOGICAL UNIT, UNITS
-1 STARTTIME ENDTIME 12 1
INPUTS 4
Q_SOLAR Q_LOAD  Q_AUX SF
Q_SOLAR Q_LOAD  Q_AUX SF
GJ GJ GJ 0


UNIT 14 TYPE 65 ONLINE PLOTTER
PARAMETERS 14
*N_top, N_bot, Y_min,1, Y_max,1, Y_min,2, Y_max,2, I_ref, I_upd
*units,N_pic,Grid,stop,symbols, on/off
8 3 0 180 0 5000 1 1 3 n_PICTURES 7 0 2 0
INPUTS 11
*VARIABLES TO BE PLOTTED
1,5 4,1 6,1 16,1 10,17 10,5 4,2 19,2 6,3 1,4 16,3
TA TPO TCOLL TTANKO TTANK TTANKCOL FLOW WATERDRAW QU I Q_aux
LABELS 4
C KG/HR
TEMPERATURE
ENERGY

END
```

TRNSYS DECK FOR A SERPENTINE COLLECTOR AND PV DRIVEN PUMP SDHW SYSTEM

```
ASSIGN C:\TRNWIN\WEATHER\albuqe.nm 10
ASSIGN M:\THESIS\wTMY\serpPV.LST 6
ASSIGN M:\THESIS\wTMY\serpPV.OUT 12
ASSIGN M:\THESIS\DRAW8760\Neuhou4.TXT 14

**********************************************************
*      LOW FLOW SOLAR DOMESTIC HOT WATER SYSTEM
*      INCORPORATING A SERPENTINE COLLECTOR AND PV DRIVEN PUMP
*      7 OCTOBER 1997
*      MYRNA DAYAN
**********************************************************

CONSTANTS 27
PI=3.14159
AREA=3.185
STARTDAY=1
STARTTIME=1
ENDTIME=8760
STEPTIME=0.1
PRINTTIME=1
CP_WATER=4.184
RHO_WATER=984
K_WATER= 2.34
mu_WATER=0.000489
PR_WATER=3.148
LATITUDE=35.1
REFL_GROUND=0.2
SLOPE=35
AZIMUTH=0
T_SET=55
T_ENV=20
T_MAINS=15
UA_TANK=1.44
V_TANK=0.4
HEIGHT_TANK=1.5
UA_HEATER=0
D_riser=0.004928
L=0.762
***** FIX THIS
W=0.11
N_SERP=19

EQUATIONS 1
n_PICTURES=(ENDTIME-STARTTIME)/24/4

SIMULATION STARTTIME ENDTIME STEPTIME
WIDTH 72
LIMITS 250 10

UNIT 1 TYPE 9 DATA READER
PARAMETERS 2
* MODE,  LOGICAL UNIT NUMBER
-1 10
*OUTPUTS
```

```
*month, hour, I_dn, I, T_db, w, W_vel, W_dir, t_d1, T-d2
*month_next, hour_next, I_dn_next, I_next, T_db_next,
*w_next, W_vel_next, W_dir_next,


UNIT 2 TYPE 16 SOLAR RADIATION PROCESSOR
PARAMETERS 9
* erbs correlation, tracking mode, tilted surface radiation mode,
* startday,latitude, solar constant, SHFT, SMOOTH, IE
3 1 1 STARTDAY LATITUDE 4871 0. 2 -1
INPUTS 6
* I, Td1, Td2, rho_g, beta, gamma
1,4 1,19 1,20 0,0 0,0 0,0
0 0 0 REFL_GROUND SLOPE AZIMUTH
*OUTPUTS
*I_o,Theta_z, Gamma_s, I, I_d, I_T1, I_b1, I_d1, Theta_1, Beta_1
*I_Ti, I_bTi, Theta_i

EQUATIONS 1
T_WATER_AV=([10,5]+[6,1])/2

UNIT 3 TYPE 88 THERMODYNAMIC PROPERTIES FOR GLYCOL
PARAMETERS 2
*substance percent
1 0
INPUTS 1
*temperature
T_WATER_AV
60
*OUTPUTS
*mu, cp, k, rho


UNIT 6 TYPE 86 SERPENTINE COLLECTOR
PARAMETERS 13
*N, D_i, D, delta, L,W,k,C_p, U_be, E_p, alpha, N_G, eta_R
*Kl, mu, Pr, K_f, rho_water
19 D_riser 0.00635 0.0002 1.524  W 1386
3.6 0.98 0.98 1 1.526  0.0524
INPUTS 14
*T_inlet, m_dot_collector, T_ambient, I_T,wind,I_h,I_d,rho_g,theta,beta
10,5 71,1 1,5 2,6 1,7 2,4 2,5 0,0 2,9 2,10 3,1 3,2 3,3 3,4
20 45 20 3600 1 3600 3600 REFL_GROUND 40 40
mu_water CP_WATER k_WATER rho_WATER
*OUTPUTS
* T_o, m_dot, Q_u,T_pm, F_R,TauAlpha, F', U_L


EQUATIONS 3
*THESE EQUATIONS ACT AS A TEMPERING VALVE
TDIFF=MAX(0.000001,([10,6]-T_MAINS))
TNKDRW=MIN(1,((T_SET-T_MAINS)/TDIFF))
M_LOAD=[19,2]*TNKDRW

UNIT 10 TYPE 60 STRATIFIED FLUID STORAGE TANK
PARAMETERS 32
*inlet position, tank volume, tank height, perimeter
*height inlet 1, height outlet 1, height inlet 2, height outlet 2
```

```
*Cp, rho, U_tank, k,  DELk, T_boil,Aux Mode, H_aux1,Hstat1
*Tset1,delTdb1, Q_aux1, H_aux2,Hstat2,Tset2,delTdb2, Q_aux2,UA_flue
*T_flue,Crit_fraction,Gas aux, hxMode,Hmode,umode
1 V_TANK HEIGHT_TANK -1 1.5 0.0 0.1 1.5 CP_WATER RHO_WATER  UA_TANK
k_WATER 0
100 2 1.2 1.2 T_SET 0 16000 0.7 0.7 T_SET 0 16000 0 20 10 0 0 0 0
INPUTS 9
*m_dot_1_in, m_dot_1_out, m_dot_2_in, m_dot_2_out
*T_1_in,T_2_in, T_env, gamma_1, gamma_2
6,2 6,2 0,0 M_LOAD 6,1 0,0 0,0 0,0 0,0
45 45 -2 12.1 15 T_MAINS T_ENV 0 0
*OUTPUTS
*m_1_in, m_1_out, m_2_in, m_2_out, T_1_out,T_2_out,Q_env , Q_1_in,Q_1_out
*Q_2_in, Q_2_out, Q_aux, Q_aux_1, Q_aux_2, Q_flue, DEL_E, T_ave
*DEL_P_1_in, DEL_P_1_out, DEL_P_2_in, DEL_P_2_out
DERIVATIVES 20
20 20 20 20 20 20 20 20 20 20
20 20 20 20 20 20 20 20 20 20

UNIT 16 TYPE 6 ON/OFF AUXILIARY HEATER
PARAMETERS 5
*Q_max, T_set, Cp, UA , eta
16000 T_SET CP_WATER UA_HEATER 1
INPUTS 4
*T_inlet, m_dot_inlet, gamma, T_env
10,6 10,4 0,0 0,0
45 45 1 T_ENV
*OUTPUTS
*T_o,m_o,Q_aux,Q_loss,Q_fluid

UNIT 19 TYPE 9 DATA READER for water draw
PARAMETERS 11
*MODE, N, deltat_d, i, mi, ai, Logical unit #, FRMT
-2 2 1 -1 1 0 2 3.785 0 14 -1
*OUTPUT
*Hour, water draw


*UNIT 12 TYPE 25 PRINTER 1
*PARAMETERS 5
*TIME INTERVAL WHICH PRINTING WILL OCCUR, TIME AT WHICH PRINTING STARTS
*TIME AT WHICH PRINTING FINISHES, LOGICAL UNIT, UNITS
*STEPTIME STARTTIME ENDTIME 11 2
*INPUTS 3
*62,1 62,2 71,1
*CURRENT VOLTAGE M_DOT

EQUATIONS 3
DHW=[10,4]*CP_WATER*(T_SET-15)+[16,4]
AUX=[16,3]
Q_ENV=[16,4]


UNIT 11 TYPE 24 INTEGRATOR
PARAMETERS 1
*TIME INTERVAL OVER WHICH INTEGRATED
-1
INPUTS 4
```

```
* SOLAR RADIATION, USEFUL ENERGY TO TANK, Q_AUX FROM TANK SOLAR FRACTION
2,6 DHW AUX Q_ENV
0.0 0.0 0.0 0.0
*OUTPUTS
*INTEGRAL OF ABOVE QUANTITIES

EQUATIONS 6
Q_SOLAR=[11,1]/1000000*AREA
Q_LOAD= [11,2]/1000000
Q_AUX=  [11,3]/1000000
Q_LOSS= [11,4]/1000000
DEN=EQL(Q_LOAD,0)+Q_LOAD
SF=1-Q_AUX/DEN

UNIT 13 TYPE 25 PRINTER 2
PARAMETERS 5
*TIME INTERVAL WHICH PRINTING WILL OCCUR, TIME AT WHICH PRINTING STARTS
*TIME AT WHICH PRINTING FINISHES, LOGICAL UNIT, UNITS
-1 STARTTIME ENDTIME 12 1
INPUTS 4
Q_SOLAR Q_LOAD Q_AUX  SF
Q_SOLAR Q_LOAD Q_AUX  SF
GJ GJ GJ GJ  0

UNIT 14 TYPE 65 ONLINE PLOTTER
PARAMETERS 14
*N_top, N_bot, Y_min,1, Y_max,1, Y_min,2, Y_max,2, I_ref, I_upd
*units,N_pic,Grid,stop,symbols, on/off
7 3 0 180 0 5000 1 1 3 n_PICTURES 7 0 2 0
INPUTS 10
*VARIABLES TO BE PLOTTED
1,5  6,1 16,1 10,17 10,5 19,2 71,1 6,3 1,4 16,3
TA  TCOLL TTANKO TTANK TTANKCOL WATERDRAW flow QU I Q_aux
LABELS 4
C KG/HR
TEMPERATURE
ENERGY

UNIT 71 TYPE 71 Pump/Motor/System
PARAMETERS 24
*mu,rho,D_pipe,L_pipe,N_bends,N,L,W,D_riser,V_threshold,curve fitting
parameters a-p
 0.005 10 4 N_serp L W D_riser 5.5 -1.0069E+01 -4.9072E+00 -6.7853E-01
-1.5984E-02 +3.551104 -3.2935E-01 +0.01149067 0.8669153 -4.3065E-02
+0.06917987
-6.1515E-04 0.4640587 -9.1174E-02 +0.01059595 +0.01497438 -7.4913E-03
INPUTS 3
*voltage
62,2 3,1 3,4
14 MU_WATER RHO_WATER
*OUTPUTS
*m_dot, current, voltage, P_pump

CONSTANTS 3
TauAlpha=0.9
T_cell_NOCT=46
G_T_NOCT=800
EQUATIONS 1
```

```
U_L_pv=TauAlpha*G_T_NOCT/(T_cell_NOCT-[1,5])*3.6

UNIT 62 TYPE 62 PHOTOVOLTAIC PANEL
PARAMETERS 17
*mode_PV,mode_CVG,G_T_ref,T_cell_ref,Isc_ref,Voc_ref,Imp_ref,Vmp_ref,MIsc
*MVoc,taualpha,E_g,NCS,width,length,Ns_pv,Np_pv
2 2 3600 25 1.45 20 1.33 13 0.001325 -0.0775 TauAlpha 1.12 36 0.35 0.66
1 1
INPUTS 6
*G_t,T_amb,U_L,I,I_pv,V_pv
2,6 1,5 0,0 71,2 62,1 62,2
2400 25 U_L_pv 1.4 1.4 15
*OUTPUTS
*I_pv  V_pv  P_pv  Imp  Vmp Pmax Isc Voc T_cell Eff_pv  utiliz

END
```

TRNSYS DECK FOR SERPENTINE COLLECTOR SDHW SYSTEM WITH A HEAT EXCHANGER

```
ASSIGN C:\TRNWIN\WEATHER\madisn.wi 10
ASSIGN d:\myrna\wTMY\serphtx.LST 6
ASSIGN d:\myrna\wTMY\serphtx.OUT 12
ASSIGN d:\myrna\THESIS\DRAW8760\Neuhou4.TXT 14

*************************************************************
*      LOW FLOW SOLAR DOMESTIC HOT WATER SYSTEM
*      INCORPORATING A CONVENTIONAL SERPENTINE COLLECTOR
*      AND A HEAT EXCHANGER.  THE HEAT EXCHANGER UA IS
*      DETERMINED IN TERMS OF FLOW RATE AND FLUID TEMPERATURES
*      11 NOVEMBER 1997
*      MYRNA DAYAN
*************************************************************

CONSTANTS 34
PI=3.14159
AREA=3.185
STARTDAY=1
STARTTIME=1
ENDTIME=8760
STEPTIME=0.1
PRINTTIME=1
CP_WATER=4.184
RHO_WATER=984
K_WATER=2.34
mu_WATER=0.000489
PR_WATER=3.148
CP_GLYCOL=3.580
RHO_GLYCOL=1058
k_GLYCOL=1.44
mu_GLYCOL=0.0011
PR_glycol=9.845
LATITUDE=43.1
REFL_GROUND=0.2
SLOPE=40
AZIMUTH=0
T_SET=55
T_ENV=20
T_MAINS=15
UA_TANK=1.44
V_TANK=0.4
HEIGHT_TANK=1.5
UA_HEATER=0
D_riser=0.004928
L=1.524
W=0.11
N_SERP=19
m_coll=0.004
m_tank=0.003
*MATCHED TO THE WATER DRAW

EQUATIONS 2
flow_TANK=m_tank*Area*3600
flow_COLL=m_coll*Area*3600
```

```
EQUATIONS 1
n_PICTURES=(ENDTIME-STARTTIME)/24/4

SIMULATION STARTTIME ENDTIME STEPTIME
WIDTH 72
LIMITS 250 50

UNIT 1 TYPE 9 DATA READER
PARAMETERS 2
* MODE,  LOGICAL UNIT NUMBER
-1 10
*OUTPUTS
*month, hour, I_dn, I, T_db, w, W_vel, W_dir, t_d1, T-d2
*month_next, hour_next, I_dn_next, I_next, T_db_next,
*w_next, W_vel_next, W_dir_next,

UNIT 2 TYPE 16 SOLAR RADIATION PROCESSOR
PARAMETERS 9
* erbs correlation, tracking mode, tilted surface radiation mode,
* startday,latitude, solar constant, SHFT, SMOOTH, IE
3 1 1 STARTDAY LATITUDE 4871 0. 2 -1
INPUTS 6
* I, Tdl, Td2, rho_g, beta, gamma
1,4 1,19 1,20 0,0 0,0 0,0
0 0 0 REFL_GROUND SLOPE AZIMUTH
*OUTPUTS
*I_o,Theta_z, Gamma_s, I, I_d, I_T1, I_b1, I_d1, Theta_1, Beta_1
*I_Ti, I_bTi, Theta_i

UNIT 4 TYPE 3 PUMP IN COLLECTOR LOOP
PARAMETERS 4
*m_dot_max, Cp, P_max, f_par
flow_coll CP_GLYCOL 1000. 0
INPUTS 3
*T_inlet, m_dot_inlet, control function
8,1 8,2 15,1
20. flow_coll 0
*OUTPUTS
*T_o,m_dot,Power consumption,Power supplied

UNIT 6 TYPE 86 SERPENTINE COLLECTOR
PARAMETERS 13
*N, D_i, D, delta, L,W,k,C_p, U_be, E_p, alpha, N_G, eta_R
*Kl, mu, Pr, K_f, rho_fluid
19 D_riser 0.00635 0.0002 1.524  W 1386
3.6 0.98 0.98 1 1.526  0.0524
INPUTS 14
*T_inlet, m_dot_collector, T_ambient, I_T,wind,I_h,I_d,rho_g,theta,beta
4,1 4,2 1,5 2,6 1,7 2,4 2,5 0,0 2,9 2,10 3,1 3,2 3,3 3,4
20 45 20 3600 1 3600 3600 REFL_GROUND 40 40 mu_GLYCOL Cp_GLYCOL k_GLYCOL
rho_GLYCOL
*OUTPUTS
* T_o, m_dot, Q_u,T_pm, F_R,TauAlpha, F', U_L

EQUATIONS 2
T_glycol_hx=([6,1]+[8,1])/2
T_water_hx=([9,1]+[8,3])/2
```

```
UNIT 3 TYPE 88 THERMODYNAMIC PROPERTIES FOR GLYCOL
PARAMETERS 2
*substance percent
2 55
INPUTS 1
*temperature
T_glycol_hx
60
*OUTPUTS
*mu, cp, k, rho

UNIT 5 TYPE 88 THERMODYNAMIC PROPERTIES FOR WATER
PARAMETERS 2
*substance percent (not used)
1 100
INPUTS 1
*temperature
T_water_hx
60
*OUTPUTS
*mu, cp, k, rho


UNIT 7 TYPE 87 UA FOR SHELL AND TUBE HEAT EXCHANGER
PARAMETERS 10
*D_i,D,S_t,S_L,L_hx,A,N_L,k_copper, N_tubes, baffle_spacing
0.0065 0.0095 0.01 0.01 0.75 2 5 401 19 0.05
INPUTS 9
*m_dot_collector,m_dot_tank,mu_collector,Cp_collector,k_collector
*mu_tank,Cp_tank,k_tank,rho_tank
6,2 9,2 3,1 0,0 0,0 5,1 0,0 0,0 0,0
*3,1 3,2 3,3 5,1 5,2 5,3 5,4
flow_coll flow_tank mu_glycol Cp_glycol k_glycol
mu_water Cp_water k_water rho_water
*OUTPUTS
*UA

UNIT 8 TYPE 5 HEAT EXCHANGER
PARAMETERS 4
*mode, dummy, Cp_hot,Cp_cold
2 1 CP_glycol CP_water
INPUTS 5
*T_hi,m_dot_hot, T_cold_inlet, m_dot_cold UA
6,1 6,2 9,1 9,2 7,1
20. flow_coll 20. FLOW_TANK 200
*OUTPUTS
*T_ho, m_dot_h, T_co, m_dot_c, Q_dot_T, Epsilon

UNIT 9 TYPE 3 PUMP - TANK SIDE
PARAMETERS 4
*m_dot_max, Cp, P_max, f_par
FLOW_TANK CP_WATER 1000. 0.
INPUTS 3
*T_inlet, m_dot_inlet, control function
10,5 10,2 15,1
20. FLOW_TANK 1.
*OUTPUTS
```

```
*T_o,m_dot,Power consumption,Power supplied

EQUATIONS 3
*THESE EQUATIONS ACT AS A TEMPERING VALVE
TDIFF=MAX(0.000001,([10,6]-T_MAINS))
TNKDRW=MIN(1,((T_SET-T_MAINS)/TDIFF))
M_LOAD=[19,2]*TNKDRW


UNIT 10 TYPE 60 STRATIFIED FLUID STORAGE TANK
PARAMETERS 32
*inlet position, tank volume, tank height, perimeter
*height inlet 1, height outlet 1, height inlet 2, height outlet 2
*Cp, rho, U_tank, k,  DELk, T_boil,Aux Mode, H_aux1,Hstat1
*Tset1,delTdb1, Q_aux1, H_aux2,Hstat2,Tset2,delTdb2, Q_aux2,UA_flue
*T_flue,Crit_fraction,Gas aux, hxMode,Hmode,umode
1 V_TANK HEIGHT_TANK -1 1.5 0.0 0.1 1.5 CP_WATER RHO_WATER  UA_TANK
k_WATER 0
100 2 1.2 1.2 T_SET 0 16000 0.7 0.7 T_SET 0 16000 0 20 10 0 0 0 0
INPUTS 9
*m_dot_1_in, m_dot_1_out, m_dot_2_in, m_dot_2_out
*T_1_in,T_2_in, T_env, gamma_1, gamma_2
8,4 8,4 0,0 M_LOAD 8,3 0,0 0,0 0,0 0,0
45 45 -2 12.1 15 T_MAINS T_ENV 0 0
*OUTPUTS
*m_1_in, m_1_out, m_2_in, m_2_out, T_1_out,T_2_out,Q_env , Q_1_in,Q_1_out
*Q_2_in, Q_2_out, Q_aux, Q_aux_1, Q_aux_2, Q_flue, DEL_E, T_ave
*DEL_P_1_in, DEL_P_1_out, DEL_P_2_in, DEL_P_2_out
DERIVATIVES 20
20 20 20 20 20 20 20 20 20 20
20 20 20 20 20 20 20 20 20 20

UNIT 16 TYPE 6 ON/OFF AUXILIARY HEATER
PARAMETERS 5
*Q_max, T_set, Cp, UA , eta
16000 T_SET CP_WATER UA_HEATER 1
INPUTS 4
*T_inlet, m_dot_inlet, gamma, T_env
10,6 10,4 0,0 0,0
45 45 1 T_ENV
*OUTPUTS
*T_o,m_o,Q_aux,Q_loss,Q_fluid

UNIT 15 TYPE 2 ON/OFF DIFFERENTIAL CONTROLLER PUMP
PARAMETERS 4
*NSTK,deltaT_h,deltaT_l,T_MAX
7 0 0 300
INPUTS 4
*T_H,T_L,T_IN,GAMMA_i
6,1 10,5 6,1 15,1
20 20 90 0
*OUTPUTS
*GAMMA_o

UNIT 19 TYPE 9 DATA READER for water draw
PARAMETERS 11
*MODE, N, deltat_d, i, mi, ai, Logical unit #, FRMT
-2 2 1 -1 1 0 2 3.785 0 14 -1
```

```
*OUTPUT
*Hour, water draw

*UNIT 12 TYPE 25 PRINTER 1
*PARAMETERS 5
*TIME INTERVAL WHICH PRINTING WILL OCCUR, TIME AT WHICH PRINTING STARTS
*TIME AT WHICH PRINTING FINISHES, LOGICAL UNIT, UNITS
*STEPTIME STARTTIME ENDTIME 11 2
*INPUTS 10
*3,1 3,2 3,3 3,4 5,1 5,2 5,3 5,4 7,1 8,6
*mu_glycol cp_glycol k_glycol rho_glycol
*mu_water cp_water k_water rho_water  UA epsilon

EQUATIONS 3
DHW=[10,4]*CP_WATER*(T_SET-15)+[16,4]
AUX=[16,3]
Q_ENV=[16,4]

UNIT 11 TYPE 24 INTEGRATOR
PARAMETERS 1
*TIME INTERVAL OVER WHICH INTEGRATED
-1
INPUTS 4
* SOLAR RADIATION, USEFUL ENERGY TO TANK, Q_AUX FROM TANK SOLAR FRACTION
2,6 DHW AUX Q_ENV
0.0 0.0 0.0 0.0
*OUTPUTS
*INTEGRAL OF ABOVE QUANTITIES

EQUATIONS 7
Q_SOLAR=[11,1]/1000000*AREA
Q_LOAD= [11,2]/1000000
Q_AUX=  [11,3]/1000000
Q_LOSS= [11,4]/1000000
DEN=EQL(Q_LOAD,0)+Q_LOAD
SF=1-Q_AUX/DEN
epsilon=[8,6]*100

UNIT 13 TYPE 25 PRINTER 2
PARAMETERS 5
*TIME INTERVAL WHICH PRINTING WILL OCCUR, TIME AT WHICH PRINTING STARTS
*TIME AT WHICH PRINTING FINISHES, LOGICAL UNIT, UNITS
-1 STARTTIME ENDTIME 12 1
INPUTS 4
Q_SOLAR Q_LOAD Q_AUX  SF
Q_SOLAR Q_LOAD Q_AUX  SF
GJ GJ GJ  0

UNIT 14 TYPE 65 ONLINE PLOTTER
PARAMETERS 14
*N_top, N_bot, Y_min,1, Y_max,1, Y_min,2, Y_max,2, I_ref, I_upd
*units,N_pic,Grid,stop,symbols, on/off
7 4 0 200 0 5000 1 1 3 n_PICTURES 7 0 2 -1
INPUTS 11
*VARIABLES TO BE PLOTTED
1,5  6,1 16,1 10,17 epsilon 19,2 3,2 6,3 1,4 16,3 7,1
TA  TCOLL TTANKO TTANK effectiveness WATERDRAW flow QU I Q_aux UA
LABELS 4
```

```
C KG/HR
TEMPERATURE
ENERGY

END
```

TRNSYS DECK FOR A SERPENTINE COLLECTOR AND PV DRIVEN SDHW SYSTEM WITH A HEAT EXCHANGER

```
ASSIGN C:\TRNWIN\WEATHER\ALBUQE.NM 10
ASSIGN M:\THESIS\wTMY\serphtxPV.LST 6
ASSIGN M:\THESIS\wTMY\serphtxPV.OUT 12
ASSIGN M:\THESIS\DRAW8760\Neuhou4.TXT 14

*************************************************************
*      LOW FLOW SOLAR DOMESTIC HOT WATER SYSTEM
*      INCORPORATING A SERPENTINE COLLECTOR, A PV DRIVEN PUMP
*      AND A HEAT EXCHANGER.  THE HEAT EXCHANGER UA IS
*      DETERMINED IN TERMS OF FLOW RATE AND FLUID TEMPERATURES
*      17 NOVEMBER 1997
*      MYRNA DAYAN
*************************************************************

CONSTANTS 33
PI=3.14159
AREA=3.185
STARTDAY=1
STARTTIME=1
ENDTIME=8760
STEPTIME=0.1
PRINTTIME=1
CP_WATER=4.184
RHO_WATER=984
K_WATER=2.34
mu_WATER=0.000489
PR_WATER=3.148
CP_GLYCOL=3.580
RHO_GLYCOL=1058
k_GLYCOL=1.44
mu_GLYCOL=0.0011
PR_glycol=9.845
LATITUDE=35.1
REFL_GROUND=0.2
SLOPE=35
AZIMUTH=0
T_SET=55
T_ENV=20
T_MAINS=15
UA_TANK=1.44
V_TANK=0.4
HEIGHT_TANK=1.5
UA_HEATER=0
D_riser=0.004928
L=0.762
*** FIX THIS
W=0.11
N_SERP=19
m_tank=0.0035
*MATCHED TO THE WATER DRAW

EQUATIONS 1
flow_TANK=m_tank*Area*3600
```

```
EQUATIONS 1
n_PICTURES=(ENDTIME-STARTTIME)/24/4

SIMULATION STARTTIME ENDTIME STEPTIME
WIDTH 72
LIMITS 250 10

UNIT 1 TYPE 9 DATA READER
PARAMETERS 2
* MODE,  LOGICAL UNIT NUMBER
-1 10
*OUTPUTS
*month, hour, I_dn, I, T_db, w, W_vel, W_dir, t_d1, T-d2
*month_next, hour_next, I_dn_next, I_next, T_db_next,
*w_next, W_vel_next, W_dir_next,

UNIT 2 TYPE 16 SOLAR RADIATION PROCESSOR
PARAMETERS 9
* erbs correlation, tracking mode, tilted surface radiation mode,
* startday,latitude, solar constant, SHFT, SMOOTH, IE
3 1 1 STARTDAY LATITUDE 4871 0. 2 -1
INPUTS 6
* I, Td1, Td2, rho_g, beta, gamma
1,4 1,19 1,20 0,0 0,0 0,0
0 0 0 REFL_GROUND SLOPE AZIMUTH
*OUTPUTS
*I_o,Theta_z, Gamma_s, I, I_d, I_T1, I_b1, I_d1, Theta_1, Beta_1
*I_Ti, I_bTi, Theta_i


UNIT 6 TYPE 86 SERPENTINE COLLECTOR
PARAMETERS 13
*N, D_i, D, delta, L,W,k,C_p, U_be, E_p, alpha, N_G, eta_R
*Kl, mu, Pr, K_f, rho_fluid
19 D_riser 0.00635 0.0002 1.524  W 1386
3.6 0.98 0.98 1 1.526  0.0524
INPUTS 14
*T_inlet, m_dot_collector, T_ambient, I_T,wind,I_h,I_d,rho_g,theta,beta
8,1 71,1 1,5 2,6 1,7 2,4 2,5 0,0 2,9 2,10 3,1 3,2 3,3 3,4
20 45 20 3600 1 3600 3600 REFL_GROUND 40 40 mu_GLYCOL Cp_GLYCOL k_GLYCOL
rho_GLYCOL
*OUTPUTS
* T_o, m_dot, Q_u,T_pm, F_R,TauAlpha, F', U_L

EQUATIONS 2
T_glycol_hx=([6,1]+[8,1])/2
T_water_hx=([9,1]+[8,3])/2

UNIT 3 TYPE 88 THERMODYNAMIC PROPERTIES FOR GLYCOL
PARAMETERS 2
*substance percent
2 55
INPUTS 1
*temperature
T_glycol_hx
60
*OUTPUTS
```

```
*mu, cp, k, rho

UNIT 5 TYPE 88 THERMODYNAMIC PROPERTIES FOR WATER
PARAMETERS 2
*substance percent (not used)
1 100
INPUTS 1
*temperature
T_water_hx
60
*OUTPUTS
*mu, cp, k, rho


UNIT 7 TYPE 87 UA FOR SHELL AND TUBE HEAT EXCHANGER
PARAMETERS 10
*D_i,D,S_t,S_L,L_hx,A,N_L,k_copper, N_tubes, baffle_spacing
0.0065 0.0095 0.01 0.01 0.75 2 5 401 19 0.05
INPUTS 9
*m_dot_collector,m_dot_tank,mu_collector,Cp_collector,k_collector
*mu_tank,Cp_tank,k_tank,rho_tank
6,2 9,2 3,1 0,0 0,0 5,1 0,0 0,0 0,0
*3,1 3,2 3,3 5,1 5,2 5,3 5,4
0.005 flow_tank mu_glycol Cp_glycol k_glycol
mu_water Cp_water k_water rho_water
*OUTPUTS
*UA

UNIT 8 TYPE 5 HEAT EXCHANGER
PARAMETERS 4
*mode, dummy, Cp_hot,Cp_cold
2 1 CP_glycol CP_water
INPUTS 5
*T_hi,m_dot_hot, T_cold_inlet, m_dot_cold UA
6,1 6,2 9,1 9,2 7,1
20. 0.005 20. FLOW_TANK 200
*OUTPUTS
*T_ho, m_dot_h, T_co, m_dot_c, Q_dot_T, Epsilon

UNIT 9 TYPE 3 PUMP - TANK SIDE
PARAMETERS 4
*m_dot_max, Cp, P_max, f_par
FLOW_TANK CP_WATER 1000. 0.
INPUTS 3
*T_inlet, m_dot_inlet, control function
10,5 10,2 15,1
20. FLOW_TANK 1.
*OUTPUTS
*T_o,m_dot,Power consumption,Power supplied

EQUATIONS 3
*THESE EQUATIONS ACT AS A TEMPERING VALVE
TDIFF=MAX(0.000001,([10,6]-T_MAINS))
TNKDRW=MIN(1,((T_SET-T_MAINS)/TDIFF))
M_LOAD=[19,2]*TNKDRW


UNIT 10 TYPE 60 STRATIFIED FLUID STORAGE TANK
```

```
PARAMETERS 32
*inlet position, tank volume, tank height, perimeter
*height inlet 1, height outlet 1, height inlet 2, height outlet 2
*Cp, rho, U_tank, k,  DELk, T_boil,Aux Mode, H_aux1,Hstat1
*Tset1,delTdb1, Q_aux1, H_aux2,Hstat2,Tset2,delTdb2, Q_aux2,UA_flue
*T_flue,Crit_fraction,Gas aux, hxMode,Hmode,umode
1 V_TANK HEIGHT_TANK -1 1.5 0.0 0.1 1.5 CP_WATER RHO_WATER  UA_TANK
k_WATER 0
100 2 1.2 1.2 T_SET 0 16000 0.7 0.7 T_SET 0 16000 0 20 10 0 0 0 0
INPUTS 9
*m_dot_1_in, m_dot_1_out, m_dot_2_in, m_dot_2_out
*T_1_in,T_2_in, T_env, gamma_1, gamma_2
8,4 8,4 0,0 M_LOAD 8,3 0,0 0,0 0,0 0,0
45 45 -2 12.1 15 T_MAINS T_ENV 0 0
*OUTPUTS
*m_1_in, m_1_out, m_2_in, m_2_out, T_1_out,T_2_out,Q_env , Q_1_in,Q_1_out
*Q_2_in, Q_2_out, Q_aux, Q_aux_1, Q_aux_2, Q_flue, DEL_E, T_ave
*DEL_P_1_in, DEL_P_1_out, DEL_P_2_in, DEL_P_2_out
DERIVATIVES 20
20 20 20 20 20 20 20 20 20 20
20 20 20 20 20 20 20 20 20 20

UNIT 16 TYPE 6 ON/OFF AUXILIARY HEATER
PARAMETERS 5
*Q_max, T_set, Cp, UA , eta
16000 T_SET CP_WATER UA_HEATER 1
INPUTS 4
*T_inlet, m_dot_inlet, gamma, T_env
10,6 10,4 0,0 0,0
45 45 1 T_ENV
*OUTPUTS
*T_o,m_o,Q_aux,Q_loss,Q_fluid

UNIT 15 TYPE 2 ON/OFF DIFFERENTIAL CONTROLLER PUMP
PARAMETERS 4
*NSTK,deltaT_h,deltaT_l,T_MAX
7 0 0 300
INPUTS 4
*T_H,T_L,T_IN,GAMMA_i
6,1 10,5 6,1 15,1
20 20 90 0
*OUTPUTS
*GAMMA_o

UNIT 19 TYPE 9 DATA READER for water draw
PARAMETERS 11
*MODE, N, deltat_d, i, mi, ai, Logical unit #, FRMT
-2 2 1 -1 1 0 2 3.785 0 14 -1
*OUTPUT
*Hour, water draw

*UNIT 12 TYPE 25 PRINTER 1
*PARAMETERS 5
*TIME INTERVAL WHICH PRINTING WILL OCCUR, TIME AT WHICH PRINTING STARTS
*TIME AT WHICH PRINTING FINISHES, LOGICAL UNIT, UNITS
*STEPTIME STARTTIME ENDTIME 11 2
*INPUTS 10
*3,1 3,2 3,3 3,4 5,1 5,2 5,3 5,4 7,1 8,6
```

```
*mu_glycol cp_glycol k_glycol rho_glycol
*mu_water cp_water k_water rho_water  UA epsilon

EQUATIONS 3
DHW=[10,4]*CP_WATER*(T_SET-15)+[16,4]
AUX=[16,3]
Q_ENV=[16,4]

UNIT 11 TYPE 24 INTEGRATOR
PARAMETERS 1
*TIME INTERVAL OVER WHICH INTEGRATED
-1
INPUTS 4
* SOLAR RADIATION, USEFUL ENERGY TO TANK, Q_AUX FROM TANK SOLAR FRACTION
2,6 DHW AUX Q_ENV
0.0 0.0 0.0 0.0
*OUTPUTS
*INTEGRAL OF ABOVE QUANTITIES

EQUATIONS 7
Q_SOLAR=[11,1]/1000000*AREA
Q_LOAD= [11,2]/1000000
Q_AUX=  [11,3]/1000000
Q_LOSS= [11,4]/1000000
DEN=EQL(Q_LOAD,0)+Q_LOAD
SF=1-Q_AUX/DEN
epsilon=[8,6]*100

UNIT 13 TYPE 25 PRINTER 2
PARAMETERS 5
*TIME INTERVAL WHICH PRINTING WILL OCCUR, TIME AT WHICH PRINTING STARTS
*TIME AT WHICH PRINTING FINISHES, LOGICAL UNIT, UNITS
-1 STARTTIME ENDTIME 12 1
INPUTS 4
Q_SOLAR Q_LOAD Q_AUX  SF
Q_SOLAR Q_LOAD Q_AUX  SF
GJ GJ GJ  0

UNIT 14 TYPE 65 ONLINE PLOTTER
PARAMETERS 14
*N_top, N_bot, Y_min,1, Y_max,1, Y_min,2, Y_max,2, I_ref, I_upd
*units,N_pic,Grid,stop,symbols, on/off
7 4 0 200 0 5000 1 1 3 n_PICTURES 7 0 2 0
INPUTS 11
*VARIABLES TO BE PLOTTED
1,5  6,1 16,1 10,17 epsilon 19,2 3,2 6,3 1,4 16,3 7,1
TA  TCOLL TTANKO TTANK effectiveness WATERDRAW flow QU I Q_aux UA
LABELS 4
C KG/HR
TEMPERATURE
ENERGY

UNIT 71 TYPE 71 Pump/Motor/System
PARAMETERS 24
*mu,rho,D_pipe,L_pipe,N_bends,N,L,W,D_riser,V_threshold,curve fitting
parameters a-p
 0.005 10 4 N_serp L W D_riser 5.5 -1.0069E+01 -4.9072E+00 -6.7853E-01
```

```
-1.5984E-02 +3.551104 -3.2935E-01 +0.01149067 0.8669153 -4.3065E-02
+0.06917987
-6.1515E-04 0.4640587 -9.1174E-02 +0.01059595 +0.01497438 -7.4913E-03
INPUTS 3
*voltage
62,2 3,1 3,4
14 MU_WATER RHO_WATER
*OUTPUTS
*m_dot, current, voltage, P_pump

CONSTANTS 3
TauAlpha=0.9
T_cell_NOCT=46
G_T_NOCT=800
EQUATIONS 1
U_L_pv=TauAlpha*G_T_NOCT/(T_cell_NOCT-[1,5])*3.6

UNIT 62 TYPE 62 PHOTOVOLTAIC PANEL
PARAMETERS 17
*mode_PV,mode_CVG,G_T_ref,T_cell_ref,Isc_ref,Voc_ref,Imp_ref,Vmp_ref,MIsc
*MVoc,taualpha,E_q,NCS,width,length,Ns_pv,Np_pv
2 2 3600 25 1.45 20 1.33 13 0.001325 -0.0775 TauAlpha 1.12 36 0.35 0.66
1 1
INPUTS 6
*G_t,T_amb,U_L,I,I_pv,V_pv
2,6 1,5 0,0 71,2 62,1 62,2
2400 25 U_L_pv 1.4 1.4 15
*OUTPUTS
*I_pv  V_pv  P_pv  Imp  Vmp Pmax Isc Voc T_cell Eff_pv  utiliz

END
```

APPENDIX C

Header-Riser Pressure Drop Calculations

Finite Difference Serpentine Collector Analysis

HEADER-RISER PRESSURE DROP CALCULATIONS

EES Program

```
"Calculates pressure drop, pressure and flow distribution for a flat
plate collector"
"Model:  Alta Energy Liquid Flat Plate Collector ATL 100-1"
"_____________________________________________________________"
Procedure MoodyChart (Re:f)

If Re<0.001 Then  "No flow"
f:=0
Else
If Re<2100  Then "Laminar"
   f:=64/Re
Else "Turbulent"
"This is a good estimate for smooth pipes"
   f:=(0.79*ln(Re)-1.64)^(-2)
EndIf
EndIf
End
"_____________________________________________________________"

"Collector Area" A_collector=22.1*convert(ft^2,m^2)
"Number of risers" N=16
"Header Length" L_header=(33+3/8)*convert(in,m)
"Length of risers " L=(97+3/8-2*D_header)*convert(in,m)
"Distance between risers" W=(2-D_riser)*convert(in,m)
"Riser inside diameter" D_riser= D_r_n
"Nominal riser diameter" D_r_n=3/8*convert(in,m)
"Header diameter" D_header=1*convert(in,m)

"Kinematic viscosity" mu=6.55e-4
"Density" rho=995
"_____________________________________________________________"

"Find head loss across the risers"
Duplicate j=1,N
H[2*j-1,2*j]=v[2*j-1,2*j]^2*f[2*j-1,2*j]*(L+2*L_eq_riser[2*j-
1,2*j])/D_riser/2*10^(-3)
End

"Find head loss across the headers"
Duplicate j=0,N-1
"Lower headers"
H[2*j-1,2*j+1]=v[2*j-1,2*j+1]^2*f[2*j-1,2*j+1]*(W+L_eq_lheader[2*j-
1,2*j+1])/D_header/2*10^(-3)
End

"Upper headers"
Duplicate j=1,N
H[2*j,2*j+2]=v[2*j,2*j+2]^2*f[2*j,2*j+2]*(W+L_eq_uheader[2*j,2*j+2])/D
_header/2*10^(-3)
End

"_____________________________________________________________"
```

```
"Mass Balances"
"Along lower header  nodes"
Duplicate j=0,N-2
m[2*j-1,2*j+1]=m[2*j+1,2*j+2]+m[2*j+1,2*j+3]
End
m[1,2]=m[2,4]
"Along upper header nodes"
Duplicate j=1,N-1
m[2*j,2*j+2]+m[2*j+1,2*j+2]=m[2*j+2,2*j+4]
End
m[2*N-1,2*N]=m[2*N-3,2*N-1]

"_____"

"Calculate pressures through the collector"
"Risers"
Duplicate j=1,N
P[2*j-1]/rho=P[2*j]/rho+H[2*j-1,2*j]
End
"Lower headers"
Duplicate j=0,N-1
P[2*j-1]/rho=P[2*j+1]/rho+H[2*j-1,2*j+1]
(P[2*j+1]-P_out)/Pressure_Drop=P_lower_header[j+1]

End
"Upper Headers"
Duplicate j=1,N
P[2*j]/rho=P[2*j+2]/rho+H[2*j,2*j+2]
(P[2*j]-P_out)/Pressure_Drop=P_upper_header[j]
End

Duplicate j=1,N
Riser[j]=j
End

"_____"


"Convert mass flow rates to velocities"
A_riser=pi*(D_riser/2)^2
A_header=pi*(D_header/2)^2

"Along risers"
Duplicate j=1,N
m[2*j-1,2*j]=rho*A_riser*v[2*j-1,2*j]
Re[2*j-1,2*j]=rho*v[2*j-1,2*j]*D_riser/mu
Call MoodyChart(Re[2*j-1,2*j]:f[2*j-1,2*j]);
End

"Lower headers"
Duplicate j=0,N-1
m[2*j-1,2*j+1]=rho*A_header*v[2*j-1,2*j+1]
Re[2*j-1,2*j+1]=rho*v[2*j-1,2*j+1]*D_header/mu
Call MoodyChart(Re[2*j-1,2*j+1]:f[2*j-1,2*j+1]);
End

"Upper headers"
```

```
Duplicate j=1,N
m[2*j,2*j+2]=rho*A_header*v[2*j,2*j+2]
Re[2*j,2*j+2]=rho*v[2*j,2*j+2]*D_header/mu
Call MoodyChart(Re[2*j,2*j+2]:f[2*j,2*j+2]);
End

"_____"

"K - factors at the tee-joints"
"Lower Headers"
"RANDOM DISTRIBUTION OF K-factors"
K_header[-1,1]=1.45
K_header[1,3]=1.6
K_header[3,5]=2.3
K_header[5,7]=1.45
K_header[7,9]=1.45
K_header[9,11]=1.45
K_header[11,13]=1.9
K_header[13,15]=1.9
K_header[15,17]=2.5
K_header[17,19]=2.7
K_header[19,21]=1.8
K_header[21,23]=1.8
K_header[23,25]=1.6
K_header[25,27]=1.45
K_header[27,29]=1.45
K_header[29,31]=1.8

Duplicate j=0,N-1
L_eq_lheader[2*j-1,2*j+1]=K_header[-1,1]*D_header/f[2*j-1,2*j+1]
End

"Risers"
{K_riser=0.9}
K_riser[1,2]=0.9
K_riser[3,4]=1.0
K_riser[5,6]=1.2
K_riser[7,8]=0.9
K_riser[9,10]=0.9
K_riser[11,12]=0.8
K_riser[13,14]=1.5
K_riser[15,16]=1.0
K_riser[17,18]=1.4
K_riser[19,20]=1.0
K_riser[21,22]=0.9
K_riser[23,24]=0.9
K_riser[25,26]=1.1
K_riser[27,28]=1.4
K_riser[29,30]=1.0
K_riser[31,32]=0.9
Duplicate j=1,N
L_eq_riser[2*j-1,2*j]=K_riser[1,2]*D_riser/f[2*j-1,2*j]
End

K_header[2,4]=1.45
K_header[4,6]=1.60
K_header[6,8]=1.8
K_header[8,10]=2.4
```

```
K_header[10,12]=1.4
K_header[12,14]=1.6
K_header[14,16]=2.2
K_header[16,18]=2.0
K_header[18,20]=1.9
K_header[20,22]=2.4
K_header[22,24]=2.3
K_header[24,26]=1.6
K_header[26,28]=2.0
K_header[28,30]=2.3
K_header[30,32]=1.6
K_header[32,34]=1.45
"Upper Headers"
Duplicate j=1,N
L_eq_uheader[2*j,2*j+2]=K_header[2,4]*D_header/f[2*j,2*j+2]
End

"_____"
"Inlet Conditions"
P[-1]=100
m[-1,1]=mass_english*convert(gpm, m^3/s)*rho
{mass_english=1.5}
P_out=p[2*N+2]
Pressure_Drop=P[-1]-P_out
Pressure_Drop_english=(P[-1]-P_out)*convert(kpa,psi)

"_____"
"Prepare plot for flow distribution"
"Use lower node"
Duplicate j=1,N
flow[j]=m[2*j-1,2*j]/m[-1,1]
End

flow\area=m[-1,1]/A_collector
xx=2/60/1000/A_collector/rho*convert(m^3/s,gpm)

flow\area=0.002
m_dot_in=m[-1,1]
flow[1]=m_dot_riser\m_dot_in[1]
```

FINITE DIFFERENCE SERPENTINE COLLECTOR ANALYSIS

EES Program

```
Procedure LAMINARTURBULENT(Re,L:friction,laminar,turbulent,nusselt)

      mu=3.6e-4
      a=0.0534
      b=0.0335
      m_ht=1.15
      nw=0.82
      kw=0.67
      mu_w=mu
      Pr=2.2 "Assume water at 80 C"
      L = 1.0 "Length of one serpentine segment"
      D_i=6.5 *10^(-3)"Tube inside diameter"
If Re<2100 Then "Laminar"
      friction:=64/Re
      laminar:=1
      turbulent:=0
      Nusselt=3.7+a*(Re*Pr*D_i/L)^m_ht/(1+b*(Re*Pr*D_i/L)^nw)
Else "Turblent"
      friction:=(0.79*ln(Re)-1.64)^(-2)
      laminar:=0
      turbulent:=1
      Nusselt=
(friction/8)*Re*Pr/(1.07+12.7*sqrt(friction/8)*(Pr^(2/3)-
1))*(mu/mu_w)^0.11
EndIf
End
"_____"

Procedure OddEven(x:odd,even)
If (Trunc(x/2)-x/2=0)  Then
   Even=1
   Odd=0
Else
   Even=0
   Odd=1
Endif
End
"_____"


k=211
delta=0.0015
D=0.0075
U_L=5
T_a=20
S=1000
L_nodes=40
R=1/(pi*D_i*h_fi)
DELTA_y=L/L_nodes
L=1.0
A_c=N*W*L
m_dot=0.014
```

```
C_p=4190
T_in=20
N=10
A_c=1
"_____________________________________________________________________"
m^2=U_L*(W-D)^2/(k*delta)
kappa=k*delta*m/((W-D)*sinh(m))

Duplicate j=0,L_nodes
Duplicate i=1,N
theta[i,j]=T[i,j]-T_a-(S/U_L)
End
End
"_____________________________________________________________________"

"HEAT TRANSFER COEFFICIENT"
D_i=6.5e-3
mu=0.00036
kw=0.67
Re_serpentine=4*m_dot/(pi*D_i*mu)
L_tube_serpentine=N*(L+W)-W
Call
LaminarTurbulent(Re_serpentine,L_tube_serpentine:friction_serpentine,d
ummy2,dummy3,Nusselt_serpentine);
h_fi={Nusselt_serpentine*kw/D_i}1500
"_____________________________________________________________________"
"Heat Transfer from fins to tube"

q_plus[1,0]=kappa*theta[1,0]*(1-cosh(m))*DELTA_y/2
q_plus[1,L_nodes]=kappa*theta[1,L_nodes]*(1-cosh(m))*DELTA_y/2
Duplicate i=2,N
q_plus[i,0]=kappa*(theta[i-1,0]-theta[i,0]*cosh(m))*DELTA_y/2
q_plus[i,L_nodes]=kappa*(theta[i-1,L_nodes]-
theta[i,L_nodes]*cosh(m))*DELTA_y/2
End

Duplicate j=1,L_nodes-1
q_plus[1,j]=kappa*theta[1,j]*(1-cosh(m))*DELTA_y
Duplicate i=2,N
q_plus[i,j]=kappa*(theta[i-1,j]-theta[i,j]*cosh(m))*DELTA_y
End
End

q_minus[N,0]=kappa*theta[N,0]*(1-cosh(m))*DELTA_y/2
q_minus[N,L_nodes]=kappa*theta[N,L_nodes]*(1-cosh(m))*DELTA_y/2
Duplicate i=1,N-1
q_minus[i,0]=kappa*(theta[i+1,0]-theta[i,0]*cosh(m))*DELTA_y/2
q_minus[i,L_nodes]=kappa*(theta[i+1,L_nodes]-
theta[i,L_nodes]*cosh(m))*DELTA_y/2
End

Duplicate j=1,L_nodes-1
Duplicate i=1,N-1
q_minus[i,j]=kappa*(theta[i+1,j]-theta[i,j]*cosh(m))*DELTA_y
End
q_minus[N,j]=kappa*theta[N,j]*(1-cosh(m))*DELTA_y
End
"_____________________________________________________________________"
```

```
"Useful heat transfer to tube and fluid"

Duplicate i=1,N
q_useful[i,0]=q_plus[i,0]+q_minus[i,0]-D*U_L*Theta[i,0]*DELTA_y/2
q_useful[i,0]=(T[i,0]-T_f[i,0])/R*DELTA_y/2
End

Duplicate i=1,N
q_useful[i,L_nodes]=q_plus[i,L_nodes]+q_minus[i,L_nodes]-
D*U_L*Theta[i,L_nodes]*DELTA_y/2
q_useful[i,L_nodes]=(T[i,L_nodes]-T_f[i,L_nodes])/R*DELTA_y/2
End

Duplicate j=1,L_nodes-1
Duplicate i=1,N
q_useful[i,j]=q_plus[i,j]+q_minus[i,j]-D*U_L*Theta[i,j]*DELTA_y
q_useful[i,j]=(T[i,j]-T_f[i,j])/R*DELTA_y
End
End
"_____________________________________________________________"
"Heat transfer to fluid"

Duplicate j=1,L_nodes-1
Duplicate i=1,N
m_dot*C_p*(gamma[i,j+1]-gamma[i,j])+(-1)^i*q_useful[i,j]=0
End
End

Duplicate i=1,N-1
Call OddEven(i:odd_i[i],even_i[i])
(m_dot*C_p*(gamma[i+1,L_nodes]-gamma[i,L_nodes])+(-
1)^i*(q_useful[i,L_nodes]+q_useful[i+1,L_nodes]))*odd_i[i]+(m_dot*C_p*
(gamma[i+1,1]-gamma[i,1])+(-
1)^i*(q_useful[i,0]+q_useful[i+1,0]))*even_i[i]=0
End

"start"
m_dot*C_p*(gamma[1,1]-T_f[1,0])=q_useful[1,0]
"end"
(m_dot*C_p*(T_f[N,0]-gamma[N,1])-
(1)^N*q_useful[N,0])*even+(m_dot*C_p*(T_f[N,L_nodes]-
gamma[N,L_nodes])-(1)^N*q_useful[N,L_nodes])*odd=0

Duplicate i=1,N
Duplicate j=1,L_nodes-1

T_f[i,j]=(gamma[i,j]+gamma[i,j+1])/2
end
end

Duplicate i=1,N-1
Call OddEven(i:oddi[i],eveni[i])
T_f[i,L_nodes]*oddi[i]+T_f[i,0]*eveni[i]=((gamma[i,L_nodes]+gamma[i+1,
L_nodes])/2)*oddi[i]+((gamma[i,1]+gamma[i+1,1])/2)*eveni[i]
End
"_____________________________________________________________"
"Boundary conditions at turns"
Duplicate i=1,N-1
```

```
Call OddEven(i:i_odd[i],i_even[i])
T_f[i+1,L_nodes]*i_odd[i]                              +T_f[i+1,0]*i_even[i]=
alpha*(T_f[i,L_nodes]*i_odd[i]+T_f[i,0]*i_even[i])
End
alpha=exp(-D*U_L*W/(m_dot*C_p*(1+R*D*U_L)))
"_____________________________________________________________________"
"Calculation of the heat removal factor"
Call OddEven(N:odd,even)
F_R=m_dot*C_p*(T_out-T_in)/(A_c*(S-U_L*(T_in-T_a)))
T_out=T_f[N,0]*even+T_f[N,L_nodes]*odd

T_in=T_f[1,0]
"_____________________________________________________________________"
"collector efficiencies"
eta_serpentine=F_R*TauAlpha-F_R*U_L*DELTA_T\G_T
eta_serpentine_ZL=F_R_ZL*TauAlpha-F_R_ZL*U_L*DELTA_T\G_T
TauAlpha=0.9
DELTA_T\G_T=0.05
"_____________________________________________________________________"

"Using Abdel-Khalik's analysis"
Kappa_ZL=k*delta*nnn/((W-D)*sinh(nnn))
nnn=(W-D)*sqrt(U_L/(k*delta))
gamma_ZL=-2*cosh(nnn)-D*U_L/Kappa_ZL
F_1_ZL=(N*Kappa_ZL*L)/(U_L*A_c)*(Kappa_ZL*R*(1+gamma_ZL)^2-1-gamma_ZL-
Kappa_ZL*R)/((Kappa_ZL*R*(1+gamma_ZL)-1)^2-(kappa_ZL*R)^2)
F_2_ZL=1/(Kappa_ZL*R*(1+gamma_ZL)^2-1-gamma_ZL-Kappa_ZL*R)
F_5_ZL=sqrt((1-F_2_ZL^2)/F_2_ZL^2)
(F_1_ZL*U_L*A_c)/(m_dot*C_p)=2*beta_1_zl
F_R_ZL/F_1_ZL=1/(2*Beta_1_ZL)*(1+(2*(1/F_2_ZL+F_5_ZL-1)*F_5_ZL)/((1-
1/F_2_ZL+F_5_ZL)*exp(-2*Beta_1_ZL*sqrt(1-F_2_ZL^2))+(1/F_2_ZL+F_5_ZL-
1))-1/F_2_ZL-F_5_ZL)
F_4_Zl=1/F_2_zl+F_5_zl-1
1/f_3_zl=(2*beta_1_zl)

unity_ZL=m_dot*c_p/(F_1_ZL*U_L*A_c)

"_____________________________________________________________________"
m_dot\A_c=m_dot/A_c
FR_ZL\F1=F_R_ZL/F_1_ZL
```

APPENDIX D

Interpretation of Manufacturer's Data

HARTELL PUMP DATA

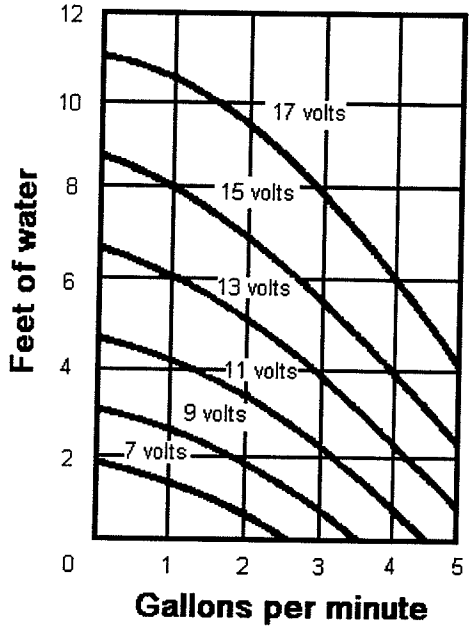

Figure D.1

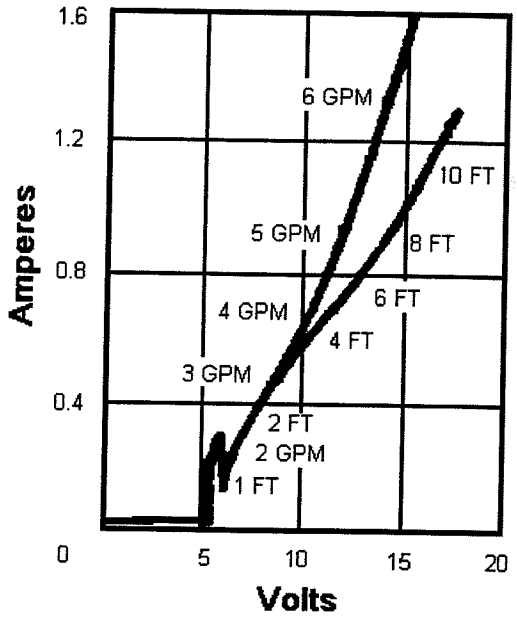

Figure D.2

Information is needed about the voltage, current, head and flow rate in order to couple the pump to a photovoltaic cell. Figure D.1 shows the typical pump curves for various voltages. Since current varies for a given voltage, Figure D.2 is used to find the current at various voltages. Two curves are presented in figure D.2; the upper curve represents the condition of no head and the lower curve represents the condition of no flow. The current can then be found at the extremes of no head and no flow for each voltage. Linear interpolation was used to find current at any intermediate head and flow rate in order to derive equations D.1 and D.2.

$$flowrate = a + b \cdot Head + c \cdot Head^2 + d \cdot Head^3 + e \cdot Voltage + f \cdot Voltage^2 + g \cdot Voltage^3 + h \cdot Head \cdot Voltage + i \cdot Head \cdot Voltage^2 + j \cdot Head^2 \cdot Voltage + k \cdot Head^2 \cdot Voltage^2 \qquad (D.1)$$

$$Current = a + b \cdot Voltage + c \cdot Voltage^2 + d \cdot Head + e \cdot Head^2 \qquad (D.2)$$

BIBLIOGRAPHY

Abdel-Khalik, S.I., "Heat Removal Factor for a Flat-Plate Solar Collector with a Serpentine Tube", *Solar Energy*, vol.18, p.59-64, 1976.

Al-Ibrahim, A.M., *Optimum Selection of Direct-Coupled Photovoltaic Pumping System in Solar Domestic Hot Water Systems*, Ph.D. Thesis, Mechanical Engineering Department, University of Wisconsin-Madison, 1997.

Avina, J., *The Modeling of a Natural Convection Heat Exchanger in a Solar Domestic Hot Water System*, M.S. Thesis, University of Wisconsin-Madison, 1994.

Bergelt, T.K., Brunger, A.P., and Hollands, K.G.T., "Optimum Hydraulic Resistance for Natural Convection SDHW Heat Exchanger Loops", *Proceedings, 19th Annual Conference of the Solar Energy Society of Canada*, Quebec City, Quebec, vol. 35(11), pp. 2969-2982, 1993.

Bradley, D., *Promising Freeze Protection Alternatives in Solar Domestic Hot Water Systems*, M.S. Thesis, University of Wisconsin - Madison, 1997.

CANMET, S2000 Program brochure, Minister of Supply and Services, Ottawa, Canada, 1993.

Chapman, A.J., *Heat Transfer*, 4th ed., Macmillan, New York, 1984.

Chiou, J.P., and Perera, D.G., "Non-Iterative Solution of Heat Transfer Equation of Fluid Flowing through a Serpentine Tube attached to a plate with radiation as a heat source", *American Society of Mechanical Engineers- Heat Transfer Division,* vol 62, pp. 89-96, ASME, New York, 1986.

Cragan, K.E., *Impact on a Utility of An Ensemble of Solar Domestic Hot Water Systems*, M.S. thesis, University of Wisconsin - Madison, 1994.

Dahl, S.D., and Davidson, J.H., "Characterization of a Tube-In-Shell Thermosyphon Heat Exchanger for Solar Water Heating", *Proceedings, ASME/JSME/JSES International Solar Energy Conference*, Maui, Hawaii, vol. 2, pp.1157-1163, 1995.

Dahl, S.D., and Davidson, J.H., "Comparison of Natural Convection Heat Exchangers for Solar Water Heating", *Proceedings, Solar '95, Annual Conference of the American Solar Energy Society*, Minneapolis, MN, pp. 288-293, 1995.

Davidson, J.H., and Dahl, S., *Natural Convection Heat Exchangers for Solar Water Heating Systems*, Technical Progress Report, University of Minnesota, May 15 - July 14, Minneapolis, MN, 1996.

Davidson, J.H., and Dahl, S.D., "Issues of Predicting Performance of Thermosyphon Heat Exchangers", *Proceedings, ASME International Solar Energy Conference*, San Antonio, TX, pp. 1-8, 1996.

Davidson, J.H., Dahl, S.D., and Long, S., "Testing, Modeling and Rating Solar Water Heaters with Side-Arm Thermosyphon Heat Exchangers", *Proceedings, Solar '97, Annual Conference of the American Solar Energy Society*, Washington, D.C, 1997.

Department of Energy (DOE) – Energy Information Administration, *Annual Energy Review 1996*, U.S. Government Printing Office, 1997.

Department of Energy (DOE) – Energy Information Administration, *Electricity Generation and Environmental Externalities: Case Studies*, Government Printing Office, Washington D.C., September 1995.

Duffie, J.A., and Beckman, W.A., *Solar Engineering of Thermal Processes*, 2nd edition, John Wiley & Sons, New York, 1991.

Dunkle, R.V., and Davey, E.T., "Flow Distribution in Solar Absorber Banks", paper presented at *Melbourne International Solar Energy Society Conference*, Melbourne, 1970.

Enstar, *USH$_2$O Utility User Group Meeting Report for March 11 – 14,* Palm Springs, California,1996.

Fanney, A.H., and Klein, S.A., "Thermal Performance Comparisons for Solar Hot Water Systems Subjected to Various Collector Array Flow Rates", *Intersol 85: Proceedings of the Ninth Biennial Congress of the International Solar Energy Society,* vol. 1, pp.538-543, Pergammon Press, New York, 1985.

Fanney, A.H., and Klein, S.A., "Thermal Performance Comparisons for Solar Hot Water Systems Subjected to Various Collector and Heat Exchanger Flow Rates", *Solar Energy*, vol. 40, No. 1, pp. 1-11, 1988.

Fraser, K.F., Hollands, K.G.T., Brunger, A.P., "Modeling Natural Convection Heat Exchangers for SDHW Systems", *Proceedings, "Renewable Energy : Technology for Today" 18th Annual Conference of the Solar Energy Society of Canada*, Edmonton, Alberta, pp. 190-195, 1992.

Fraser, K.F., *Modeling Natural Convection Heat Exchangers in Solar Domestic Hot Water Systems*, M.S. Thesis, University of Waterloo, Canada, 1992.

Gerhart, P.M., and Gross, R.J., *Fundamentals of Fluid Mechanics*, Addison-Wesley Publishing Company, Massachusetts, 1985.

Hartell, *Direct Current Circulating Pumps*, Catalog, Ivyland, PA, 1991.

Hicks, T.G., *Pump Selection and Application*, McGraw-Hill, 1st ed., New York, 1957.

Hirsch, U.T., *Control Strategies for Solar Water Heating Systems*, M.S. Thesis, University of Wisconsin - Madison, 1985.

Hollands, K.G.T., and Brunger, A.P., "Optimum Flow Rates in Solar Water Heating Systems with a Counterflow Exchanger", *Solar Energy*, vol. 48(1), pp. 15-19, 1992.

Hunn, B.D., ed., Solar Energy Research Institute (SERI), *Engineering Principles and Concepts for Active Solar Systems*, U.S. Government Printing Office, 1981.

Incropera, F.P., and DeWitt, D.P., *Fundamentals of Heat and Mass Transfer*, 3rd ed., John Wiley & Sons, Singapore, 1990.

International Energy Agency (IEA), Duff, W.(ed.), *Advanced Solar Domestic Hot Water Systems*- A report of the Task 14 Advanced Solar Domestic Hot Water Systems Working Group, April 1996.

Kakaç, S., Shah, R.K., Aung, W., *Handbook of Single-Phase Convective Heat Transfer,* John-Wiley & Sons, New York, 1987.

Klein, S.A., "Calculation of Flat-Plate Collector Loss Coefficients", *Solar Energy*, vol. 17, No. 1, pp. 79-80, 1975.

Klein, S.A. and Alvarado, F.L, EES – Engineering Equation Solver, F-Chart Software, Middleton, WI, 1997.

Klein, S.A. et al., TRNSYS – A Transient System Simulation Program, Version 14.2, University of Wisconsin-Madison Solar Energy Laboratory, 1996.

Kou, Q., *A Method for Estimating the Long-term Performance of Photovoltaic Pumping System,* M.S. Thesis, Mechanical Engineering Department, University of Wisconsin-Madison, 1997.

Lindeburg, M.R., *Mechanical Engineering Review Manual*, 7th ed., Professional Publications, San Carlos, 1984.

Lund, K.O., "General Thermal Analysis of Serpentine-Flow Flat-Plate Solar Collector Absorbers", *Solar Energy,* vol. 42, pp. 133-142, 1989.

Lyons, R.L and Comer, J.C., *Business Opportunity Prospectus for Utilities in Solar Water Heating*, Energy Alliance Group, Boston, 1997.

Madison Gas and Electric, *Water Heaters*, brochure, Madison, 1995.

Murphy, J., Ridout, D., and McShane, B., *Numerical Analysis, Algorithms and Computation*, Ellis Horwood Limited, Chichester, 1988.

Rabehl, R.J., *Parameter Estimation and the Use of Catalog Data with TRNSYS*, M.S. Thesis, Mechanical Engineering Department, University of Wisconsin-Madison, 1997.

Solar Energy Research Institute (SERI), *Photovoltaics Technical Information Guide*, 2nd ed., U.S. Government Printing Office, 1988.

Solar Rating and Certification Corporation, *Solar Products Specification Guide*, Washington, D.C., 1982.

Solar Rating and Certification Corporation, *Directory of SRCC Certified Solar Collector and Water Heating System Ratings*, Washington, D.C., December, 1994.

Tadros, W.H., Abdel-Salam, M.S., Salama, M.W., "Temperature Profiles of Serpentine-flow Flat-Plate Solar Collectors, *Journal of The Institution of Engineers (India) :Interdisciplinary*, vol. 74, pp. 32-37, 1994.

Trzesniewski, J.A., *Electric Utility Interest in Solar Energy Systems*, M.S. thesis, University of Wisconsin - Madison, 1995.

Van Koppen, C.W.J., Thomas, J.P.S., and Veltkamp, W.B., "The actual benefits of thermally stratified storage in small – and medium – size storage system", *Proceedings of Sun II, Biennial Meeting, ISES, Atlanta, GA*, Vol.2, Pergammon Press, New York, pp. 576-580 (1979).

Williams, P.M., *Development and Analysis Tool for Photovoltaic-Powered Solar Water Heating Systems*, M.S. Thesis, Mechanical Engineering Department, University of Wisconsin-Madison, 1996.

Williams, P.M.,, Al-Ibrahim, A.M., Eckstien, Y., Madison, WI, personal communication, 1997.

Wuestling, M.D., *Investigation of promising control alternatives for solar domestic water heating systems*, M.S. Thesis, Mechanical Engineering Department, University of Wisconsin-Madison, 1983.

Wuestling, M.D., Klein, S.A., and Duffie, J.A., "Promising Control Alternatives for Solar Water Heating Systems", *Trans. ASME, Journal of Solar Energy Engineering*, vol. 107, p.215, 1985.

Zhang, H., and Lavan, Z., "Thermal Performance of a Serpentine Absorber Plate", *Solar Energy,* vol. 34, p.175-177, 1985.

Advisor S. A. Klein

Title Professor

Date 12/17/97